

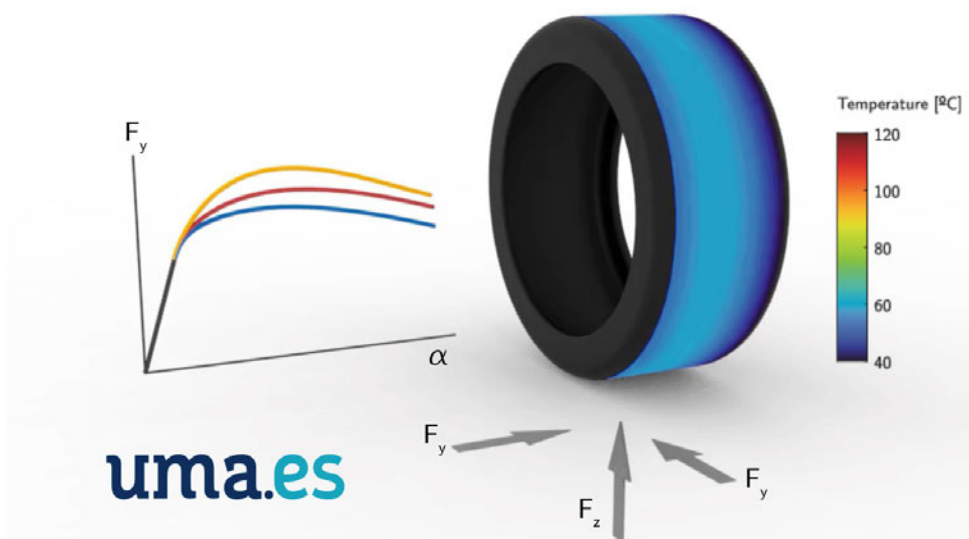


Study of the fundamental parameters affecting tire models for use in active safety systems in vehicles

Ingeniería Mecánica y Eficiencia Energética
Universidad de Málaga
Escuela de Ingenierías Industriales
2022

Author: Manuel G. Alcázar Vargas

Advisors: Juan A. Cabrera Carrillo
Juan J. Castillo Aguilar




uma.es



UNIVERSIDAD
DE MÁLAGA

AUTOR: Manuel Gonzalo Alcázar Vargas

 <https://orcid.org/0000-0001-6737-0880>

EDITA: Publicaciones y Divulgación Científica. Universidad de Málaga



Esta obra está bajo una licencia de Creative Commons Reconocimiento-NoComercial-SinObraDerivada 4.0 Internacional:

<http://creativecommons.org/licenses/by-nc-nd/4.0/legalcode>

Cualquier parte de esta obra se puede reproducir sin autorización pero con el reconocimiento y atribución de los autores.

No se puede hacer uso comercial de la obra y no se puede alterar, transformar o hacer obras derivadas.

Esta Tesis Doctoral está depositada en el Repositorio Institucional de la Universidad de Málaga (RIUMA): riuma.uma.es



University of Malaga

Department of Mechanical Engineering and Fluid Mechanics

STUDY OF THE FUNDAMENTAL PARAMETERS AFFECTING TIRE MODELS FOR USE IN ACTIVE SAFETY SYSTEMS IN VEHICLES

DISSERTATION

submitted in partial fulfillment
of the requirements for the degree of

Doctor of Philosophy

in Ingeniería Mecánica y Eficiencia Energética

by

Manuel Gonzalo Alcázar Vargas

Malaga, November 2022



University of Malaga

Department of Mechanical Engineering and Fluid Mechanics
PhD Dissertation

STUDY OF THE FUNDAMENTAL PARAMETERS AFFECTING TIRE MODELS FOR USE IN ACTIVE SAFETY SYSTEMS IN VEHICLES

Author: Manuel Gonzalo Alcázar Vargas

Supervisors: Dr. Juan Antonio Cabrera Carrillo
Full Professor, Mechanical Engineering

Dr. Juan Jesús Castillo Aguilar
Full Professor, Mechanical Engineering

Malaga, November 2022

DECLARACIÓN DE AUTORÍA Y ORIGINALIDAD DE LA TESIS PRESENTADA PARA OBTENER EL TÍTULO DE DOCTOR

D. Manuel Gonzalo Alcázar Vargas

Estudiante del programa de doctorado Ingeniería Mecánica y Eficiencia energética de la Universidad de Málaga, autor de la tesis, presentada para la obtención del título de doctor por la Universidad de Málaga, titulada: *Study of the fundamental parameters affecting tire models for use in active safety systems in vehicles*

Realizada bajo la tutorización de Juan Antonio Cabrera Carrillo y dirección de Juan Antonio Cabrera Carrillo y Juan Jesús Castillo Aguilar

DECLARO QUE:

La tesis presentada es una obra original que no infringe los derechos de propiedad intelectual ni los derechos de propiedad industrial u otros, conforme al ordenamiento jurídico vigente (Real Decreto Legislativo 1/1996, de 12 de abril, por el que se aprueba el texto refundido de la Ley de Propiedad Intelectual, regularizando, aclarando y armonizando las disposiciones legales vigentes sobre la materia), modificado por la Ley 2/2019, de 1 de marzo.

Igualmente asumo, ante a la Universidad de Málaga y ante cualquier otra instancia, la responsabilidad que pudiera derivarse en caso de plagio de contenidos en la tesis presentada, conforme al ordenamiento jurídico vigente.

Doctorando:	Tutor:
Directores:	

AUTORIZACIÓN DE LECTURA

D. Juan Antonio Cabrera Carrillo y D. Juan Jesús Castillo Aguilar,
Catedráticos de la Universidad de Málaga, en calidad de directores

CERTIFICAN:

Que las publicaciones que avalan la tesis de Manuel Gonzalo Alcázar Vargas, titulada *Study of the fundamental parameters affecting tire models for use in active safety systems in vehicles*, no han sido utilizadas en tesis anteriores; y que ha alcanzado los objetivos de investigación propuestos, estando debidamente cualificada para su defensa

Director y tutor de tesis:	Director de tesis:

ACKNOWLEDGMENTS

In this dissertation I would like to thank all the people who have helped me during these years, which have not been few.

First and foremost, I want to thank my advisors, 'los Juanes'. Juan Cabrera and Juan Castillo have always supported me, guided me and given me advice looking for the best for me, not for them. That is why I am most grateful to them. Also, the group of people who make up 'Taller 31' and the working environment are undoubtedly praiseworthy due to their incredible work in MotoStudent and at the school for many years. I hope that, when the time comes, those who follow can do half as well as them.

I also want to thank all the colleagues who have been and are in 'Taller 31'. The first one who deserves a special mention is Javi. You have been an ideal partner from day one and you have opened, with a lot of effort, a difficult path that I am also traveling, but I must thank you for the enormous effort you have made being the first. Besides, this dissertation has been possible thanks to the countless hours we have spent on the tire bench, fixing and testing it.

To the rest of the members of the lab, 'los tíos', I have a lot to thank you for. Going to work with you is an absolute pleasure. Juanma, Nacho, Ilde and Manu: you guys are great. Also, to the members of the MotoStudent teams, especially the 2018 and 2021 editions, the project we do every two years is one of the most beautiful things an engineer can do and truly a pleasure to be a part of.

I do not forget Caro, whom I met almost by necessity during my stay in London. Thank you for those months on 'the island without fish' and for your vision of things, which clearly complements mine. You have given me a lot and I wish you all the best, colleague.

I don't want to forget my roots, the University of Jaén, either. I have to thank my TFG and MotoStudent tutor, Pepe Mata. You have transmitted the interest in this field of vehicle dynamics and motorcycles to me. I would also like to thank my TFM tutor, Patricio. I ended up in Malaga partly thanks to you and I thank you for that. To both of you: it was a pleasure to be your student.

I also want to thank Ernesto, my friend and flatmate, for the almost five years I have been in Malaga. You have been an important support, both on and off the tatami.

Last but not least, this dissertation is dedicated to my parents and my sister. Without them, none of this would have been possible. This work is also yours.

Thank you all very much.



Motostudent 2021 team members and the 2018 and 2021 electric motorcycles.

*Tires are perhaps the least well
understood parts of road-going
vehicles despite the fact that they
are one of the most studied.*

- Dave Kaemmer -

ABSTRACT

Active safety in vehicles is a topic of enormous interest to society. In this line, a better knowledge of tire-road interaction broadens the possibilities of improving these safety systems. This thesis analyzes several aspects related to traction, braking and cornering in ground vehicles. Specifically, three papers published in high-impact peer-reviewed journals study each aspect.

First, the power transmission in a motorcycle when passing over an uneven road is analyzed. It demonstrates how the motion of the swingarm, engine and wheel are related. This paper proposes an optimized motorbike transmission system design that maximizes the power transmitted to the wheel. For this purpose, genetic algorithms have been used to maximize the distance traveled during a given time. The result is an arrangement of the final drive elements that acts like a mechanical traction control system by delaying and controlling wheel slip under hard acceleration.

Second, an algorithm for measuring angular velocities whose delay is known, controllable and independent of speed is developed. This algorithm is compared to current methods of measuring wheel velocities. Results demonstrate the superiority of the proposed approach, providing more robust results compared to its competitors.

Third, the influence of various parameters on pure lateral dynamics in tires, both in transient and steady state, is studied. It is observed how temperature dramatically affects the maximum lateral acceleration that a vehicle can experience. The delay in the onset of lateral forces as a function of speed and vertical load is also modeled. These results are of great interest to braking and traction control algorithms since the dynamic response of the tire can be considered to improve the performance of these systems.

Finally, the results and conclusions of this work are grouped, as well as future lines of research related to the thesis.

SUMMARY

In this PhD dissertation, tire dynamics are simulated, measured and modeled under certain conditions. The PhD has been funded through two contracts, the first one for 18 months through the national youth guarantee system, within research project TRA2015-67920-R - Real-time determination of tire-road contact characteristics using bio-inspired algorithms for the improvement of active safety in vehicles. The second has been a contract from the Ministry of Universities through university teacher training grant (FPU18/00450), which started in September 2019.

The dissertation focuses on a specific study of tires, within a broader field of knowledge that the research group has studied for years. Several group members, including the dissertation supervisor, have done their doctorates on this subject. Among them, we can highlight the dissertation by Dr. Cabrera Carrillo (2004), titled '*Modelización en banco de ensayo de sistema inteligente de frenado*' (Intelligent braking system test bench modeling), the one by Dr. Ortiz Fernández (2005) titled '*Desarrollo de técnicas experimentales en la modelización de neumáticos*' (Development of experimental techniques in tire modeling) and the one by Dr. Carabias Acosta (2022) titled '*Metodología experimental para la identificación de los parámetros de suspensión en vehículos automóviles*' (Experimental methodology for the identification of suspension parameters in automotive vehicles). In addition, the research group has been responsible for several regional and national research projects on the study of tires and the application of this knowledge to the design of traction and braking control algorithms and road type estimation, among others. One of these projects allowed the design and construction of a flat-trac type tire-testing machine on which most of the experiments of this doctoral dissertation have been carried out. The doctoral dissertation is the result of three journal articles published in high-impact international journals. In addition, the candidate has carried out a three-month stay abroad within the FPU short-stay program at the Imperial College in London so that the PhD will obtain international mention. As indicated at the beginning of this summary, this dissertation aims to

simulate, measure and parameterize tire dynamics. Therefore, three publications have been made, each of them related to each of the following aspects: simulation of planar vehicle dynamics with emphasis on tire-road contact under highly variable and transient conditions; development and validation of a wheel angular velocity measurement algorithm based on sin-cos encoders with a particular interest in the accuracy and minimization of the delay in the measurement of angular velocities close to wheel locking; and finally the parameterization of tires, both under transient conditions to obtain relaxation parameters and the influence of other variables, such as temperature, in the estimation of maximum available lateral grip. These three works, as a whole, allow the possibility of developing real-time controllers with better knowledge of the system and more robustness in obtaining some variables of interest, thus improving active safety in vehicles.

In the first paper, titled 'Motorcycle final drive geometry optimization on uneven roads', published in 2019 in the Mechanism and Machine Theory journal, a 2D simulation of a motorcycle was performed. An exhaustive study of the rear axle was carried out, analyzing the influence of the position of the engine sprocket with respect to the swingarm axis, the rear suspension and the tire model implemented. Two main phenomena were observed. The first is related to the arrangement of the final drive geometry on the motorcycle: an optimized geometry maximizes the power transmitted to the road. The second is that the tire model greatly affects the simulation results. This is because road irregularities cause a significant fluctuation in the vertical load, as well as oscillations in the swingarm that cause rapid variations in the angular speed of the wheel and, therefore, in the slip. Thus, it is necessary to use a nonlinear transient tire model to analyze the power transmission more adequately.

In this work, a motorcycle system composed of 6 bodies, 6 degrees of freedom and 39 coordinates has been modeled using natural coordinates. The system of differential-algebraic equations has been solved with a predictor-corrector integrator. This is due to the stiffness of the contact problem between the tire and road. This work has implemented the fully nonlinear tire model described by Pacejka. A multitude of remarkable phenomena could be observed in the multibody dynamic simulations. On one side, the importance of the integrator used in solving the system of equations. On the other hand,

the highly stiff nature of the contact problems and, more specifically, the tire-road interaction problem.

This last aspect has turned out to be the most relevant, as it has the following points to highlight. Firstly, *modeling* the system. Secondly, *solving* the system. Thirdly, the *computational cost* of solving this interaction. Finally, checking the influence of a correct *parameterization* of the tire.

In terms of modeling, the main difficulty is the problem at low speeds. The so-called starts from standstill or changes of direction greatly determine both the mathematical formulation used and the stiffness of the problem. Stiff problems are those in which the variables change very rapidly, or at least some of them. This stiffness, in the case of tire-road interaction, has two sources. The first is vertical load fluctuations, more specifically, impacts. The lift-off of the tire originates discontinuities in the equations that can cause the integrator to be unable to converge to the solution. The second problem is caused by those mentioned earlier: low speeds and changes in direction. A powerful motorcycle at low speed generates enormous fluctuations in the slip level, which causes both the coordinates associated with the rear axle and friction forces to vary very rapidly. All this, consequently, considerably increases the stiffness of the problem.

For the resolution of the system, the main difficulty presented by multibody dynamics problems is the type of equations that govern their behavior. The kinematic constraints are those due to the kinematic pairs connecting the bodies and whose unknowns are the coordinates. Therefore, they are of the *algebraic* type. On the other hand, the dynamic constraints are those in which forces appear, among which it is necessary to include, at least, those of inertial origin. Thus, the unknowns are at least the second derivative of the coordinates. Therefore, these equations are of a *differential* type. These two systems of equations constitute the so-called *differential-algebraic systems of equations* (DAEs). Moreover, in the case of multibody dynamics, the kinematic constraints are usually nonlinear, whereas, in vehicular dynamics problems, the differential equations are highly nonlinear, as in the case of Pacejka's magic formula. Finally, as mentioned above, in the 6-body and plane dynamics case studied, the number of coordinates increased to 39, which

makes it necessary to solve at least 39 equations. All of this makes solving the problem considerably complex.

The third point mentioned is the computational cost. The more complex the modeled system is, a priori, the higher its computational cost will be. This is why it is necessary to determine the nature of the problem and correctly choose the integrator(s) and the time step. In any case, an error is constantly made, which must be known and bounded.

Finally, and this is the most challenging point, it is necessary to talk about the influence of correct tire parameterization. Obtaining the parameters that characterize a tire is complex, costly and of limited reliability. This is because, although the parameters are known on the bench or even on the road, they have been obtained in conditions that will most likely not be those in which the tire will be working, as they change rapidly and continuously. Therefore, simulations in this field of knowledge are not as realistic as they are in other fields such as mechanism theory, where the models fit much better to reality. Hence, the problem of determining to what extent an error in the parameterization of the tire conditions the simulation results.

In this work, in addition to a dynamic study of the vehicle, an optimization of the position of the engine sprocket with respect to the swingarm axis has also been carried out. For this purpose, an objective function has been proposed to maximize the distance traveled in a specific period of time while limiting the chain slack. Thus, it has been observed that an optimized arrangement of the final drive elements allows maximizing the power at the wheel, acting similarly to a mechanical traction control. This optimization has been carried out using genetic algorithms, since the problem to be optimized is highly nonlinear. These algorithms have been developed in the research group over the years, being incorporated in several journal articles and PhD dissertations such as those by Dr. Cabrera Carrillo, Dr. Nadal Martínez or Dr. Carabias Acosta. The results of such optimizations agreed with what is observed in commercial and racing motorcycles.

All this system modeling and integration of problem equations has been done using MATLAB software and not with commercial multibody dynamics

software. This has primarily been for two reasons. The first was that modeling the chain drive when the positions of the mechanism vary was not easily done in multibody simulation software, as these simply model the chain drive as a constant ratio of angular velocities. The other reason was that correctly modeling the tire-road interaction in multibody dynamics software, although possible, is more complex than using well-known and well-established software such as MATLAB. Furthermore, it is possible to go down to such a low level as deemed necessary and analyze the computational cost of each subprocess. Finally, although this was seen years later, having the model in MATLAB allows it to be transferred to the real-time control system *speedgoat*, recently acquired by the research group, which has been specially designed to work with Simulink and Simulink Real-Time.

With this first work it was possible to observe firsthand the importance and complexity of a correct approach to the tire-road interaction. This, as indicated by most authors, is the most complex issue to model and characterize, as it is the only one responsible for the forces that modify the trajectory of the vehicle in a controlled manner and ensure its maneuverability. The importance of correctly determining the slip, or sliding speed, was also emphasized. As all authors suggest, either the former or the latter is crucial for generating contact forces. Although less discussed, the stability of the system is just as important. It is known that longitudinal and lateral forces present a maximum for a certain slip value, which means that, if that value is exceeded, the system becomes unstable. For this reason, it was decided to continue working on this area, thus giving rise to this doctoral dissertation, which aims to shed some light on the complex and exciting subject of tire dynamics.

Given the results of the first work, it was decided to further investigate a key aspect in the generation of forces in the tire, which is the correct measurement of the slip level. The slip level, slip ratio or simply slip, is the relationship between the speed that the wheel would have if it were geared to the road and the speed it would have if it were skidding on it. Thus, it is necessary to measure three parameters: linear velocity of the vehicle, radius of the tire and angular velocity of the wheel. Because the forces acting on the vehicle are bounded, the acceleration of the vehicle cannot be very high. Therefore, the variation in the velocity of the vehicle cannot change very

quickly. On the other hand, the radius of the tire remains virtually constant. So the most rapidly varying quantity is the angular velocity of the wheel. Comparatively speaking, the (angular) accelerations experienced by a wheel in a sudden acceleration or braking process are much higher than the (linear) accelerations experienced by a vehicle. For example, a vehicle traveling at 100 km/h can lock its wheels in a fraction of a second, making it impossible for the vehicle to stop in that time.

Therefore, to correctly determine the level of slip and the force generated, the critical parameter is the angular velocity of the wheels. In this context the second paper, titled 'A Novel Method for Determining Angular Speed and Acceleration Using Sin-Cos Encoders', surfaced, published in 2020, appearing in the journal titled *Sensors*. Angular velocity measurement on wheels is usually performed with phonic wheels, also sometimes called incremental encoders. A phonic wheel is a type of sensor, which can be magnetic or optical, that provides a digital signal whose frequency is proportional to the angular velocity of the measured element. What happens is that, at low speed, the output of this sensor is very poor, which makes it very challenging to measure low angular speeds. This complicates determining if a wheel is moving slowly or if, on the contrary, it has already stopped. Hence, the different ABS control algorithms use, in addition to angular velocity, other types of inputs such as angular acceleration to properly operate.

With the advent of electric vehicles, another type of angular position sensor has arisen. These are sin-cos encoders. This type of sensor provides two analog outputs, representing the sine and cosine of the angle between the rotor and the stator. This technology has been widely used in recent years due to the operation principle of permanent magnet synchronous motors (PMSM), which are very common in electric vehicles. In PMSMs, the position of the rotor with respect to the stator must be perfectly known in order to generate the magnetic field in the stator correctly. In low-power vehicles (scooters, bicycles, electric mopeds, etc.) this type of motor is generally not used due to its cost. In the case of medium and high-power electric vehicles, the advantages of this type of motor are undeniable: higher efficiency, lower maintenance and higher power density, among others. All this has led to the increasing use and lower cost of these sensors.

The advantage of this type of sensor is that it provides two continuous signals, so there are no problems when measuring low speeds that do occur in the case of incremental encoders. Thus, the second paper proposes an algorithm for measuring angular velocity and acceleration from the two signals of this sensor. This algorithm presents many advantages, among which can be highlighted:

- They provide a continuous velocity and acceleration output at the desired frequency.
- Signals are filtered by least squares, significantly reducing noise.
- The delay in calculating the variables is known, controllable and independent between velocity and acceleration.
- The computational cost is meager since only additions and multiplications are used. This allows its implementation, for example, in FPGAs.
- It is not necessary to calculate the position of the rotor with respect to the stator, so it is not necessary to perform the arc tangent operation (atan2) or access look-up-tables to calculate the position, therefore reducing the computational cost.

All this allows low-speed applications to perform better by replacing an incremental encoder with a sin-cos encoder. In this second work, both sensors are installed on a wheel and a comparison is made between them. The proposed algorithm is also validated and the required parameters for the angular velocity measurement are tuned.

The basis of the algorithm is quite simple and efficient. The position of the rotor with respect to the stator is determined by applying the arc tangent function and the angular velocity by differentiating it with respect to time. The advantage is that the derivative of the arc tangent function only consists of additions and multiplications, so it is computationally cheap. In addition, it does not have the discontinuities that occur in $\pm\pi$. The same is true for acceleration: only additions and multiplications are required. The Savitzky-Golay filter is used to differentiate the sine and cosine signals. This algorithm is valid for signals acquired at a constant frequency and performs a

polynomial least squares fit. It is necessary to indicate the number of points considered for the polynomial fitting and its order. Another advantage of this method is that it is only necessary to perform a dot product between the vector of measurements and the vector of weights. The latter is constant and it is the one obtained by the Savitzky-Golay method. Thus, the computational cost is very low. Moreover, the measurement delay is proportional to the number of points considered, making it possible to know and control it.

With this work, it was possible to significantly improve the measurement of low angular velocities of the wheels while ensuring measurement accuracy. The error and delay in the measurement do not depend on the angular velocity, as is the case with the methods used with incremental encoders. Finally, another advantage of this method is that the rotating direction is determined, in contrast with incremental encoders in which, to determine the rotating direction, it is usually necessary to use two sensors that are 90 degrees out of phase with each other.

As described at the beginning of this introduction, correct tire parameterization is one of the determining factors for a correct simulation of tire-road interaction. The third paper, titled 'Modeling of the influence of operational parameters on tire lateral dynamics', published in 2022 in the journal *Sensors*, sheds some light on tire parameterization. In this paper, the most specific and extensive literature review of the currently existing tire models is carried out for the first time, as far as the study of tires is concerned. A distinction is made between physical and empirical models as well as stationary and transient ones. As far as the developers of these models are willing to disclose, the generation of contact forces in each available model is studied. A trend towards increasingly physical models is observed. The reason given by the authors for this trend is that outside the conditions under which the empirical models have been tested, their reliability is not guaranteed.

On the contrary, physical models, *a priori*, work under virtually any conditions because the physical laws governing their behavior are assumed to be known. Moreover, although one of the problems with physical models is their higher computational cost compared to empirical ones, increasingly higher computational costs can be assumed. Therefore, many current

software packages indicate that they are based on physical principles for generating contact forces, although they rarely indicate how these models work.

Thus, the third paper analyzes the influence of various operating parameters on the generation of forces in the tire. The parameters analyzed are the following: linear speed of the vehicle, tire pressure, vertical load, frequency of the steering wheel and tire temperature. Tire temperature is undoubtedly the most complex parameter to study, and this is because the tire has a highly variable and highly heterogeneous temperature field. Therefore, speaking of tire temperature is an imprecise term, only valid in the case of using tire warmers for an extended period of time and immediately after removing them. There are several approaches to deal with this aspect. The most complex and probably the most realistic one is to perform a finite element analysis of several systems. The most common one is to compute three simultaneous simulations, using simplified finite elements or finite volume models, which are as follows:

- Mechanical simulation of the tire carcass to study tire deformation, pressure distribution and the contact patch area.
- Thermal simulation of the tire, where the heat generated by hysteresis and friction is analyzed and the heat evacuated by convection to the air and by conduction to the road. The air inside the tire is studied as an ideal gas at constant volume, modifying its pressure and temperature as a function of the heat that reaches it. Some models also analyze the heat radiated by the brake disc.
- Simulation of the contact patch to study the generation of normal and tangential forces from the pressure distribution, sliding velocities and temperature distribution.

These three simulations are the most common although some models perform other simulations such as wear or modal analysis (high frequency).

Other authors treat temperature as a single value, usually taking just one measurement on the tread, using an infrared sensor. With that value, it is usual to modify one or more parameters of Pacejka's magic formula. These

parameters are usually related to the maximum coefficient of friction and stiffness. Sometimes, the 'lambdas' associated with these parameters are modified while other times the parameters themselves are modified. What happens is that a single temperature measurement cannot predict tire performance for the following reasons.

The first reason is that two mechanisms, indentation and molecular adhesion, generate friction forces. The first is associated with macroroughness and the second with microroughness. The most accepted theory explains that, due to the viscoelasticity of the compound, it is necessary to apply more energy to compress it than it returns when the load that deforms it is released. Thus, when the rubber slides over a roughness, the resulting forces from viscoelasticity oppose the sliding and, consequently, friction arises. As for microroughness, the molecules on the tire surface and the molecules on the road surface, in close contact, generate Van der Waals bondings. These bonds stick the tire to the road, so they oppose sliding, resulting in friction as well. As indicated, viscoelasticity plays a crucial role in generating these forces. However, the viscoelastic parameters of the tire compound are strongly influenced by the temperature of the tire at a given moment, and more specifically, the temperature at a given moment with respect to the vitrification temperature. In the case of macroroughness, both the surface and the temperature of the inner layers affect it, as they deform when the road aggregates penetrate the compound. On the contrary, in the case of microroughness, only the surface temperature of the tire affects it since its innermost part does not contribute anything to this mechanism.

Another reason to consider is the generation of pure lateral forces. The pressure distribution in the contact patch of a tire in standstill is strongly conditioned by vertical load, camber angle and tire pressure, mainly. In a moving tire, this pressure distribution is also modified by tire hysteresis, which displaces the center of pressure forwards, generating rolling resistance. By imposing a slip angle, the pressure distribution is also modified for several reasons: the lateral load transfer causes some wheels to have more vertical load than others and some areas of the tire will stick to the road while others will slip (stick-slip theory). In addition, these loads modify the suspension and steering mechanisms, modifying camber and slip angles. All this means that, under typical driving conditions, the distribution of pressures in the contact

patch of a tire is quite complex, making some areas work harder than others. Thus, precisely those areas that work harder heat up more.

Temperature and internal air pressure are closely related. It is common to model tire air by the ideal gas equation considering constant volume so that pressure and temperature are directly coupled. Thus, tire air temperature affects the generation of contact forces in the same way as pressure does, but drastically different from how the temperature of the tread or inner layers of the tire does.

Therefore, in the third paper of the compilation of publications for this dissertation, one of the contributions is the proposal of a method to calculate a representative value of tire temperature from a series of measurements to consider the different mechanisms involved and to estimate the maximum available grip. Knowing the maximum available grip is of great interest for predictive control since it makes it possible to estimate to what extent the tire and the road can generate lateral accelerations to modify the trajectory of the vehicle. However, it is also necessary to know how long it takes to generate these forces. The second aspect dealt with in this third paper is the study of lateral relaxation parameters. Cornering stiffness and relaxation length are included in this group.

As mentioned above, for efficient predictive control of the vehicle to perform, for example, an evasive maneuver (lane-change maneuver), it is necessary to know the system to be controlled as accurately as possible. The most critical parameters are probably the maximum lateral force that the tire can generate, the relationship between the angle of the steering wheel and the lateral force generated and the time it takes for this force to be generated. The parameters associated with these three effects are the maximum lateral friction coefficient, the cornering stiffness and the relaxation length, respectively. The last two are the two parameters that characterize a first-order linear system: proportionality and a time constant. In vehicle dynamics, this time constant of the first-order system is usually replaced by the length that the vehicle would travel, called the relaxation length, which some authors consider a constant value.

Thus, the latter work also analyzes the influence of vehicle speed, vertical load, tire pressure and average tire temperature on these two linear parameters. It has been shown that certain variables are most relevant in the generation of lateral forces, the most important ones being vertical load, followed by vehicle linear speed. On the other hand, pressure and temperature have been found not to affect so much in the linear range of lateral behavior of the tire, as opposed to the nonlinear range where temperature is highly relevant. A polynomial model has been proposed to estimate the relaxation length where the vertical load affects quadratically while the longitudinal speed affects linearly. As for the cornering stiffness, it has been observed that the formula established by Pacejka fits experimental data perfectly. Therefore, this last work has made it possible to develop simple and low-computational-cost models that allow their implementation in control systems to be applied to predictive control in vehicles, primarily focused on crash-avoidance maneuvers.

Thus, this dissertation makes three main contributions to the field of knowledge of vehicle dynamics, which are:

- The analysis, modeling, simulation and optimization of the final drive configuration in a motorcycle, focusing on the optimal arrangement of the sprocket, swingarm and wheel axles in order to maximize power at the wheel. In addition, the need to measure the angular velocity of the wheels as accurately as possible is justified to estimate what forces will be generated and when they will be generated.
- The development and validation of a novel algorithm that measures angular velocities and accelerations in an accurate, delay-controlled and computationally inexpensive manner. Sin-cos encoders are the most extensively used encoders in electric vehicles and increasingly in different applications, since their use has spread enormously while its cost has been reduced.
- The analysis of the most influential parameters in the generation of lateral forces in tires. The influence of several operating variables on the generation of the maximum lateral friction coefficient is studied, proposing a model that considers an averaged tread temperature. In addition, the relaxation parameters are analyzed and studied as a first-

order linear system, characterized by the proportionality constant and by the time delay of the system.

All these contributions have been published in high-impact peer-reviewed journals, proving the relevance and novelty of the work. Future lines of research have also been opened, including the implementation of these developments in the control of a test vehicle. This vehicle is currently being developed by the research group through the project 'Regenerative braking system based on bio-inspired algorithms' (UMA18-FEDERJA-109). This project will allow further research on active safety in vehicles and energy efficiency, two topics of great interest to society.

RESUMEN

En esta tesis doctoral se simula, mide y modela la dinámica de los neumáticos en determinadas condiciones. La tesis doctoral ha sido financiada a través de dos contratos, el primero durante 18 meses a través del sistema nacional de garantía juvenil, dentro del proyecto de investigación TRA2015-67920-R - Determinación en tiempo real de las características de contacto neumático-carretera mediante algoritmos bioinspirados para la mejora de la seguridad activa en vehículos. El segundo ha sido un contrato del Ministerio de Universidades a través de la beca de formación del profesorado universitario (FPU18/00450) que comenzó en septiembre de 2019.

La tesis se centra en un estudio específico de los neumáticos, dentro de un campo de conocimiento más amplio que el grupo de investigación ha estudiado durante años. Varios miembros del grupo, incluido el director de la tesis, han realizado sus doctorados sobre este tema. Entre ellos destacan la tesis del Dr. Cabrera Carrillo (2004), titulada 'Modelización en banco de ensayo de sistema inteligente de frenado', la del Dr. Ortiz Fernández (2005) titulada 'Desarrollo de técnicas experimentales en la modelización de neumáticos' y la del Dr. Carabias Acosta (2022) titulado 'Metodología experimental para la identificación de los parámetros de suspensión en vehículos automóviles'. Además, el grupo de investigación ha sido responsable de varios proyectos de investigación regionales y nacionales sobre el estudio de los neumáticos y la aplicación de estos conocimientos al diseño de algoritmos de control de tracción y frenado y a la estimación del tipo de carretera, entre otros. Uno de estos proyectos permitió el diseño y la construcción de una máquina de ensayos de neumáticos de tipo flat-trac en la que se han realizado la mayoría de los experimentos de esta tesis doctoral. La tesis doctoral es el resultado de tres artículos publicados en revistas internacionales de alto impacto. Además, el doctorando ha realizado una estancia de tres meses en el extranjero dentro del programa de estancias cortas de la FPU en el Imperial College de Londres para que la tesis doctoral obtenga mención internacional. Como se ha indicado al principio de este resumen, esta

tesis pretende simular, medir y parametrizar la dinámica de los neumáticos. Por ello, se han realizado tres publicaciones, cada una de ellas relacionada con cada uno de estos aspectos: la simulación de la dinámica de vehículos planos con énfasis en el contacto neumático-carretera en condiciones altamente variables y transitorias; el desarrollo y validación de un algoritmo de medición de la velocidad angular de las ruedas basado en encoders sin-cos con un interés particular en la precisión y la minimización del retardo en la medición de las velocidades angulares cercanas al bloqueo de las ruedas; y por último la parametrización de los neumáticos, tanto en condiciones transitorias para obtener los parámetros de relajación como la influencia de otras variables, como la temperatura, en la estimación de la máxima adherencia lateral disponible. Estos tres trabajos, en su conjunto, permiten la posibilidad de desarrollar controladores en tiempo real con mejor conocimiento del sistema y mayor robustez en la obtención de algunas variables de interés, mejorando así la seguridad activa en los vehículos.

En el primer artículo, titulado ‘Motorcycle final drive geometry optimization on uneven roads’, publicado en 2019 en la revista *Mechanism and Machine Theory*, se realiza una simulación en 2D de una motocicleta. Se realiza un estudio exhaustivo del tren trasero, analizando la influencia de la posición del piñón del motor con respecto al eje del basculante, la suspensión trasera y el modelo de neumático implementado. Se observan dos fenómenos principales. El primero está relacionado con la disposición de la geometría de la transmisión final en la motocicleta: una geometría optimizada maximiza la potencia transmitida a la carretera. El segundo es que el modelo de neumático afecta en gran medida a los resultados de la simulación. Esto se debe a que las irregularidades de la carretera provocan una fluctuación significativa de la carga vertical, así como oscilaciones en el basculante que causan rápidas variaciones en la velocidad angular de la rueda y, por tanto, en el deslizamiento. Por ello, es necesario utilizar un modelo de neumático transitorio no lineal para analizar la transmisión de potencia de forma más adecuada.

En este trabajo se modeló un sistema de motocicletas compuesto por 6 cuerpos, 6 grados de libertad y 39 coordenadas utilizando coordenadas naturales. El sistema de ecuaciones diferenciales-algebraicas se resolvió con un integrador predictor-corrector. Esto se debe a la rigidez del problema de

contacto entre el neumático y la carretera. Este trabajo implementó el modelo de neumático totalmente no lineal descrito por Pacejka. En las simulaciones dinámicas multicuerpo se pudieron observar multitud de fenómenos notables. Por un lado, la importancia del integrador utilizado en la resolución del sistema de ecuaciones. Por otro, la naturaleza altamente rígida de los problemas de contacto y, más concretamente, del problema de interacción neumático-carretera.

Este último aspecto se consideró el más relevante, ya que tiene los siguientes puntos a destacar. El primero, la *modelización* del sistema. El segundo, la *resolución* del sistema. El tercero, el *coste computacional* de la resolución de esta interacción. Por último, comprobar la influencia de una correcta *parametrización* del neumático.

En términos de modelización, la principal dificultad es el problema a bajas velocidades. Los llamados arranques desde la parado o los cambios de dirección determinan en gran medida tanto la formulación matemática utilizada como la rigidez del problema. Los problemas rígidos son aquellos en los que las variables cambian muy rápidamente, o al menos algunas de ellas. Esta rigidez, en el caso de la interacción neumático-carretera, tiene dos orígenes. El primero son las fluctuaciones de la carga vertical, más concretamente, los impactos. El despegue del neumático origina discontinuidades en las ecuaciones que pueden hacer que el integrador no pueda converger a la solución. El segundo problema está causado por las bajas velocidades y los cambios de dirección. Una motocicleta potente a baja velocidad genera enormes fluctuaciones en el nivel de deslizamiento, lo que hace que tanto las coordenadas asociadas al eje trasero como las fuerzas de fricción varíen muy rápidamente. Todo esto, por tanto, aumenta considerablemente la rigidez del problema.

Para la resolución del sistema, la principal dificultad que presentan los problemas de dinámica multicuerpo es el tipo de ecuaciones que gobiernan su comportamiento. Las restricciones cinemáticas son las debidas a los pares cinemáticos que conectan los cuerpos y cuyas incógnitas son las coordenadas. Por tanto, son de tipo *algebraico*. Por otro lado, las restricciones dinámicas son aquellas en las que aparecen fuerzas, entre las que hay que incluir, al menos, las de origen inercial. Así, las incógnitas son, al menos, la segunda derivada

de las coordenadas. Por lo tanto, estas ecuaciones son de tipo *diferencial*. Estos dos sistemas de ecuaciones constituyen los llamados *sistemas de ecuaciones diferenciales-algebraicas* (DAE). Además, en el caso de la dinámica multicuerpo, las restricciones cinemáticas suelen ser no lineales, mientras que, en los problemas de dinámica vehicular, las ecuaciones diferenciales son altamente no lineales, como en el caso de la fórmula mágica de Pacejka. Por último, como se ha mencionado anteriormente, en el caso de la dinámica de 6 cuerpos y del plano estudiado, el número de coordenadas aumentó a 39, lo que hace necesario resolver al menos 39 ecuaciones. Todo ello hace que la resolución del problema sea considerablemente compleja.

El tercer punto mencionado es el coste computacional. Cuanto más complejo sea el sistema modelado, a priori, mayor será su coste computacional. Por eso es necesario determinar la naturaleza del problema y elegir correctamente el o los integradores y el paso de tiempo. En cualquier caso, se comete constantemente un error, que debe ser conocido y acotado.

Por último, y este es el punto más desafiante, es necesario hablar de la influencia de una correcta parametrización del neumático. La obtención de los parámetros que caracterizan un neumático es compleja, costosa y de fiabilidad limitada. Esto se debe a que, aunque los parámetros se conozcan en el banco o incluso en la carretera, se han obtenido en condiciones que muy probablemente no serán aquellas en las que trabajará el neumático, ya que cambian rápida y continuamente. Por lo tanto, las simulaciones en este campo del conocimiento no son tan realistas como lo son en otros campos como la teoría de mecanismos, donde los modelos se ajustan mucho mejor a la realidad. De ahí el problema de determinar hasta qué punto un error en la parametrización del neumático condiciona los resultados de la simulación.

En este trabajo, además de un estudio dinámico del vehículo, se llevó a cabo una optimización de la posición del piñón del motor con respecto al eje del basculante. Para ello, se propuso una función objetivo que maximizara la distancia recorrida en un tiempo determinado limitando la holgura de la cadena. Así, se observó que una disposición optimizada de los elementos de transmisión final permite maximizar la potencia en la rueda, actuando de forma similar a un control de tracción mecánico. Esta optimización se llevó a cabo mediante algoritmos genéticos, ya que el problema a optimizar es

altamente no lineal. Estos algoritmos han sido desarrollados en el grupo de investigación a lo largo de los años, siendo incorporados en varios artículos de revistas y tesis doctorales como las del Dr. Cabrera Carrillo, el Dr. Nadal Martínez o el Dr. Carabias Acosta. Los resultados de dicha optimización coinciden con lo observado en motocicletas comerciales y de competición.

Todo este modelado del sistema y la integración de las ecuaciones del problema se realizó con el software MATLAB y no con un software comercial de dinámica multicuerpo. Esto se debió principalmente a dos razones. La primera fue que el modelado de la transmisión por cadena cuando las posiciones del mecanismo varían no era fácil de realizar en un software de simulación multicuerpo, ya que éstos simplemente modelan la transmisión por cadena como una relación constante de velocidades angulares. La otra razón fue que modelar correctamente la interacción neumático-carretera en un software de dinámica multicuerpo, aunque es posible, es más complejo que utilizar un software reconocido como MATLAB. Además, es posible programar en un nivel tan bajo como se considere necesario y analizar el coste computacional de cada subproceso. Por último, aunque esto se vio años después, tener el modelo en MATLAB permite transferirlo al sistema de control en tiempo real *speedgoat*, recientemente adquirido por el grupo de investigación, que ha sido especialmente diseñado para trabajar con Simulink y Simulink Real-Time.

Con este primer trabajo se pudo observar de primera mano la importancia y la complejidad de un correcto planteamiento de la interacción neumático-carretera. Ésta, como indican la mayoría de los autores, es la más compleja de modelar y caracterizar, a la vez que es la única responsable de las fuerzas que modifican la trayectoria del vehículo de forma controlada y aseguran su maniobrabilidad. También se destacó la importancia de determinar correctamente el deslizamiento, o la velocidad de deslizamiento. Como sugieren todos los autores, la primera o la segunda son cruciales para generar fuerzas de contacto. Aunque se discute menos, la estabilidad del sistema es igual de importante. Se sabe que las fuerzas longitudinales y laterales presentan un máximo para un determinado valor de deslizamiento, lo que significa que, si se supera ese valor, el sistema se vuelve inestable. Por este motivo, se decidió seguir trabajando en este campo, dando lugar a esta

tesis doctoral, que pretende arrojar algo de luz sobre el complejo y apasionante tema de la dinámica de los neumáticos.

Dados los resultados del primer trabajo, se decidió investigar más a fondo un aspecto clave en la generación de fuerzas en el neumático, que es la correcta medición del nivel de deslizamiento. El nivel de deslizamiento, relación de deslizamiento o simplemente deslizamiento, es la relación entre la velocidad que tendría la rueda si estuviera engranada a la carretera y la velocidad que tendría si patinara sobre ella. Por lo tanto, es necesario medir tres parámetros: la velocidad lineal del vehículo, el radio del neumático y la velocidad angular de la rueda. Dado que las fuerzas que actúan sobre el vehículo están acotadas, la aceleración del vehículo no puede ser muy elevada; por lo tanto, la variación de la velocidad del vehículo no puede cambiar muy rápidamente. Por otro lado, el radio de la rueda permanece prácticamente constante. Así que la magnitud que varía más rápidamente es la velocidad angular de la rueda. Comparativamente, las aceleraciones (angulares) que experimenta una rueda en un proceso de aceleración o frenado brusco son mucho mayores que las aceleraciones (lineales) que experimenta un vehículo. Por ejemplo, un vehículo que circula a 100 km/h puede bloquear las ruedas en una fracción de segundo, mientras que es imposible detener el vehículo en ese tiempo.

Por tanto, para determinar correctamente el nivel de deslizamiento y la fuerza generada, el parámetro crítico es la velocidad angular de las ruedas. En este contexto surge el segundo artículo titulado 'A Novel Method for Determining Angular Speed and Acceleration Using Sin-Cos Encoders', publicado en 2020 en la revista Sensors. La medición de la velocidad angular en las ruedas suele realizarse con ruedas fónicas, también llamadas a veces encoders incrementales. Una rueda fónica es un tipo de sensor, que puede ser magnético u óptico, que proporciona una señal digital cuya frecuencia es proporcional a la velocidad angular del elemento medido. Lo que ocurre es que, a baja velocidad, la salida de este sensor es muy pobre, lo que hace muy difícil medir velocidades angulares bajas. Esto complica determinar si una rueda se está moviendo lentamente o si, por el contrario, ya se ha detenido. Por ello, los diferentes algoritmos de control del ABS utilizan, además de la velocidad angular, otro tipo de entradas como la aceleración angular para funcionar correctamente.

Con la llegada de los vehículos eléctricos, ha surgido otro tipo de sensor de posición angular. Se trata de los encoders sin-cos. Este tipo de sensor proporciona dos salidas analógicas que representan el seno y el coseno del ángulo entre el rotor y el estator. Esta tecnología se ha utilizado ampliamente en los últimos años debido al principio de funcionamiento de los motores síncronos de imanes permanentes (PMSM), muy comunes en los vehículos eléctricos. En los PMSM, la posición del rotor con respecto al estator debe ser perfectamente conocida para generar correctamente el campo magnético en el estator. En los vehículos de baja potencia (Scooter, bicicletas, ciclomotores eléctricos, etc.) este tipo de motor no suele utilizarse debido a su coste. En el caso de los vehículos eléctricos de media y alta potencia, las ventajas de este tipo de motor son innegables: mayor eficiencia, menor mantenimiento y mayor densidad de potencia, entre otras. Todo ello ha propiciado el uso creciente y el abaratamiento de estos sensores.

La ventaja de este tipo de sensor es que proporciona dos señales continuas, por lo que no hay problemas a la hora de medir velocidades bajas que sí se dan en el caso de los encoders incrementales. Así, el segundo trabajo propone un algoritmo para medir la velocidad angular y la aceleración a partir de las dos señales de este sensor. Este algoritmo presenta muchas ventajas, entre las que cabe destacar

- Proporcionan una salida continua de velocidad y aceleración a la frecuencia deseada.
- Las señales se filtran por mínimos cuadrados, lo que reduce significativamente el ruido.
- El retraso en el cálculo de las variables es conocido, controlable e independiente entre la velocidad y la aceleración.
- El coste computacional es reducido, ya que sólo se realizan sumas y multiplicaciones. Esto permite su implementación, por ejemplo, en FPGAs.
- No es necesario calcular la posición del rotor con respecto al estator, por lo que no es necesario realizar la operación de arco tangente (atan2) ni acceder a look-up-tables para calcular la posición, lo que reduce el coste computacional.

Todo ello permite que, al sustituir un encoder incremental por un encoder sin-cos, las aplicaciones de baja velocidad tengan un mejor funcionamiento. En este segundo trabajo, se instalan ambos sensores en una rueda y se realiza una comparación entre ellos. Se compara con los métodos más comunes, como son el método M, el método T, y el método MT. También se valida el algoritmo propuesto y se ajustan los parámetros necesarios para la medición de la velocidad angular.

La base del algoritmo es bastante sencilla y eficaz. La posición del rotor con respecto al estator se determina aplicando la función arco tangente, y la velocidad angular derivándola con respecto al tiempo. La ventaja es que la derivada de la función arco tangente consiste sólo en sumas y multiplicaciones, por lo que es computacionalmente barata. Además, es continua, al contrario que la función arco tangente, que presenta discontinuidades en $\pm\pi$. Lo mismo ocurre con la aceleración: tan sólo se requieren sumas y multiplicaciones. El filtro Savitzky-Golay se utiliza para derivar las señales de seno y coseno. Este algoritmo es válido para las señales adquiridas a una frecuencia constante y realiza un ajuste polinómico por mínimos cuadrados. Es necesario indicar el número de puntos considerados para el ajuste polinómico y su orden. Otra ventaja de este método es que sólo es necesario realizar un producto escalar entre el vector de medidas y el vector de pesos. Este último es constante y es el obtenido por el método Savitzky-Golay. Así, el coste computacional es muy bajo. Además, el retraso de las medidas es proporcional al número de puntos considerados, lo que permite conocerlo y controlarlo. Por último, cabe decir que el ajuste es casi perfecto, puesto que se aproxima una función senoidal (seno y coseno) por un polinomio de bajo grado, habitualmente tres. Esto ocasiona que tanto la propia señal como las sucesivas derivadas sean muy limpias.

Con este trabajo, se ha podido mejorar significativamente la medición de las bajas velocidades angulares de las ruedas, garantizando al mismo tiempo la precisión de la medición. El error y el retraso en la medición no dependen de la velocidad angular, como ocurre con los métodos utilizados con los encoders incrementales. Por último, otra ventaja de este método es que se determina el sentido de giro, a diferencia de lo que ocurre con los encoders incrementales en los que, para determinar el sentido de giro, suele ser necesario utilizar dos sensores desfasados 90 grados entre sí.

Como se ha descrito al principio de este resumen, la correcta parametrización de los neumáticos es uno de los factores determinantes para una correcta simulación de la interacción neumático-carretera. El tercer artículo, titulado 'Modeling of the influence of operational parameters on tire lateral dynamics', publicado en 2022 en la revista *Sensors*, arroja algo de luz sobre la parametrización de los neumáticos. En este artículo, el más específico en cuanto al estudio de los neumáticos, se realiza en primer lugar una amplia revisión bibliográfica de los modelos de neumáticos existentes en la actualidad. Se distingue entre modelos físicos y empíricos, así como estacionarios y transitorios. En la medida en que los desarrolladores de estos modelos están dispuestos a revelar, se estudia la generación de fuerzas de contacto en cada modelo disponible. Se observa una tendencia hacia modelos cada vez más físicos. La razón que dan los autores para esta tendencia es que, fuera de las condiciones en las que se han probado los modelos empíricos, su fiabilidad no está garantizada.

Por el contrario, los modelos físicos, a priori, funcionan prácticamente en cualquier condición porque se supone que se conocen las leyes físicas que rigen su comportamiento. Además, aunque uno de los problemas de los modelos físicos es su mayor coste computacional en comparación con los empíricos, aunque hoy en día se pueden asumir costes computacionales cada vez más elevados. Por ello, muchos softwares actuales indican que se basan en principios físicos para generar fuerzas de contacto, aunque rara vez indican cómo funcionan estos modelos.

Así, el tercer artículo analiza la influencia de varios parámetros de funcionamiento en la generación de fuerzas en el neumático. Los parámetros analizados son los siguientes: velocidad lineal del vehículo, presión del neumático, carga vertical, frecuencia de giro del volante y temperatura del neumático. La temperatura es, sin duda, el parámetro más complejo de estudiar, y esto se debe a que el neumático tiene un campo de temperatura altamente variable y muy heterogéneo. Por lo tanto, hablar de la temperatura del neumático es un término impreciso, sólo válido en el caso de utilizar calentadores de neumáticos durante un tiempo prolongado e inmediatamente después de retirarlos. Existen varios enfoques para tratar este aspecto. El más complejo y probablemente el más realista es realizar un análisis de elementos finitos de varios sistemas. Lo más habitual es realizar tres simulaciones

simultáneas, utilizando modelos simplificados de elementos finitos o de volúmenes finitos, que son los siguientes:

- Simulación mecánica de la carcasa del neumático para estudiar la deformación de este y la distribución de las presiones normales en la zona de contacto con la carretera.
- Simulación térmica del neumático, donde se analiza el calor generado por histéresis y rozamiento, así como el calor evacuado por convección al aire y por conducción a la carretera. Habitualmente el aire del interior del neumático se estudia como un gas ideal a volumen constante, modificando su presión y temperatura en función del calor que entra o sale del sistema. Algunos modelos analizan también el calor generado e irradiado por el disco de freno a la llanta.
- Simulación del área de contacto para estudiar la generación de fuerzas de rozamiento a partir de la distribución de la presión normal, las velocidades de deslizamiento y la distribución de temperatura.

Aunque estas tres simulaciones son las más comunes, aunque algunos modelos realizan otras adicionales, entre las que se incluyen el desgaste del neumático o análisis modales (alta frecuencia).

Otros autores tratan la temperatura como un valor único, y suelen tomar una sola medida en la banda de rodadura mediante un sensor de infrarrojos. Con ese valor, es habitual modificar uno o varios parámetros de la fórmula mágica de Pacejka. Estos parámetros suelen estar relacionados con el coeficiente máximo de fricción y la rigidez. A veces, se modifican las ‘lambdas’ asociadas a estos parámetros, mientras que otras veces se modifican los propios parámetros. Lo que ocurre es que una sola medición de la temperatura no puede predecir el rendimiento del neumático, por las siguientes razones.

La primera razón es que dos mecanismos, habitualmente conocidos por sus términos en inglés *indentation* y *molecular adhesion*, generan fuerzas de fricción. El primero está asociado a la macrorrugosidad y el segundo a la microrrugosidad. La teoría más aceptada explica que, debido a la viscoelasticidad del compuesto, es necesario aplicar más energía para

comprimirlo que la que devuelve cuando se libera la carga que lo deforma. Así, cuando el neumático se desliza sobre una rugosidad, primero se éste se comprime y luego se relaja, de manera que las fuerzas resultantes de la viscoelasticidad se oponen al deslizamiento y, por tanto, surge la fricción. En cuanto a la microrrugosidad, las moléculas de la superficie del neumático y las moléculas de la superficie de la carretera, en estrecho contacto, generan enlaces de Van der Waals. Estos enlaces pegan el neumático a la carretera, por lo que se oponen al deslizamiento, dando lugar también a la fricción. Como se ha indicado, la viscoelasticidad desempeña el papel fundamental en la generación de estas fuerzas tangenciales. Sin embargo, los parámetros viscoelásticos del compuesto del neumático están fuertemente influenciados por la temperatura a la que se encuentra el neumático, y más concretamente, la temperatura a la que se encuentra con respecto a la temperatura de vitrificación. En el caso de la macrorrugosidad, tanto la temperatura de la superficie como la de las capas internas le afectan, ya que se deforman cuando el árido de la carretera penetra en el compuesto. Por el contrario, en el caso de la microrrugosidad, sólo le afecta la temperatura de la superficie del neumático, ya que su parte más interna no contribuye nada a este mecanismo.

Otra razón para tener en cuenta es la generación de fuerzas laterales puras. La distribución de la presión en la zona de contacto de un neumático parado está muy condicionada por la carga vertical, el ángulo de inclinación y la presión del neumático, principalmente. En un neumático en movimiento, esta distribución de la presión también se ve modificada por la histéresis del neumático, que desplaza el centro de presión hacia delante, generando resistencia a la rodadura. Al imponer un ángulo de deslizamiento, la distribución de la presión también se modifica por varias razones: la transferencia de carga lateral hace que algunas ruedas tengan más carga vertical que otras, y algunas zonas del neumático se adherirán a la carretera mientras otras deslizarán (teoría de *stick-slip*). Además, estas cargas modifican los mecanismos de la suspensión y la dirección, modificando los ángulos de caída y deslizamiento. Todo esto significa que, en condiciones típicas de conducción, la distribución de presiones en la zona de contacto de un neumático es bastante compleja, haciendo que algunas zonas trabajen más que otras. De esta manera, esas zonas que trabajan más duramente se calientan más.

La temperatura y la presión interna del aire están estrechamente relacionadas. Es habitual modelar el aire del neumático mediante la ecuación de los gases ideales considerando un volumen constante, de modo que la presión y la temperatura están directamente relacionadas. Así, la temperatura del aire del neumático afecta a la generación de fuerzas de contacto de la misma manera que lo hace la presión, pero de forma drásticamente diferente a como lo hace la temperatura de la banda de rodadura o de las capas internas del neumático.

Por ello, en el tercer trabajo del compendio de publicaciones de esta tesis, una de las aportaciones es la propuesta de un método para calcular un valor representativo de la temperatura de la superficie del neumático a partir de una serie de medidas para considerar los diferentes mecanismos implicados y estimar la máxima adherencia disponible. Conocer la adherencia máxima disponible es de gran interés para el control predictivo, ya que permite estimar hasta qué punto el neumático y la carretera pueden generar aceleraciones laterales para modificar la trayectoria del vehículo. Sin embargo, también es necesario saber cuánto tiempo se necesita para generar estas fuerzas. El segundo aspecto tratado en este tercer trabajo es el estudio de los parámetros de relajación lateral. Se incluyen en este grupo la rigidez lateral y la constante de tiempo del sistema o longitud de relajación.

Como se ha mencionado anteriormente, para un control predictivo eficaz del vehículo para realizar, por ejemplo, una maniobra evasiva (*lane-change maneuver*), es necesario conocer el sistema que se va a controlar con la mayor precisión posible. Los parámetros más críticos son probablemente la fuerza lateral máxima que puede generar el neumático, la relación entre el ángulo del volante y la fuerza lateral generada, y el tiempo que tarda en generarse esta fuerza. Los parámetros asociados a estos tres efectos son el coeficiente de fricción lateral máximo, la rigidez lateral y la longitud de relajación, respectivamente. Los dos últimos son los dos parámetros que caracterizan a un sistema lineal de primer orden: la proporcionalidad y la constante de tiempo. En la dinámica de vehículos, esta constante de tiempo del sistema de primer orden suele sustituirse por la longitud que recorrería el vehículo, denominada longitud de relajación, que algunos autores consideran un valor constante.

Así, este último trabajo analiza también la influencia de la velocidad del vehículo, la carga vertical, la presión del neumático y el valor representativo de la temperatura de la superficie en estos dos parámetros lineales. Se demostró que ciertas variables son las más relevantes en la generación de fuerzas laterales, siendo la más importante la carga vertical, seguida de la velocidad lineal del vehículo. Por otro lado, se comprobó que la presión y la temperatura no afectan tanto en el rango lineal del comportamiento lateral del neumático, a diferencia del rango no lineal donde la temperatura es muy relevante. Se propuso un modelo polinómico para estimar la longitud de relajación en el que la carga vertical afecta de forma cuadrática mientras que la velocidad longitudinal lo hace de forma lineal. En cuanto a la rigidez lateral, se observó que la fórmula establecida por Pacejka se ajusta perfectamente a los datos experimentales. Por lo tanto, este último trabajo permitió desarrollar modelos sencillos y de bajo coste computacional que permiten su implementación en sistemas de control para ser aplicados al control predictivo en vehículos, principalmente enfocados a las maniobras de evasión de obstáculos.

Así, esta tesis hace tres contribuciones principales al campo del conocimiento de la dinámica de los vehículos, avalándose cada contribución con una publicación en revista de alto impacto, que son:

- El análisis, el modelado, la simulación y la optimización de la configuración de la transmisión secundaria en una motocicleta, centrándose en la disposición óptima del piñón, el basculante y los ejes de las ruedas para maximizar la potencia en la rueda. Además, se justifica la necesidad de medir con la mayor precisión posible la velocidad angular de las ruedas para estimar qué fuerzas se generarán y cuándo se generarán.
- El desarrollo y la validación de un algoritmo nuevo que mide las velocidades angulares y las aceleraciones de forma precisa, de retraso conocido y controlable y computacionalmente barata. Estos encoders sin-cos son los más utilizados en los vehículos eléctricos y cada vez más en diferentes aplicaciones, ya que su uso se ha extendido enormemente a la vez que se ha reducido su coste.

- Análisis de los parámetros más influyentes en la generación de fuerzas laterales en los neumáticos. Se estudia la influencia de diversas variables de funcionamiento en la generación del máximo coeficiente de fricción lateral, proponiendo un modelo que considera una temperatura media de la banda de rodadura. Además, se analizan los parámetros de relajación y se estudian como un sistema lineal de primer orden, caracterizado por la constante de proporcionalidad y por el retardo temporal del sistema.

Todas estas contribuciones han sido publicadas en revistas de alto impacto revisadas por pares, lo que demuestra la relevancia y novedad del trabajo. Asimismo, se han abierto futuras líneas de investigación, incluyendo la implementación de estos desarrollos en el control de un vehículo de pruebas. Este vehículo se desarrolla actualmente en el grupo de investigación a través del proyecto ‘Sistema de frenado regenerativo basado en algoritmos bioinspirados’ (UMA18-FEDERJA-109). Esto permitirá seguir investigando sobre la seguridad activa en los vehículos y la eficiencia energética, dos temas de gran interés para la sociedad.

CONTENTS

Acknowledgments	5
Abstract	9
Summary	11
Resumen	25
Contents	39
1 Introduction	1
1.1 Background.....	1
1.2 Problem statement.....	3
1.3 Literature review	4
1.4 Purpose of the study.....	19
1.5 Published works.....	22
2 Methods	25

2.1 Vehicle simulation	25
2.2 Angular speed measurement	27
2.3 Tire dynamics	28
3 Results and discussion	31
3.1 Vehicle simulation	31
3.2 Angular speed measurement	33
3.3 Tire dynamics	35
4 Conclusions	41
5 Future work	43
6 References	45
7 Appended papers	53
7.1 Paper #1	55
7.2 Paper #2	79
7.3 Paper #3	103

FIGURES

Figure 1. Measured variables for the four different methods mentioned. (M. Alcázar Vargas <i>et al.</i> , 2021)	8
Figure 2. Dual-Phase-Locked Loop (PLL) scheme for estimation of angular speed and acceleration. (M. Alcázar Vargas <i>et al.</i> , 2021)	10
Figure 3. Graphical demonstration of Pacejka's first Magic Formula. 12	
Figure 4. Four categories of possible types of approaches to develop a tire model. Reproduced from (Pacejka, 2012).	14
Figure 5. Scope of tire models, adapted from (Leister, 2015).	15
Figure 6. Thesis overview	20
Figure 7. Motorcycle model and genetic algorithm optimization explained (Alcazar <i>et al.</i> , 2020).	26
Figure 8. Angular speed measurement sensors. Left: SKF VKBA 6634. Right: Kistler Roadyn P625.	27
Figure 9. Ingeniería Mecánica Málaga (IMMa) Flat trac with speed sensors depicted. (M. Alcázar Vargas <i>et al.</i> , 2021)	28
Figure 10. Arrangement of temperature sensors.	29
Figure 11. Linear velocity of the vehicle and wheel axle and equivalent linear velocity of the contact point (Alcazar <i>et al.</i> , 2020).	32

Figure 12. Errors that can occur in the measurement of sin—cos encoder signals (Manuel Alcázar Vargas *et al.*, 2021).34

Figure 13. Relaxation length for different vertical loads and longitudinal speeds. Experimental data and fitted data (Alcázar Vargas *et al.*, 2022).....36

Figure 14. Friction coefficient against temperature (Alcázar Vargas *et al.*, 2022).....37

Figure 15. Test vehicle.44

ABBREVIATIONS

ABS: Anti-lock braking system

TCS: Traction control system

ESP: Electronic stability program

MF: Magic formula

PMSM: Permanent magnet synchronous motor

GPS: Global positioning system

TPMS: Tire pressure monitoring system

IMMa: Ingeniería mecánica Málaga

PCB: Printed circuit board

1 INTRODUCTION

1.1 BACKGROUND

Vehicle safety systems have always been of great interest. Today, three types of safety systems can be distinguished. Primary or active safety systems try to prevent an accident from occurring (ABS, TCS, etc.); passive or secondary safety elements reduce the severity of an accident (seat belts, airbags, etc.); and tertiary safety systems prevent aggravating events after an accident (automatic engine shutdown). The trend is to progressively oblige manufacturers to incorporate most of these systems on both four-wheeled and two-wheeled vehicles, where applicable.

Improvements in active safety have been shown to significantly reduce the number and severity of road accidents (Dirección General de Tráfico, 2021). However, these systems still have much potential for improvement, especially with the revolution that is taking place with autonomous or semi-autonomous vehicles.

Many research groups are working on the improvement of active safety in vehicles, especially on road type determination (Shi *et al.*, 2018), (Castillo *et al.*, 2015), tire dynamics (Riehm *et al.*, 2018), tire-road interaction (Acosta, Kanarachos and Blundell, 2017) and the development of control algorithms

(Pérez *et al.*, 2018). Along these lines lie almost all the improvements in active safety that have been developed in recent years.

A more precise knowledge of tire behavior directly leads to improved active safety in vehicles and, more specifically, in traction control and braking systems. This is because the forces that allow a ground vehicle to follow the desired trajectory and modify its speed are the ones that arise between the tire and road.

The research group where the dissertation was carried out has worked extensively in the study of tire characteristics (Castillo Aguilar *et al.*, 2017), (Ortiz Fernández, 2005), road type detection algorithms (Cabrera *et al.*, 2018) and advanced control systems related to traction and braking systems (Cabrera Carrillo, 2003; Castillo *et al.*, 2017; Pérez *et al.*, 2018). Thus, the fundamental line of the research group and the dissertations being developed within it are based on the improvement of active safety in vehicles, focusing on:

- Modeling of complex dynamic systems.
- Parameter estimation.
- Modeling of the tire and the variables that influence tire-road contact.
- Development of advanced and robust control algorithms for real-time systems.

This dissertation fits within the first three aspects, publishing a paper on each of them, leaving the last one as future work. Interest in this topic arises from the observation that tire models increasingly include thermal parameters, but without specifying how temperature influences contact dynamics. Specifically, Michelin, in the documentation of its TameTire model (Durand-Gasselin *et al.*, 2010; Grob, Blanco-Hague and Spetler, 2015), justifies the need to investigate the influence of tire temperature by feedback from F1 engineers from the McLaren team in 2001. The quote reads:

“Tyre temperature is known to have a significant effect on tyre characteristics with maximum performance only available in a small temperature band. The current model (Pacejka), which is called by many of the simulations used to analyse car performance, takes no

account of temperature effect. This is due to an inability to model the thermal behaviour of a tyre"

Although the quote is twenty years old, the subject is still being researched, as there is currently no universally accepted model to account for the influence of temperature on tire dynamics. In addition to temperature, speed also strongly influences the generation of forces in the contact patch, with no universally accepted theory either.

1.2 PROBLEM STATEMENT

It is known that, a priori, the better the knowledge of the system to be controlled, the better the controller will be. In fact, the modeling of physical systems has two main applications. The first is to estimate the state in which a system will be from a set of inputs and outputs: stress state of a mechanical element when loads are applied, temperature that an object will reach when it is heated after a specific time, weather predictions, etc. The second is to optimize controllers by including knowledge of the plant.

This way, the better the knowledge one has of a system, the better one can predict and control its behavior. Therefore, to improve active safety in vehicles, it is necessary to model all the agents involved in the best possible way. This problem is immense, ranging from psychological studies of the driver, state of the road, deterioration of vehicle elements, visibility, etc. In this dissertation, only the mechanical systems involved in generating contact forces between the road and tire are studied. This field of knowledge, known as tire dynamics, is probably the most uncertain area in vehicle dynamics.

Therefore, this work addresses three problems, each associated with one of the three publications supporting this dissertation. The first one is the correct modeling of the drivetrain of a vehicle, specifically of a high-performance motorcycle. Next, and following the results obtained in the first work, another study is carried out on the measurement of angular speeds in wheels, proposing an algorithm that optimizes this measurement using sin-cos sensors, which are increasingly used. The third and last work analyses the influence of several variables, such as vertical load, linear velocity,

temperature and pressure on some of the most critical parameters in tire lateral dynamics, such as the maximum friction coefficient, cornering stiffness and relaxation length.

1.3 LITERATURE REVIEW

This section contains the literature reviewed in the articles that support the dissertation and some other references related to these topics. This section has been divided into subsections, each of them on a specific topic. An attempt has been made to follow the order of the articles although this has not always been possible. In addition, the importance of each topic is highlighted.

1.3.1 Multibody dynamics and vehicle dynamics

There is a great deal of literature on multibody dynamics, since it is a well-established subject. Vehicular dynamics belongs to multibody dynamics, with some particularities. When a multibody system modeling problem is posed, the first thing that has to be established is the type of coordinates to be used, usually depending on the nature of the problem. They are divided into two main groups: independent coordinates and dependent coordinates. In the former, the number of coordinates equals the number of unknowns, so a system of differential equations is obtained. The disadvantage they present is that, apart from elementary problems, modeling with these coordinates becomes very complicated, making it virtually impossible to use them in real multibody systems. The latter, the dependent coordinates, use more coordinates than degrees of freedom of the system. Therefore, it is necessary to impose kinematic constraints, resulting in systems of differential-algebraic equations. This increases the computational cost of solving the system but greatly simplifies its modeling.

Within the dependent coordinates, there are mainly three types: relative coordinates, reference point coordinates and natural coordinates. A more complete description can be found in books by Jalon and Bayo (Garcia de Jalon and Bayo, 1994), Shabana (Shabana, 2020) and Haug (Haug, 1989).

Basically, *relative coordinates* are the most appropriate ones for open chain systems, which are very common in the field of robotics and biomechanics. On the other hand, reference point coordinates and natural coordinates are more common in closed-chain systems. Most multibody simulation packages employ *reference point coordinates* because the modeling of the system is more easily automated from a software point of view. It is necessary to define three coordinates for the position of each solid in space and at least three other coordinates for its spatial orientation. The spatial orientation is more complex to determine because, if Euler angles are used, the singularity of the gimbal lock may occur. Therefore, more and more multibody dynamics software programs employ quaternions to indicate spatial orientation. This way, to indicate the position of a solid, it is necessary to use seven coordinates. In the case of using rotation matrices, the number of components increases even more. ADAMS and Simscape Multibody are among the multibody dynamics software programs that use these coordinates.

On the other hand, *natural coordinates* lead to smaller systems, although the modeling process is not that automatic. Therefore, general-purpose software does not typically use these coordinates although they are well suited for modeling systems that share the same topology, such as vehicular dynamics systems. Among the advantages of natural coordinates, the following can be highlighted (De Jalon, 2007):

- The constraints imposed by almost all kinematic pairs can be written in simple algebraic expressions.
- The constraint equations are easily understood by the reader and easily modifiable in case of changing the topology or configuration of the mechanism.
- The results are obtained in absolute coordinates, so the visualization of the solids is straightforward.
- Typically, fewer coordinates are used than in the case of reference point coordinates, so the systems to be solved are smaller.

- Usually, the mass matrix is constant, so it is not necessary to explicitly model Coriolis or inertial forces.
- The manual programming and implementation for its computational resolution are much simpler than in the other cases, this being the most important advantage of this type of coordinates.

Once the coordinates have been described and the choice has been justified, it is time to solve the system. As indicated, unless independent coordinates are used, the system of equations to be solved is of the differential-algebraic type since the dynamic constraints lead to differential equations and the kinematic constraints to algebraic ones. Thus, the differential equations obtained are of second order in most mechanical engineering problems of regular dimensions (excluding particle dynamics and astrophysics). Therefore, to homogenize the system, it is usually necessary to differentiate the algebraic equations twice and, in doing so, information is lost. This information must be preserved, so there are several methods, among which the augmented Lagrange method (Bayo and Ledesma, 1996) stands out. This method replaces the kinematic constraints, such as a constant length between two points belonging to a rigid solid, by a spring-damper that maintains that distance constant. Therefore, the constraint is rewritten in terms of second-order differential equations. Another advantage is that this method allows one to determine the force exerted by the constraint.

As for integrators, there is a multitude of integrators of first-order differential equations. Therefore, it is necessary to transform the system of second-order differential equations into a first-order one. To do so, the number of variables is doubled: now the positions and velocities are unknowns. Thus, the first derivative of the variables will be the velocities and accelerations.

The selection of the optimal integrator is not trivial, a subject still being studied extensively. Selecting one type of integrator or another mainly depends on the stiffness of the problem. Shampine has done much work on this subject, being the primary reference author in the MATLAB help documentation. (Shampine and Gordon, 1975; Shampine, 1994; Shampine and Reichelt, 1997).

Within the field of multibody dynamics, one of the main applications, and the one that is of interest in this dissertation, is vehicle dynamics. Within vehicular dynamics, different complete motorcycle models can be found. Among them, the following two can be highlighted, both being spatial (3D):

- The model published by Sharp and Limebeer in 2001, written in independent coordinates (Sharp and Limebeer, 2001). This model, slightly modified, is used by the Bikesim software.
- The model published by Cossalter and Lot in 2003 uses natural coordinates (Cossalter and Lot, 2003). It is implemented in the FastBike program.

These models are responsible for simulating and studying the behavior of the vehicle. One of the key aspects in ground vehicles with pneumatic tires is the generation of contact forces between the tire and road. This aspect, known as *tire dynamics*, is one of the fundamental topics of this dissertation and is therefore analyzed in a separate section.

1.3.2 Angular speed measurement

One of the critical parameters of ground vehicles is the angular speed of the wheels. It is especially interesting because it is the main input to traction control (TCS), braking (ABS) and stability (ESP) systems. The fundamental reason is that a tire rotating much faster or much slower than it would if it were simply rolling will generate a high longitudinal force at the expense of not generating lateral forces. In other words, the vehicle will lose its steerability. Therefore, in traction control systems, it is necessary to determine whether the wheel is spinning at an abnormally high speed. The opposite is true for braking control applications: it is necessary to measure low angular speeds to determine whether the wheel is still rotating or if it has already locked up.

Currently, the sensors used in angular speed measurement on wheels are of the incremental encoder type (Robert Bosch GmbH, 2007; Reif, 2014). The main characteristic of these sensors is that they provide a digital output whose frequency is proportional to the angular speed. These sensors can be magnetic

or optical, signal processing being similar in both cases. Currently, there are basically two methods to calculate the angular speed from the signal of these sensors. These methods are the *M-method* and the *T-method*. In addition, there are two derived from these, the *MT-method* and the *divisionless MT-method*. Figure 1 shows a scheme indicating the measurement performed in each method.

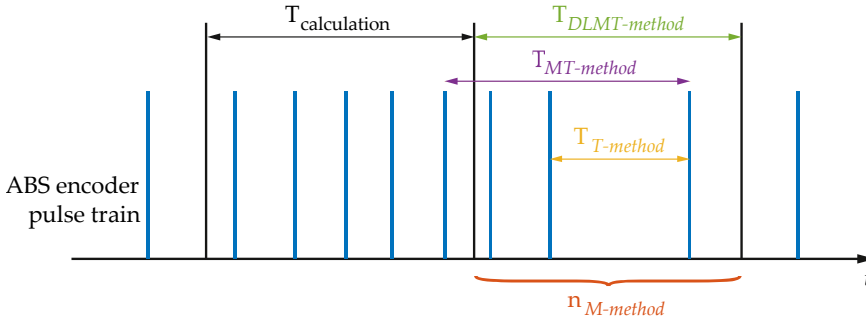


Figure 1. Measured variables for the four different methods mentioned. (M. Alcázar Vargas *et al.*, 2021)

The first method, the M-method, is based on measuring the number of pulses that enter in a given period of time. The computational cost is the lowest, but the accuracy at low speeds is very poor. In addition, if the sensor generates few pulses per revolution, it is necessary to leave more time between readings for more pulses to enter, so the delay in the measurement is greater. At very low speeds, for example, if, on average, 10.5 pulses enter in the calculation period, sometimes 10 and sometimes 11 will enter, so the error (or noise) at the output will be approximately 10%. To reduce it, it is necessary to filter the output, which is equivalent to delaying the measurement.

On the other hand, the T-method is based on measuring the time between pulses. This way, the time between pulses is counted, and the last value is stored in memory. The speed is updated with the last stored value. In this method, it is necessary to consider several aspects. The first is that what is being counted are ticks of a clock, so the time measurement is discrete.

The second problem is that any error in the manufacturing process of the sensor, such as slight differences between pulse widths, translates into noise in the reading. In addition, to obtain the speed, it is necessary to perform a

division, so the computational cost increases considerably. The last of the relevant problems is that only the time between the last two pulses is considered, which has the following drawback. For example, if the speed is being updated at a frequency of 100 Hz (10 ms) and pulses enter every 100 μ s, considerable noise at the output is expected due to the asymmetry of the edges. Moreover, it is not necessary to update the velocity with the last edge and neglect all the flanks entered in the last calculation period, since this information is being lost, which greatly cleans the velocity signal of the output. For all these reasons, the MT-method arises, which combines the advantages of the M and T methods.

This way, the MT-method (Ohmae and Tachikawa, 1982) takes into account, not the time between the last two pulses, but the time between the pulse that entered just before the beginning of this period and the last pulse. In addition, it considers the periods in which no pulses enter. However, it is more complex to program and has a slightly higher computational cost than the T-method (and much higher than the M-method) (Kavanagh, 2001).

To avoid performing the division in the MT-method, with the fundamental objective of implementing this method on FPGAs, Hace proposed the divisionless MT-method (DLMT-method), slightly modifying the MT-method at the expense of losing some accuracy (Hace and Curkovic, 2018; Hace and Čurković, 2018; Hace, 2019).

In any case, none of the methods can generate more information than the sensor can provide. Therefore, for applications where it is required to properly measure speeds where sensors of this type fail, magnetic sensors with many more pulses per revolution are normally used at a much higher cost, generally intended for research purposes.

On the other hand, resolvers have traditionally been used in industry to determine angular position. This type of sensor generates an electrical signal in a coil coupled to a rotating element that is transmitted to two coils by transformer action. This way, the output of these elements will be proportional to the angle between the rotor and the stator. More specifically, if these coils are arranged perpendicularly to each other, the outputs will be proportional to the sine and cosine of the relative angle between the rotor and the stator. A high-frequency electrical carrier signal is required to magnetically couple the rotor and the stator. Subsequently, in the post-

processing of the signals, it is necessary to eliminate this carrier signal from the output signals, leaving only the sine and cosine signals. These types of sensors are large, robust, heavy and expensive. They are usually used in harsh industrial applications, whose main purpose is to determine the angle between two elements. As for determining the angular speed, literature is very scarce on methods for its estimation, the main one being the Dual-Phase-Locked Loop method. This method, belonging to the so-called closed loop, basically works as follows (Figure 2). The measured sine and cosine signals are multiplied by the estimated ones, so that the trigonometric identity $\sin^2(x) + \cos^2(x) = 1$ will be fulfilled. This output goes through a PI controller and then through an integrator to close the first control loop. This way, just before the integrator, the output will be the angular speed if the controller is well-tuned. A similar scheme is performed in the case one wants to obtain the angular acceleration, hence the *dual* name. This method is the most common one for estimating velocity and angular accelerations for resolvers. Different versions of this algorithm and its advantages and disadvantages can be consulted in the following works: (Al-Emadi, Ben-Brahim and Benammar, 2014; Liu and Wu, 2018).

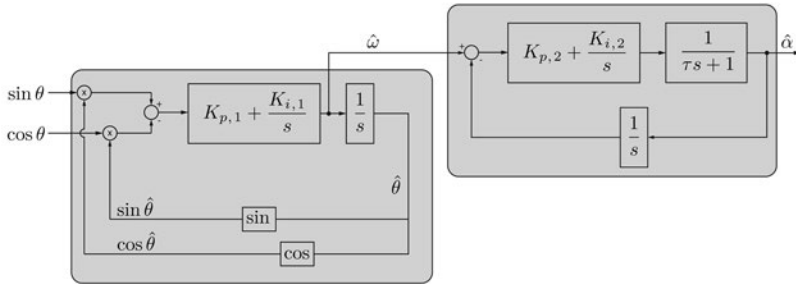


Figure 2. Dual-Phase-Locked Loop (PLL) scheme for estimation of angular speed and acceleration. (M. Alcázar Vargas *et al.*, 2021)

Other authors have used either the opened loop methods, which seek to obtain the position and differentiate it (Sarma, Agrawal and Udupa, 2008) or extended Kalman filters to determine the velocity although it is necessary to adjust various parameters for its correct operation (Harnefors, 1996).

1.3.3 Tire dynamics

The field of tire dynamics is undoubtedly the broadest field and the one with the most current theories of all those addressed in this dissertation. A historic milestone in this field is the publication of what later became known as Pacejka's Magic Formula, in 1987, in the article '*Tyre Modelling for Use in Vehicle Dynamics Studies*' (Bakker, Nyborg and Pacejka, 1987). Until then, theories on the generation of contact forces between the tire and road were varied and imprecise. Bakker, Nyborg and Pacejka proposed a purely empirical model that fitted the experimental data very accurately. This first formulation, although much simpler than the present one, allowed from a few parameters to estimate both the longitudinal force, F_x , and the lateral force, F_y , and the self-aligning moment, M_z . Their first formulation was (1):

$$y = D \cdot \sin[C \cdot \text{atan}(B \cdot x)] \quad (1)$$

Analyzing it in detail and seeing its intrinsic power is pretty interesting. Figure 3 shows a graphical interpretation of this very first formulation. Given an input, x , a multiplier factor B is applied and a representative angle $\text{atan}(Bx)$ is obtained. This arctangent function gives much importance to small values, linearizing the zero region. It also saturates the output at very high values. If one were to apply the sine function to this angle, one would obtain a sigmoid function, where the identity $\sin[\text{atan}(Bx)] = Bx / \sqrt{(Bx)^2 + 1}$ is satisfied. This function, quite common in fields such as artificial intelligence, approximates the behavior of tires poorly since it lacks a maximum. To solve that problem, one multiplies that angle $\text{atan}(Bx)$ by a factor C , which is usually slightly greater than unity. This way, the angle, now $C \cdot \text{atan}(Bx)$, can indeed exceed $\pi/2$, so function $D \cdot \sin[C \cdot \text{atan}(Bx)]$ has a maximum. Moreover, as long as $1 < C < 2$ is satisfied, the function will have a maximum, but it will never cross zero again, which is valid for longitudinal and lateral forces. In the case of the self-aligning moment, by ensuring that $C > 2$, the sign is reversed beyond a certain slip angle. The latter phenomenon, which is demonstrated experimentally, has been complicated to explain with physical models, being solved in this way with Pacejka's formulation.

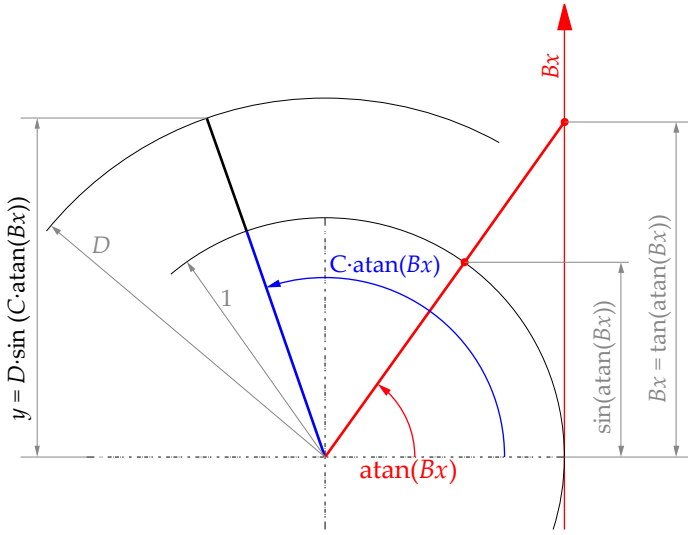


Figure 3. Graphical demonstration of Pacejka's first Magic Formula.

It should be noted that equation (1) is not the original magic formula. It has been used here for didactic purposes since the author of this dissertation has not found a reasoned explanation of the origin of this formula; in literature it is simply indicated as *magic*. The formulation of the first paper on this subject replaced the term Bx by a somewhat more complex expression, introducing an additional term, E . Thus, the original expression was the following (2):

$$y = D \cdot \sin[C \cdot \operatorname{atan}\{Bx - E(Bx - \operatorname{atan} Bx)\}] \quad (2)$$

Furthermore, horizontal and vertical offsets were added to this function to include conicity and ply steer although these terms are assumed to be zero in virtually all cases. Successive modifications of Pacejka's formula have complicated it, mainly by making each coefficient dependent on several variables. Some authors (Farroni and Sakhnevych, 2022) call parameters B , C , D and E *macrocoefficients*, while the polynomial terms that constitute these coefficients are called *microcoefficients*. This terminology has become necessary since, in the latest version, characterizing a tire requires in the order of 100 microcoefficients. As a result, vehicle simulation software now allows tire data to be entered in a plain text file, usually with a '.tir' extension, in which all these coefficients are grouped. Obtaining these coefficients is costly and

outside the conditions where the tire has been tested, the reliability of the results cannot usually be guaranteed. For a more in-depth analysis on this subject, it is recommended to consult the book that is undoubtedly the reference: *tire and vehicle dynamics* by Professor Pacejka (Pacejka, 2012). After the edition of the book, Siemens acquired this tire model, currently named Siemens Simcenter MF-Tyre/MF-SWIFT package.

It can safely be said that the state of the art in tire dynamics is the magic formula. Moreover, the magic formula is an excellent solution for vehicle design and, more specifically, for commercial vehicle suspension and steering designs. It just so happens that there are applications where the magic formula does not stand out against its competitors. These applications include the following:

- Racing applications.
- Tire design and manufacturing.
- Driving simulators.
- Development of active safety systems in vehicles.
- Research on friction generation mechanisms between the tire and road.

As a result, various models have emerged that attempt to understand and explain how tires work. There are two extremes when it comes to classifying tire models: empirical and physical models. The former, to which the magic formula belongs, adjust experimental data by mathematical expressions, more or less complex, to predict behavior under certain conditions. The latter tries to understand the physical principles behind tires to determine, through mathematical expressions with physical meaning, the forces and moments that tires will generate. No model is purely empirical or physical. The magic formula, although fundamentally empirical, does have physical parameters, such as parameter D , which represents the maximum friction coefficient, or the product of BCD , which represents the stiffness (longitudinal or cornering) of the tire. The so-called physical models, such as some that are supposedly used in driving simulators, are not entirely physical either, as they require empirical adjustments of specific parameters. Therefore, although the empirical-physical classification is the most widely used, it is not the only one. A graph analyzing this classification can be found in (Pacejka, 2012). Figure 4 is a reproduction of the one in the book:

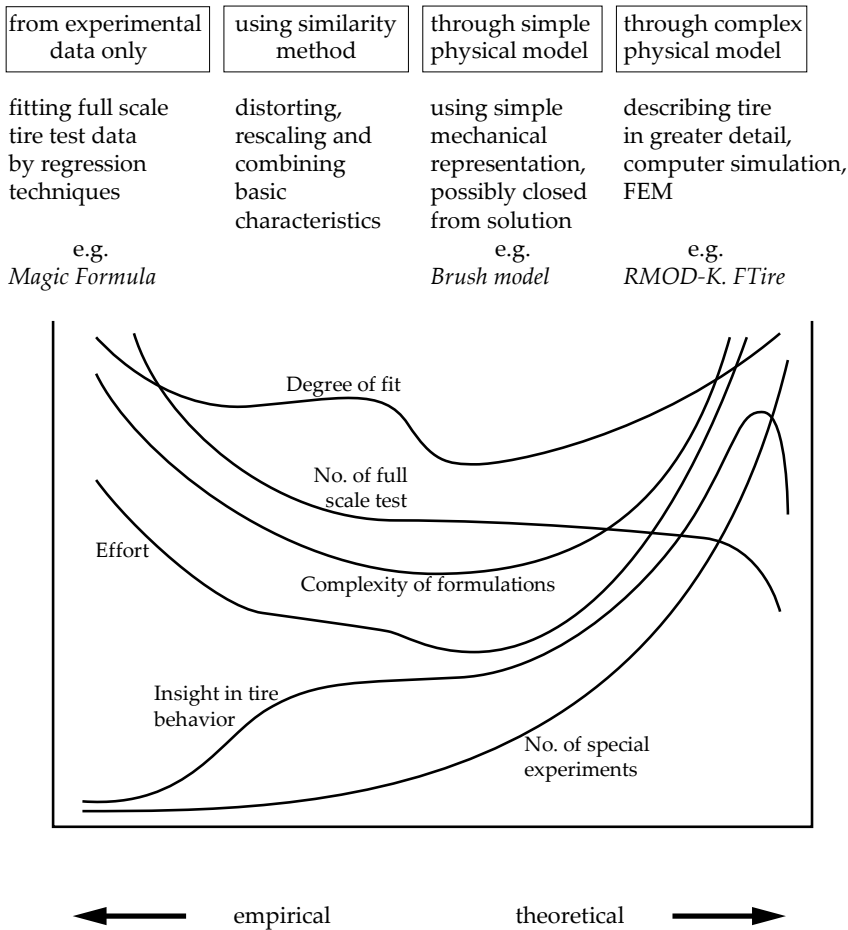


Figure 4. Four categories of possible types of approaches to develop a tire model. Reproduced from (Pacejka, 2012).

This figure is quite illustrative, giving a broad view of tire models, their advantages and their disadvantages. It can be seen that both empirical and physical models fit pretty well. However, a large number of real experiments are necessary for the former and the latter. A large number of specific experiments are required. In both cases, the formulations are complex and the effort is high. In the case of physical models, the effort is even greater than for empirical models although, in theory, it is possible to understand the internal behavior of tires. Intermediate models, either semi-empirical or simple

physical models, have the advantages of requiring fewer tests, fewer parameters and less effort, at the expense of a worse system modeling.

Another aspect studied in tire dynamics is the behavior of tires at high frequency. High frequency is understood as vibrations induced by irregularities in the road as well as fast maneuvers in which longitudinal or lateral slip varies rapidly and vibrations that occur due to unbalance in the wheel when it rotates at high speed. Depending on the phenomenon to be captured, it is necessary to consider one model or another. Thus, Pacejka's formula was adapted for low-frequency irregularities and renamed SWIFT: *Short Wavelength Intermediate Frequency Tire Model*. This new model allows us to simulate situations where input variables, such as slip angle, longitudinal slip, or vertical load, vary with low frequency. Leister (Leister, 2015) proposed a scheme, as shown in Figure 5, where different models and their frequency ranges are observed.

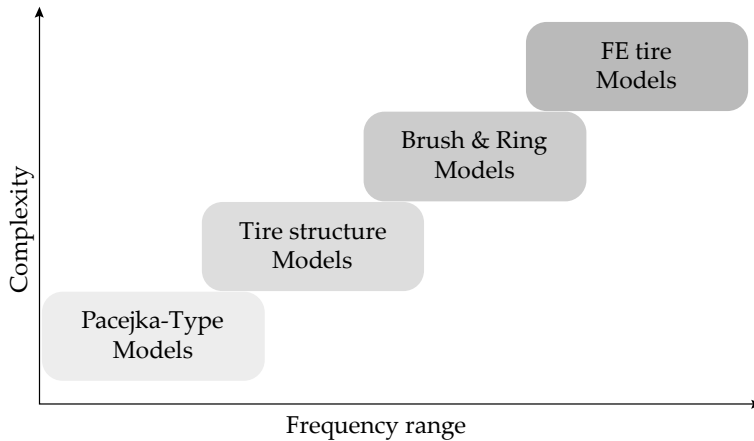


Figure 5. Scope of tire models, adapted from (Leister, 2015).

In order to try to capture the phenomena occurring at medium and high frequency, it is necessary to analyze tires from a physical point of view.

Among the physical models, probably the simplest one is the *brush model*. This model considers the tire a rigid disk, to which *bristles* of known stiffness and friction coefficient are connected at the perimeter. Friction is modeled

using Coulomb's law, either with a single coefficient or distinguishing between static and dynamic friction. The problem has an analytical solution if the expression for the normal pressure in the contact patch is simple and known. This model, which is easily understandable, shows the approximate behavior of what happens in the tire contact patch.

Moreover, under certain conditions with an analytical solution, the computational cost of solving the tire-road interaction is just evaluating the expression. This model allows, for example, determining the approximate longitudinal and lateral force against slip curves. In addition, in the case of using a friction model with two coefficients, it is able to capture the maximum one that occurs in the previously mentioned curves. It can simulate combined cases directly without using complex functions to fit data obtained in pure cases. As references on this topic, although it has been addressed in literature for a long time, it is advisable to consult the book by Pacejka (Pacejka, 2012) and the works by Romano (Romano *et al.*, 2019; Romano, Bruzelius and Jacobson, 2021), specifically the book titled '*Advanced Brush Tyre Modeling*', published in 2022 (Romano, 2022).

In an intermediate category between physical and empirical models, one could include the *TameTire* model, developed by Michelin (Fevrier and Fandard, 2008; Durand-Gasselin *et al.*, 2010; Grob, Blanco-Hague and Spetler, 2015). This model arose in 2001 from F1 teams' need to consider thermal effects, as tire behavior is known to be strongly affected by temperature. Although it sits between physical and empirical models, this model will be discussed in more detail at the end of this chapter, along with those of driving simulators.

As for complex physical models, there is a multitude of them. Perhaps the best known is the *FTire*, developed by Professor Gisper (Gisper, 2016; Hofmann and Gisper, 2017), and the *RMODK*, developed by Oertel and Fandre (Oertel and Fandre, 2001, 2009). The former, the *FTire*, is based on modeling a flexible structure of the carcass and the belt. This joint is performed by nonlinear spring-dampers, both in-plane and out-of-plane. This makes it possible to work at high frequency and the authors claim that using this model makes it possible to understand the operation of tires. As for the *RMODK* model, it is essentially a simplified finite element model. It analyzes the deformations of the carcass and the belt, allowing adaptation to road irregularities and considering high frequencies. These last two models also

allow modeling the contact forces at low and even zero speed, something that the magic formula cannot do. They can also estimate the resisting moment in parking maneuvers and consider the inversion of the sign of the self-aligning moment. On the other hand, many experiments are necessary to characterize tires and the computational cost is much higher than the one of empirical models.

From the point of view of physical modeling, the highest level of complexity is finite element modeling. During the first years of the 21st century, especially in the journal '*Tire, Science and Technology*', numerous studies were published on this subject. These include the following: (Ebbott *et al.*, 1999; Peters, 2001; Hall, 2004; Jeong *et al.*, 2007; Wang *et al.*, 2012). Finite element analysis has the disadvantage that it is necessary to know the tire in detail and the computational cost of solving it makes it unfeasible to be used in real-time applications. However, it is beneficial for vehicle manufacturers and particular applications, such as: designing tread patterns, studying the arrangement of internal fibers in tire manufacturing, internal heat transfer in the rubber, wear and, perhaps most important, generating simplified finite element models for use in real-time applications.

From this last point and going a bit beyond conventional publications in peer-reviewed journals, one can look at how driving simulators model tires. In this section, two models used by widely recognized driving simulators and the Michelin simulation package, Tametire, will be discussed. All these models are black boxes since the developers seek to sell the software, not to explain its inner workings. In any case, they do indicate, roughly speaking, their general operation. These three models have been grouped since their operation is similar: they perform three simultaneous simulations: carcass deformation, generation of contact forces in the contact patch and heat generation and transfer. The first simulator analyzed, Project Cars 2, uses the *SETA tire model* (Studios, 2014). The other simulator analyzed is iRacing, which employs *New Tire Model V7* (NTM V7) (Kaemer, 2018). Both simulators perform the mechanical simulation of carcass deformation and pressure distribution in the contact patch from the results obtained in the finite element analysis. For thermal analysis of the tire, a finite volume analysis is performed where the generated, evacuated and conducted heats inside the tire are considered. As for the generation of contact forces in the patch, this is the aspect that almost all models are most cautious about. They indicate that it affects temperature, wear, sliding speed, vertical load, camber, etc... but do

not indicate how. Tametire indicates that friction against temperature has a Gaussian shape and that friction is affected by sliding velocity. This approach is similar to the one proposed by Kelly and Sharp in one of the most relevant works on this subject (Kelly and Sharp, 2012).

1.4 PURPOSE OF THE STUDY

The purpose of this dissertation is to conduct research on pneumatic tires, aiming to apply this knowledge to improve active safety in vehicles. First, the dynamics of the drivetrain of motorcycles is studied to determine the influence of the arrangement of the engine sprocket and the swingarm in the power transmitted to the wheel. Furthermore, the modeling of multibody dynamic systems and their possibility to implement them in real-time systems is evaluated.

Subsequently, given the importance of correctly measuring slip speed in vehicle control systems, an angular speed measurement algorithm is developed using these increasingly common sin-cos encoders. These sensors generate two signals indicating the sine and cosine of the relative angle between the rotor and the stator. The advantage is that these analog signals can be acquired at any desired frequency and are continuous and differentiable. In addition, they fulfill certain trigonometric relationships with each other. All this makes it possible to determine low angular speeds much more accurately, a problem often encountered in braking control algorithms. In addition, obtaining the acceleration is simple, the delay in the speed estimation is known and controllable and the adjustment of the algorithm is straightforward, requiring the tuning of practically one single parameter. Moreover, these sensors are used in PMSM control, increasingly present in the automotive industry.

Finally, the influence of several parameters on lateral dynamics of tires is studied. Vehicle linear speed, vertical wheel load, pressure and temperature distribution on the tire tread are among these parameters. Two new models are proposed. The first one is for the relaxation length as a function of vertical load and linear speed of the vehicle, while the other is for the maximum lateral friction coefficient as a function of one single representative value of tread temperature.

In this dissertation, the vehicle drivetrain is analyzed, the measurement of determinant variables in the generation of friction forces is improved and models are proposed to determine the relaxation length and the maximum friction coefficient. Therefore, this dissertation contributes to improving

active safety systems in vehicles, a topic of great interest to society. Figure 6 shows the overview of the thesis.

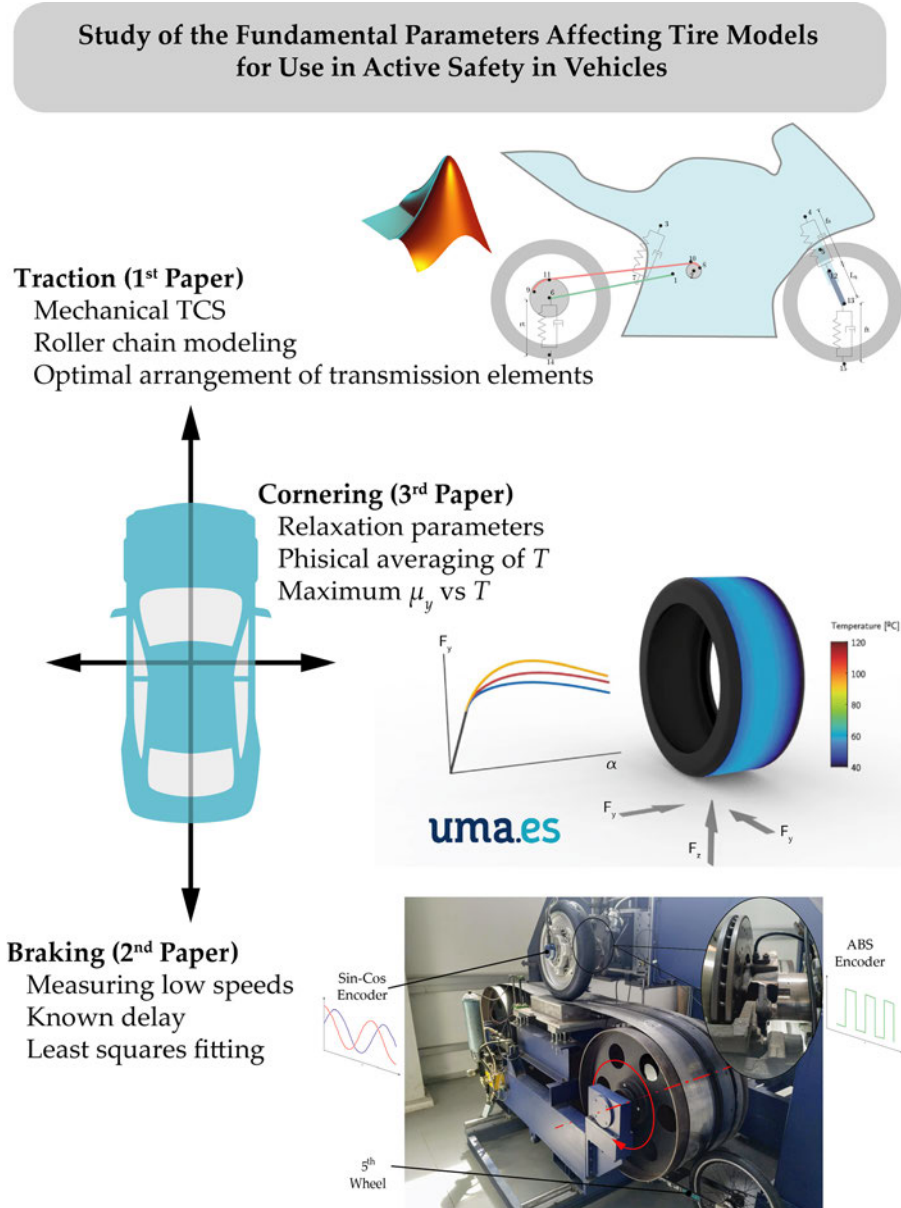


Figure 6. Thesis overview

1.5 PUBLISHED WORKS

According to MDPI and CRediT (Contributor Roles Taxonomy) classification, the author of the thesis has contributed to the articles as follows:

- Articles [1–3]: Conceptualization, Data curation, Investigation, Methodology, Software, Visualization, Writing – original draft.
- Articles [4, 6–7]: Writing – review & editing.
- Articles [5, 8]: Software.

In conference papers, all authors have contributed equally.

1.5.1 Appended papers

[1] Alcazar Vargas, M. *et al.* (2020) “Motorcycle final drive geometry optimization on uneven roads,” *Mechanism and Machine Theory*, 144, p. 103647. doi: 10.1016/j.mechmachtheory.2019.103647.

[2] Alcázar Vargas, M. *et al.* (2021) “A novel method for determining angular speed and acceleration using sin-cos encoders,” *Sensors (Switzerland)*, 21(2), pp. 1–21. doi: 10.3390/s21020577.

[3] Alcázar Vargas, M. *et al.* (2022) “Modeling of the Influence of Operational Parameters on Tire Lateral Dynamics,” *Sensors*, 22(17), p. 6380. doi: 10.3390/s22176380.

1.5.2 Related papers

[4] Pérez Fernández, J. *et al.* (2019) “Low-cost FPGA-based electronic control unit for vehicle control systems,” *Sensors (Switzerland)*, 19(8). doi: 10.3390/s19081834.

- [5] Carabias Acosta, E. *et al.* (2020) “Modeling of Tire Vertical Behavior Using a Test Bench,” *IEEE Access*, 8, pp. 106531–106541. doi: 10.1109/ACCESS.2020.3000533.
- [6] Pérez Fernández, J. *et al.* (2021) “A biological-like controller using improved spiking neural networks,” *Neurocomputing*, 463, pp. 237–250. doi: 10.1016/j.neucom.2021.08.005.
- [7] Pérez Fernández, J. *et al.* (2021) “Coevolutionary Optimization of a Fuzzy Logic Controller for Antilock Braking Systems under Changing Road Conditions,” *IEEE Transactions on Vehicular Technology*, 70(2), pp. 1255–1268. doi: 10.1109/TVT.2021.3055142.
- [8] Carabias Acosta, E. *et al.* (2023) “Non-intrusive determination of shock absorber characteristic curves by means of evolutionary algorithms,” *Mechanical Systems and Signal Processing*, 182(July 2022). doi: 10.1016/j.ymssp.2022.109583.

1.5.3 Conference papers

- [9] Pérez Fernández, J. *et al.* (2019) “Influence of System Dynamics in Brake Blending Strategies for Electric Vehicles,” in *IAVSD Symposium on Dynamics of Vehicles on Roads and Tracks*, pp. 1555–1564. doi: 10.1007/978-3-030-38077-9_178.
- [10] Alcazar Vargas, M. *et al.* (2019) “Influencia de la temperatura y la velocidad en la dinámica del contacto neumático-carretera,” in FEIBIM (ed.) *XIV Congreso Iberoamericano de Ingeniería Mecánica, realizado en la ciudad de Cartagena*. Cartagena, Colombia: FEIBIM, pp. 1–4. Available at: <https://www.researchgate.net/publication/342466756>.
- [11] Alcázar Vargas, M. *et al.* (2021) “Estimación de la resistencia a la rodadura en neumáticos mediante banco de ensayos de tracción compresión,” in *XXIII Congreso Nacional de Ingeniería Mecánica*. Jaén, Spain: Universidad de Jaén, pp. 1–6.
- [12] Castillo Aguilar, J. J. *et al.* (2021) “UMA Racing Team: Una experiencia en participación en competiciones universitarias. - [UMA Racing Team: An experience in participation in university competitions],” in *Innovaciones*

docentes en tiempos de pandemia. Madrid: Servicio de Publicaciones Universidad, pp. 268–273. doi: 10.26754/CINAIC.2021.0052.

[13] Alcazar Vargas, M. *et al.* (2021) “Aplicación de las T.I.C. para optimizar el trabajo en equipo en el ámbito de la ingeniería industrial,” in *8º Congreso Internacional sobre Buenas prácticas con TIC*. Málaga, Spain: Universidad de Málaga, pp. 562–566.

[14] Pérez Fernández, J. *et al.* (2021) “Influence of tire dynamics on a braking process with ABS,” in *XIV Congreso de Ingeniería del Transporte (CIT 2021)*. Burgos, Spain: Universidad de Burgos, pp. 3517–3519. doi: <https://doi.org/10.36443/9788418465123>.

[15] Pérez Fernández, J. *et al.* (2022) “Reward-modulated learning using spiking neural networks for vehicle lateral control,” in *15th International Symposium on Advanced Vehicle Control*. Tokio, Japan: Society of Automotive Engineers of Japan.

2 METHODS

This section briefly describes the methods used in each of the papers that support the dissertation. Therefore, they are grouped into three categories, each belonging to a corresponding publication.

2.1 VEHICLE SIMULATION

The process of the first paper, which deals with multibody dynamics, is described below. The problem has first been identified: the arrangement of the final drive elements determines the power delivered to the wheel. More specifically, it has been observed that the *squat* value in most racing motorcycles is around unity. Subsequently, the system has been modeled, emphasizing the power transmission through the chain, something multibody simulation software programs model as a constant speed ratio. For this purpose, natural coordinates have been used due to all the advantages described in the previous section. Finally, at least as far as multibody simulation is concerned, the equations have been integrated using integrators of the predictor-corrector type (Adams-Bashforth-Moulton). In addition, it was observed that the tire model implemented in the simulations modified the results considerably. Therefore, the most realistic model among those

described by Pacejka was implemented: the fully nonlinear transient model. This, among other reasons, justified the need for further research on tire models. As a novelty, in addition to demonstrating the importance of a correct arrangement of the final drive elements, this configuration has been optimized to maximize power transmission. In a way, a mechanical traction control has been designed. A scheme of the modeled mechanical system and the optimization process can be seen in Figure 7.

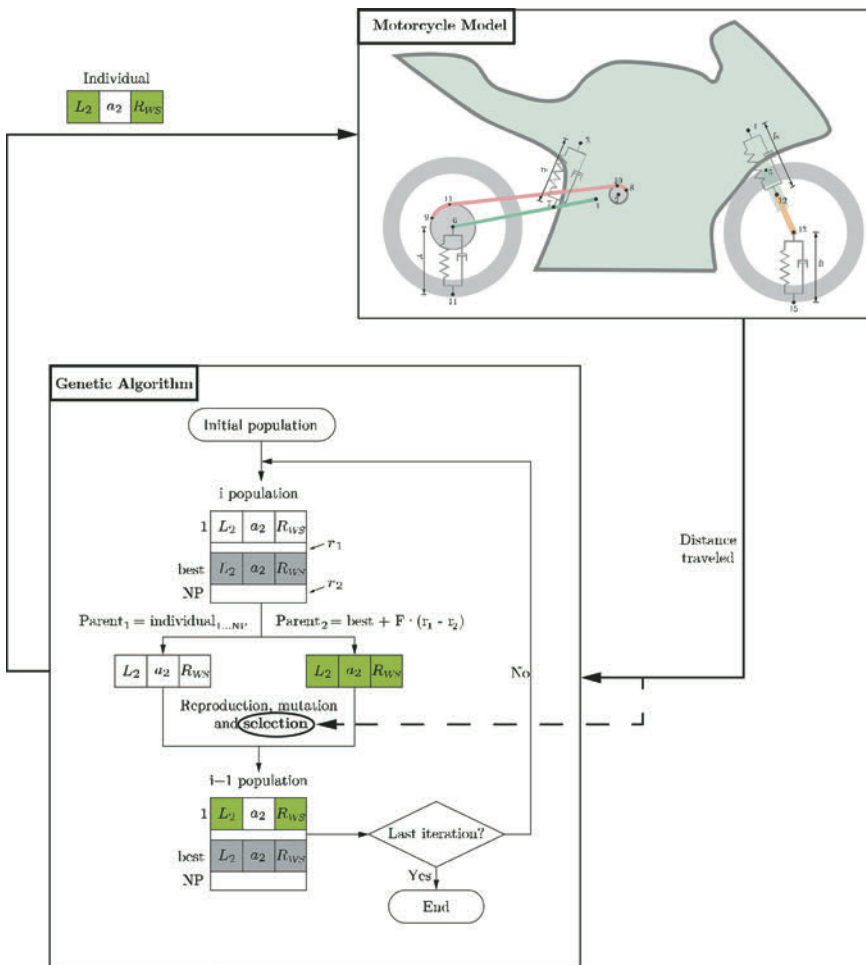


Figure 7. Motorcycle model and genetic algorithm optimization explained (Alcazar *et al.*, 2020).

2.2 ANGULAR SPEED MEASUREMENT

As for the angular speed measurement, two angular measurement sensors have been installed on the tire test bench. The first is an ABS magnetic encoder included within the wheel bearing, reference SKF VKBA 6634. The second sensor is included inside the Kistler Roadyn P625 wheel force transducer. Both sensors can be seen in figure 8:



Figure 8. Angular speed measurement sensors. Left: SKF VKBA 6634. Right: Kistler Roadyn P625.

This rim needs the sine and cosine signals to provide the output of the three forces and the three torques acting on the wheel with respect to the xyz reference system. Acquiring the signals from both sensors and the rest of the signals needed to control the tire testing machine is made with the National Instruments™ sbRIO-9637 real-time controller and the company's LabVIEW software. The research group has entirely manufactured the tire test bench, while the author of this dissertation and Dr. Perez have recently modified much of its hardware and software. Figure 9 shows a photograph of the test bench where the installed sensors can be seen.

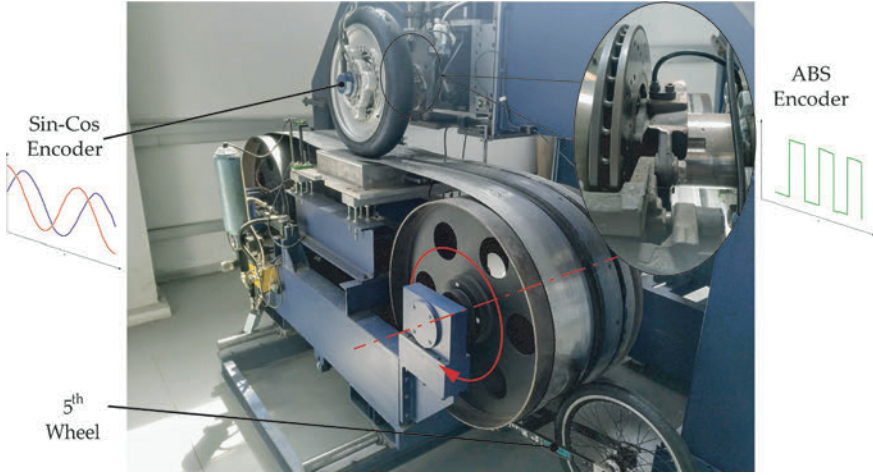


Figure 9. Ingeniería Mecánica Málaga (IMMa) Flat trac with speed sensors depicted. (M. Alcázar Vargas *et al.*, 2021)

This machine has led to the completion of several doctoral dissertations, contracts with companies, and research articles.

2.3 TIRE DYNAMICS

The same machine explained in the previous section has been used for tire modeling. For tire surface temperature measurement, Melexis MLX90614 infrared sensors have been used. These sensors measure a wide temperature range with high accuracy. Figure 10 shows the arrangement of the temperature sensors. It is vital to ensure that the distance between the sensors and the measured surface is controlled. As the sensor measures a more extensive area, the greater the distance to the object.



Figure 10. Arrangement of temperature sensors.

In order to implement this temperature measurement technology in more vehicles, it has been designed as follows. First, a microprocessor reads the signals sent by the sensors through the I²C protocol. These signals are the surface temperature and the temperature at which the sensor is located. The median of the sensor temperatures is taken to measure the ambient temperature. As for object temperature, each value is considered separately. Then, the message is encoded by the CAN protocol, having two advantages. First, it does not have any distance communication problems. The second is that it is the most common communication protocol in vehicles.

This developed product can be used in vehicles with more or fewer sensors. If one wants to use it in motorcycles, which lack a flat tread, the temperature sensors can be arranged on a flexible PCB and attached to the fender.

3 RESULTS AND DISCUSSION

This section will present the results of the three papers that constitute the dissertation and their discussion. Emphasis is placed on the discussion of the results since the results have already been presented in each article.

3.1 VEHICLE SIMULATION

The *results* of the first work are threefold. Firstly, determining the importance of a correct angular speed measurement to estimate the slip speed as evidenced by tire models (see figure 11). Secondly, demonstrating the importance of correctly arranging the final drive elements to maximize the power transmitted from the engine to the wheel. Thirdly, optimizing this arrangement to maximize the power transmitted to the wheel, acting as a mechanical traction control system.

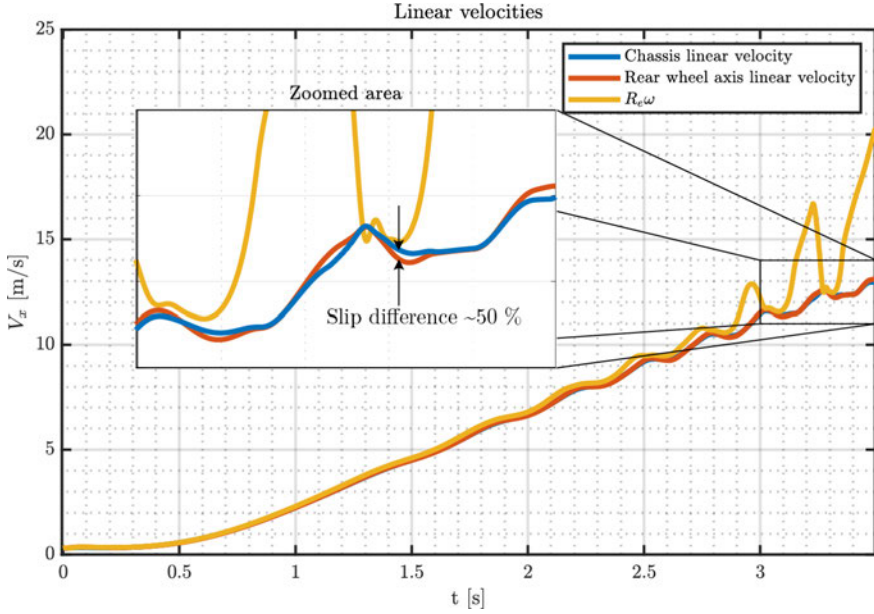


Figure 11. Linear velocity of the vehicle and wheel axle and equivalent linear velocity of the contact point (Alcazar *et al.*, 2020).

As for the *discussion of the results*, it should be said that, with our current knowledge, the system would have been modeled in Simscape Multibody, which belongs to MATLAB Simulink. This software, which has evolved enormously in recent years, has the advantages of multibody simulation software and allows the full power of MATLAB Simulink. Therefore, modeling the final drive, the most complex task since this kinematic pair is not one of the usual ones in system modeling, could have been written as a MATLAB function. As for the integrator, the programming of a variable step integrator is much more complex than the one of constant step. In fact, the efficiency of the simulation performed in the paper supporting this dissertation is limited because of the need for using a small time step for the times when the stiffness of the problem is high (starting from standstill and tire impacts). All this would have been simplified and optimized using variable step integrators available in Simulink. In addition, Simscape Multibody has recently implemented the latest versions of Pacejka's magic formula (Furlan, 2022), so there is no need to program it. As a final point to note, having performed the optimization by genetic algorithms in MATLAB,

the iterative simulation-optimization process is perfectly integrated. This work led to the next one since it demonstrated the importance of adequately measuring the angular speed of the wheels, given that the slip speed is the most important parameter in the generation of friction.

3.2 ANGULAR SPEED MEASUREMENT

As in the previous section, the *results* can be found in the corresponding article. The main result of this work is the development of a low computational cost algorithm for the measurement of angular velocities and accelerations from the sine and cosine signals coming from this type of encoder. It has two advantages over the most used method for measuring angular speed from this type of encoder (Dual-Phase-Locked Loop (PLL), Figure 2). The first is that tuning the algorithm parameters is much simpler: it is only necessary to determine the number of points to be used for the Savitzky-Golay filter and the order of the polynomial although this will usually be in the order of 3 or 4. Second, the signal delay is half the number of points used multiplied by the sampling time, so it is known and controllable.

As for the *discussion of the results*, both behave the same in measuring high angular speed from incremental encoders, making the computational cost of the M-method lower. In contrast, the incremental encoders do not work at low speeds, so a proper angular speed measurement, either by using the PLL method or the one proposed in this work, will be better. What happens is that these sensors have two drawbacks.

The first is that the correct installation of the encoder magnet on the axis of rotation is decisive since errors caused by sensor misalignment condition the measurement (Figure 12).

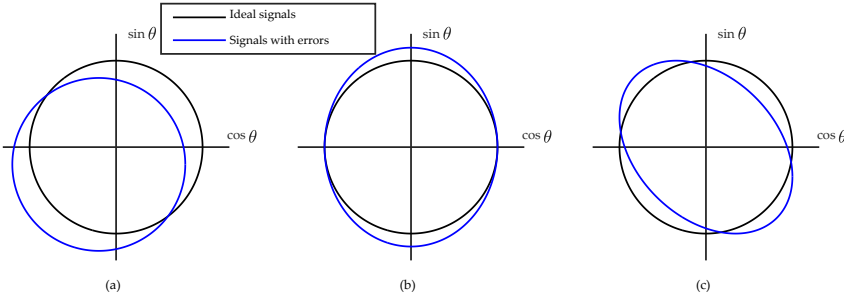


Figure 12. Errors that can occur in the measurement of sin—cos encoder signals (Manuel Alcázar Vargas *et al.*, 2021).

The left figure shows offset errors in both signals, causing the mean value of both signals to be non-zero. The figure in the center shows different gains for each signal, since the maximum values of both signals are not equal. The right one shows a lag in the acquisition of the signals, so that the theoretical circle degenerates into an ellipse whose inclination depends on the speed of rotation of the sensor. These three errors do not occur in isolation but are usually combined. These errors can indeed be corrected, but ideally, they should be avoided, as they worsen the quality of the measurement.

The other disadvantage is that for incremental encoders, it is only necessary to acquire a single *digital* signal (two signals in case one wants to determine the direction of rotation). For sin-cos encoders, the acquisition of two *analog* signals is required. In addition, manufacturing wheel bearings with the incremental encoder already integrated inside is widespread, so the cost of this sensor has decreased considerably. In any case, the trend is undeniably towards the electrification of vehicles and, for the time being, the motors used are of the PMSM type. Hence, if the speed ratio between the rotational speed of the electric motor and the rotational speed of the wheel is known, which in the absence of clutches and differentials is trivial, the rotational speed of the wheel can be known using this method. Therefore, it is a relevant contribution to this field as it expands knowledge and allows, under certain conditions, avoiding the measurement of angular speed on wheels from incremental encoders (also known as ABS encoders). In addition, the signal acquisition and processing of the cosine and sine encoders are

required to control the PMSMs, so there is no need to install additional sensors or acquire extra signals.

3.3 TIRE DYNAMICS

As indicated above, tire dynamics is the most varied field of those studied in this dissertation. In contrast to multibody dynamics, where there are several theories, one or the other being used to solve the problems more efficiently depending on what one is trying to study, in tire dynamics there are multitudes of theories, but none that stand out. One only has to look at the racing world: there are many more problems associated with tires, more uncertainty, and more variability than in any other aspect, including multibody dynamics. Having stated this, the *results* of this dissertation in the field of tire dynamics are presented. However, it is advisable to consult the publication that supports the dissertation related to this topic for further information.

Two critical aspects of lateral tire dynamics have been studied. The first is the relaxation parameters, namely cornering stiffness and relaxation length. These two parameters characterize a first-order system with a time and gain constant. As for the cornering stiffness, the model proposed by Pacejka fits experimental data perfectly, so no other is proposed. On the other hand, the relaxation length is strongly dependent on vertical load and linear velocity. Therefore, a 2D polynomial model is proposed (3):

$$L_{Fy} = c_1 + c_2 V_x + c_3 F_z + c_4 F_z^2 \quad (3)$$

Which fits correctly, as shown in Figure 13:

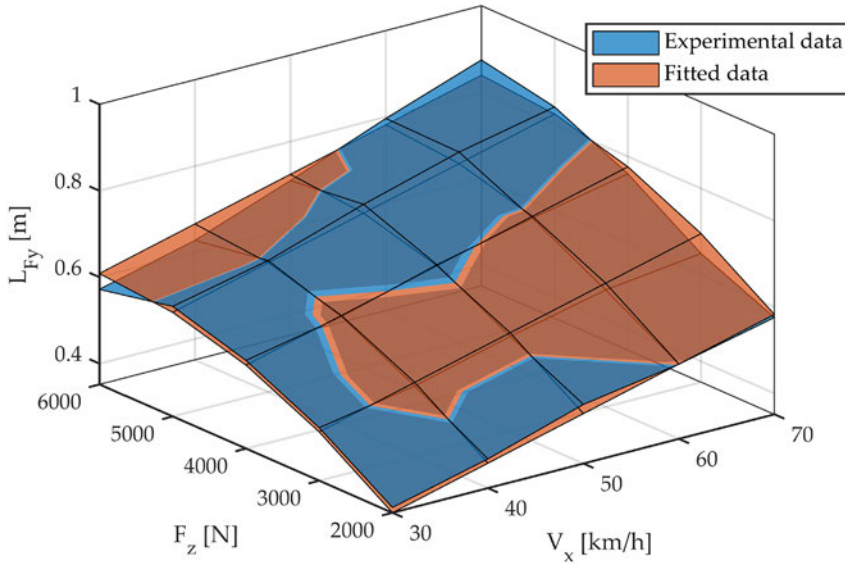


Figure 13. Relaxation length for different vertical loads and longitudinal speeds. Experimental data and fitted data (Alcázar Vargas *et al.*, 2022).

On the other hand, the maximum coefficient of lateral friction generated between the tire and road is studied. This, together with the relaxation parameters, allows for predictive control since it is possible to know the maximum acceleration a vehicle can experience and how long it will take to be generated. In order to estimate the maximum friction coefficient, a PCB with nine infrared sensors has been developed and manufactured to measure the surface temperature of the tire sidewalls (four sensors) and the one of the tread (five sensors). This board costs approximately 100 €. Therefore, it is a low-cost PCB. In addition, a method has been proposed to take a representative value of the temperature. This is also novel since it is usual to read only one temperature value or, if more than one measurement is taken, to simply average it arithmetically. No method for assigning weights to each measured temperature has been found in literature. The published article proposes a method, based on the fundamental mechanisms of heat generation

and transmission, which allows working with a single representative value of the surface temperature. Equation (4) and figure 14 show the results:

$$\mu_y(T) = \mu_y^{\max} + \left[1 - \cosh\left(\frac{T_{\text{averaged}} - T_{\text{opt}}}{T_{\text{dispersion}}}\right) \right] \quad (4)$$

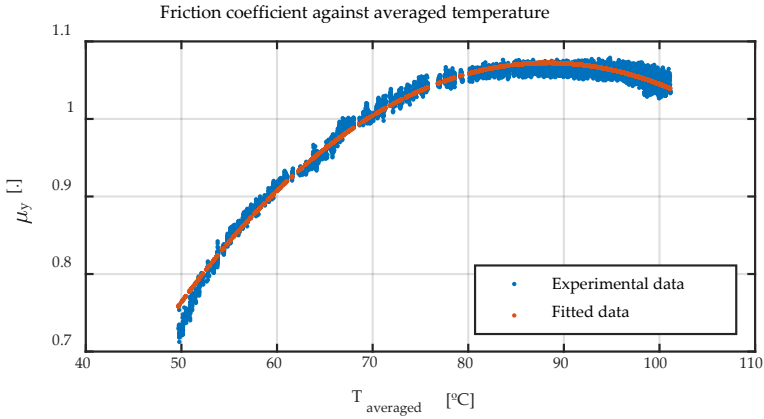


Figure 14. Friction coefficient against temperature (Alcázar Vargas *et al.*, 2022).

As for the *discussion of the results*, there is more to discuss in this section. It is important to highlight that a sensor has been designed and manufactured to measure surface temperatures at moderately high frequencies (~ 2 Hz). Also, a method has been proposed to weigh the temperature measurements more realistically. Finally, a simple method has been proposed to estimate the relaxation length from easily measurable or estimated variables. However, the advances in the field of tire dynamics are very scattered, there is very little information available in literature and the physical principles of friction generation, although assumed to be known, are not easily shapeable. The increasing trend is to use tire modeling software, which are black boxes, requiring many input parameters that are virtually impossible to have in a commercial vehicle. Whatever the tire model, they all require the slip speed (or slip ratio) to be known and this parameter is very complex to determine in commercial vehicles. Measuring the instantaneous speed of the vehicle is not

simple and the reason is as follows. During smooth driving, the speed varies slowly and the tires work in a linear range so there is no major complication. It is possible to work with a single value of cornering stiffness and longitudinal stiffness and simulation and control work more than adequately.

Problems arise when the maneuvers performed are aggressive or severe. This is the case of emergency brakings or lane-change-maneuvers to avoid obstacles. This is where it is crucial to know what forces the tire can generate and how and when they are generated. In all these cases, linear speed varies very rapidly. Hence, GPS data is of no use and the estimation of linear speed of the vehicle from the angular speed of the wheels is not valid either since the slip ratio is high. There are several data fusion techniques, using accelerometers and Kalman filters, as well as other techniques, but none of them prevail. In instrumented vehicles, a fifth wheel is used, with a negligible slip level, allowing one to know the velocity of the vehicle (speed and direction). Another type of sensor, *Correxit*, measures velocity very precisely but at a cost that is unaffordable in a commercial vehicle.

Even if the problem of slip speed measurement is solved, many other variables affect it. One of them, perhaps the most important one, is the road type. This field, the estimation of road types, is also very interesting and is being extensively investigated. Most tire models focus on studying asphalt in good, clean and dry conditions. The racing industry and the simulation video game industry have made great efforts to have reliable models of the behavior of racing tires on clean, dry tracks. These models are not publicly available, so very little is known. When the asphalt is not excellent, the models usually adopt two approaches. Either penalty factors are applied, the so-called *lambdas* of Pacejka's magic formula or several groups of roads are modeled: dry asphalt, wet asphalt, concrete, snow, etc., and one type of road or another is assumed.

In the work of this dissertation, we wanted to analyze the influence of temperature on tire dynamics. This subject is known to be decisive, especially in racing fields. As an example, in Figure 12, it can be seen that the friction coefficient increases by 50% ($0.70 \rightarrow 1.05$) when the tire is at its optimum temperature, these results coming from a street tire. What happens is that talking about temperature as if it was a scalar parameter is usually a mistake.

Within a tire, there is a very uneven temperature distribution as long as the vehicle has been driven more or less aggressively. The reason for this heterogeneity is that heat is generated in certain areas, depending on the type of maneuver performed. Heat conduction in a tire is very low, so the temperature is not homogenized quickly. In addition, measuring the surface temperature of the tire is relatively simple to perform. It is also easy to measure the air temperature since some TPMS sensors provide it directly at a very low cost. What happens is that the temperature of the innermost layers of the tire is not easily measurable. Some models allow us to estimate it using heat transfer equations and finite volume methods. In competition, it is usually measured by lightly pinching the tire with a sensor to read the temperature of the somewhat innermost layers since the surface temperature cools it down very fast as it is complicated to conduct heat into the tire. In addition, the state of the contact patch is very complex.

Some models assume one type, generally parabolic, to obtain an analytical solution of the models and explain the friction generation mechanisms. The brush model is one of them although there are more. However, the pressure distribution is exceptionally complex, affected by camber and slip angles, tire pressure, wear level or road type. Even the angular speed of the wheel affects it since the mass of the tread, when rotating at high speed, generates a similar effect to that of increasing air pressure. This effect can be seen in F1 cars, where ground clearance is decisive for the correct functioning of the aerodynamic elements.

On the other hand, some companies have invested vast amounts of money, time, and experimentation in obtaining results that allow them to validate their models for use in competition or to sell simulation software (either video games or simulators). These models are obviously not public. Therefore, as a discussion of the results obtained in this work, we have contributed to shedding some light on this field. The results allow us to get to know the system better and develop more efficient controllers. However, there is still much work to be done and published.

4 CONCLUSIONS

This work presents an introduction to the problems studied, a bibliographic analysis and explanations of the methods followed to achieve the objectives and the results. Also, as a contribution to the articles supporting the dissertation, the results of the works have been discussed further. The scope, the drawbacks that have been found and the impact that the dissertation might cause have been discussed. The dissertation is set in the context of the modeling of tires and some subsystems associated with the wheels, aiming to improve active safety in vehicles. The dissertation is an important contribution to the work developed by the *Ingeniería Mecánica Málaga* (IMMa) research group for many years, where research in vehicle dynamics is carried out. The conclusions drawn from the three journal papers that support the dissertation and from the dissertation itself are listed below:

- The importance of correctly modeling the system has been highlighted since it allows capturing phenomena that are impossible to capture with simpler models. Specifically, the first work of the dissertation demonstrates a relationship between the position of the engine sprocket with respect to the swingarm axis and the power transmitted to the wheel in a motorcycle. In addition, a deficiency in multibody dynamics modeling programs when studying power transmission by belt or chain (kinematically equivalent) is revealed.

- An optimal solution to the final drive geometry of a motorcycle is proposed, maximizing power transmission in a pure traction case scenario and considering only longitudinal dynamics.
- Given the need to know the instantaneous angular speed of the wheels in a vehicle and the trend towards electrification, an algorithm for measuring this parameter has been designed and proposed. This algorithm allows measuring angular speed and accelerations at a low cost, with a known and controllable delay. In addition, it is only necessary to tune two simple parameters for the correct operation of the algorithm.
- An in-depth literature review of tire models has been carried out. The trends have been observed, both those arising from academia and those from the automotive and videogame industries. The complexity of studying friction between tires and roads has been explained and it has been made clear that it is a field in continuous research. In addition, the difference between simulation and control-oriented approaches has been explained. In the former, useful for the design of suspension or steering systems as well as for entertainment, all the input variables to the models are known: vertical load, speeds, angles, temperature distribution, wear level, etc. These models are highly complex, computationally expensive and usually require much more data than is available for an active safety controller in a commercial vehicle. On the other hand, approaches toward active safety performance need few reliable variables whose delay and uncertainty are known. In this line, a simple method has been proposed for the dynamic characterization of tires in cases of pure lateral dynamics. The first one considers the surface temperature distribution of the tire to estimate the maximum lateral friction the tires can generate. The second one models the delay of the system (relaxation length) as a function of the vertical load and vehicle speed. All this can be applied to vehicle control systems, thus improving active safety in vehicles.

5 FUTURE WORK

The dissertation has deepened in aspects related to tires and wheels. This field is still a tool for improving control systems in vehicles, whether for active safety, energy efficiency or racing purposes. Aspects such as suspension, road type estimation, energy efficiency in the drivetrain of an electric vehicle or brake blending algorithms have not been discussed throughout the document. All these aspects are being studied by the research group to which the author of the dissertation belongs. Other researchers in the group are working on these aspects, which complement perfectly with those studied in this dissertation. Two evident future lines can be distinguished.

The first one is to continue studying *tire dynamics*. Aspects such as pure or combined longitudinal dynamics, longitudinal relaxation lengths for the optimization of ABS systems and, above all, tire characterization testing on real tracks are key aspects fascinating to investigate. Thus, bench tests of longitudinal and combined tire characterization, similar to those performed in the last article of this dissertation will be carried out as soon as possible. For those who are on track, it will be necessary to wait for the test vehicle for a few months until the research group has finished manufacturing it (Figure 15):

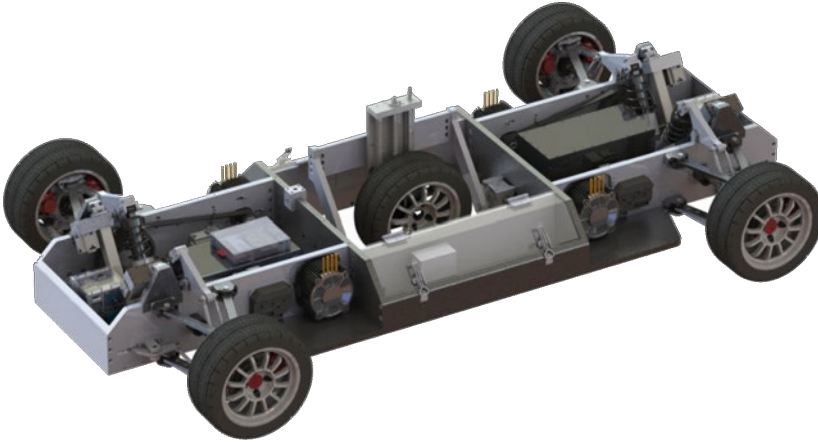


Figure 15. Test vehicle.

Once the test vehicle is available, it will be possible to work on the other research line, which is *active safety in vehicles* and *energy efficiency*. The development of traction control algorithms in electric vehicles is an intriguing topic. So is the study of braking distribution between friction braking and regenerative braking. *Road type estimation* is perhaps the most striking aspect and the most studied subject by the scientific community of all those indicated in this section. All this will be possible to investigate in the coming months and years, thanks to the knowledge acquired by the research group members, including the author of this dissertation.

6 REFERENCES

- Acosta, M., Kanarachos, S. and Blundell, M. (2017) "Road Friction Virtual Sensing: A Review of Estimation Techniques with Emphasis on Low Excitation Approaches," *Applied Sciences*, 7(12), p. 1230. doi: 10.3390/app7121230.
- Al-Emadi, N., Ben-Brahim, L. and Benammar, M. (2014) "A new tracking technique for mechanical angle measurement," *Measurement: Journal of the International Measurement Confederation*, 54, pp. 58–64. doi: 10.1016/j.measurement.2014.04.011.
- Alcazar, M. *et al.* (2020) "Motorcycle final drive geometry optimization on uneven roads," *Mechanism and Machine Theory*, 144, p. 103647. doi: 10.1016/j.mechmachtheory.2019.103647.
- Alcázar Vargas, Manuel *et al.* (2021) "A novel method for determining angular speed and acceleration using sin-cos encoders," *Sensors (Switzerland)*, 21(2), pp. 1–21. doi: 10.3390/s21020577.
- Alcázar Vargas, M. *et al.* (2021) "A Novel Method for Determining Angular Speed and Acceleration Using Sin-Cos Encoders," *Sensors (Basel, Switzerland)*, 21(2). doi: 10.3390/s21020577.
- Alcázar Vargas, M. *et al.* (2022) "Modeling of the Influence of Operational

- Parameters on Tire Lateral Dynamics,” *Sensors*, 22(17), p. 6380. doi: 10.3390/s22176380.
- Bakker, E., Nyborg, L. and Pacejka, H. B. (1987) “Tyre Modelling for Use in Vehicle Dynamics Studies,” *SAE Technical Paper Series*. doi: 10.4271/870421.
- Bayo, E. and Ledesma, R. (1996) “Augmented Lagrangian and mass-orthogonal projection methods for constrained multibody dynamics,” *Nonlinear Dynamics*, 9(1–2), pp. 113–130. doi: 10.1007/BF01833296.
- Cabrera Carrillo, J. (2003) *Modelización en banco de ensayo de sistema inteligente de frenado*. Universidad de Málaga.
- Cabrera, J. A. *et al.* (2018) “A procedure for determining tire-road friction characteristics using a modification of the magic formula based on experimental results,” *Sensors (Switzerland)*, 18(3). doi: 10.3390/s18030896.
- Castillo Aguilar, J. J. *et al.* (2017) “Optimization of an optical test bench for tire properties measurement and tread defects characterization,” *Sensors (Switzerland)*, 17(4). doi: 10.3390/s17040707.
- Castillo, J. *et al.* (2015) “Robust Road Condition Detection System Using In-Vehicle Standard Sensors,” *Sensors*, pp. 32056–32078. doi: 10.3390/s151229908.
- Castillo, J. *et al.* (2017) “Regenerative Intelligent Brake Control for Electric Motorcycles,” *Energies*. doi: 10.3390/en10101648.
- Cossalter, V. and Lot, R. (2003) “A Motorcycle Multi-Body Model for Real Time Simulations Based on the Natural Coordinates Approach,” *Vehicle System Dynamics*, 37(6), pp. 423–447. doi: 10.1076/vesd.37.6.423.3523.
- Dirección General de Tráfico (2021) “Balance de las cifras de siniestralidad vial 2020. Anexo estadístico,” p. 26.

- Durand-Gasselín, B. *et al.* (2010) "Assessing the thermo-mechanical TaMeTirE model in offline vehicle simulation and driving simulator tests," *Vehicle System Dynamics*, 48(SUPPL. 1), pp. 211–229. doi: 10.1080/00423111003706730.
- Ebbott, T. G. *et al.* (1999) "Tire temperature and rolling resistance prediction with finite element analysis," *Tire Science and Technology*, 27(1), pp. 2–21. doi: 10.2346/1.2135974.
- Farroni, F. and Sakhnevych, A. (2022) "Tire multiphysical modeling for the analysis of thermal and wear sensitivity on vehicle objective dynamics and racing performances," *Simulation Modelling Practice and Theory*, 117(January), p. 102517. doi: 10.1016/j.simpat.2022.102517.
- Fevrier and Fandard (2008) "Thermal and Mechanical Tyre Modelling," 110.
- Furlan, M. (2022) *MFeval*. Available at: <https://es.mathworks.com/matlabcentral/fileexchange/63618-mfeval> (Accessed: September 16, 2022).
- García de Jalon, J. and Bayo, E. (1994) *Kinematic and Dynamic Simulation of Multibody Systems*. New York: Springer New York. doi: 10.1007/978-1-4612-2600-0.
- Gipser, M. (2016) "FTire and puzzling tyre physics: Teacher, not student," *Vehicle System Dynamics*, 54(1), pp. 113–127. doi: 10.1080/00423114.2015.1117116.
- Grob, M., Blanco-Hague, O. and Spetler, F. (2015) "Tametire's testing procedure outside michelin," in *4th International Tyre Colloquium*. doi: 10.1115/1.2895925.
- Hace, A. (2019) "The improved division-less mt-type velocity estimation algorithm for low-cost fpgas," *Electronics (Switzerland)*, 8(3). doi: 10.3390/electronics8030361.
- Hace, A. and Curkovic, M. (2018) "A Novel Divisionless MT-Type Velocity

- Estimation Algorithm for Efficient FPGA Implementation," *IEEE Access*, 6, pp. 48074–48087. doi: 10.1109/ACCESS.2018.2867510.
- Hace, A. and Čurkovič, M. (2018) "Accurate FPGA-based velocity measurement with an incremental encoder by a fast generalized divisionless MT-type algorithm," *Sensors (Switzerland)*, 18(10). doi: 10.3390/s18103250.
- Hall, W. (2004) "Tire Modeling Methodology with the Explicit Finite Element Code LS-DYNA," *Tire Science and Technology*, 32(4), p. 236. doi: 10.2346/1.2186783.
- Harnefors, L. (1996) "Speed estimation from noisy resolver signals," (429), pp. 279–282. doi: 10.1049/cp:19960927.
- Haug, E. J. (1989) "Computer-Aided Kinematics and Dynamics of Mechanical Systems," *Allyn and Bacon*, (January 1989). Available at: <http://www.computer.org/csdl/proceedings/cmcsn/2012/4738/00/4738z014-abs.html%5Cnhttp://scholar.google.com/scholar?hl=en&btnG=Search&q=intitle:Computer-Aided+Kinematics+and+Dynamics+of+Mechanical+Systems.+Volume+I:Basic+Methods#1>.
- Hofmann, G. and Gipser, M. (2017) "FTire - Flexible Structure Tire Model," p. 64.
- De Jalon, J. G. (2007) "Twenty-five years of natural coordinates," *Multibody System Dynamics*, 18(1), pp. 15–33. doi: 10.1007/s11044-007-9068-0.
- Jeong, K. M. *et al.* (2007) "Finite Element Analysis of Nonuniformity of Tires with Imperfections," *Tire Science and Technology*, 35(3), pp. 226–238. doi: 10.2346/1.2768607.
- Kaemer, D. (2018) *Physics modeling NTM V7*. Available at: <https://www.iracing.com/physics-modeling-ntm-v7-info-plus/> (Accessed: June 9, 2022).

- Kavanagh, R. C. (2001) "Performance analysis and compensation of M/T-type digital tachometers," *IEEE Transactions on Instrumentation and Measurement*, 50(4), pp. 965–970. doi: 10.1109/19.948308.
- Kelly, D. P. and Sharp, R. S. (2012) "Time-optimal control of the race car: Influence of a thermodynamic tyre model," *Vehicle System Dynamics*, 50(4), pp. 641–662. doi: 10.1080/00423114.2011.622406.
- Leister, G. (2015) "The role of tyre simulation in chassis development – challenge and opportunity," in *4th International Tyre Colloquium*. Surrey, pp. 1–10.
- Liu, H. and Wu, Z. (2018) "Demodulation of angular position and velocity from resolver signals via chebyshev filter-based type III phase locked loop," *Electronics (Switzerland)*, 7(12). doi: 10.3390/electronics7120354.
- Oertel, C. and Fandre, A. (2001) "RMOD-K tyre model system," *ATZ worldwide*, 103(11), pp. 23–25. doi: 10.1007/bf03224524.
- Oertel, C. and Fandre, A. (2009) "Tire model RMOD-K 7 and misuse load cases," *SAE Technical Papers*, (April 2009). doi: 10.4271/2009-01-0582.
- Ohmae, T. and Tachikawa, M. (1982) "Microprocessor-Controlled High-Accuracy Wide-Range Speed Regulator for Motor Drives sponse , the detecting time is almost the same as that of the M," *I(3)*, pp. 207–211.
- Ortiz Fernández, A. (2005) *Desarrollo de técnicas experimentales en la modelización de neumáticos*.
- Pacejka, H. B. (2012) *Tire and Vehicle Dynamics*. 3rd ed. Elsevier.
- Pérez, J. et al. (2018) "Bio-inspired spiking neural network for nonlinear systems control," *Neural Networks*, 104, pp. 15–25. doi: 10.1016/j.neunet.2018.04.002.
- Peters, J. M. (2001) "Application of the Lateral Stress Theory for Groove Wander Prediction Using Finite Element Analysis," *Tire Science and*

- Technology*, 29(4), pp. 244–257. doi: 10.2346/1.2135242.
- Reif, K. (2014) *Brakes, Brake Control and Driver Assistance Systems - Bosch Professional Automotive Information*. Springer. doi: 10.1007/978-3-658-03978-3.
- Riehm, P. *et al.* (2018) “3D brush model to predict longitudinal tyre characteristics,” *Vehicle System Dynamics*, 3114, pp. 1–26. doi: 10.1080/00423114.2018.1447135.
- Robert Bosch GmbH (2007) *Bosch Automotive Electrics and Automotive Electronics*. 5th ed. Edited by R. B. GmbH. Springer. doi: 10.1007/978-3-658-01784-2.
- Romano, L. *et al.* (2019) “A novel brush-model with flexible carcass for transient interactions,” *Meccanica*, 54(10), pp. 1663–1679. doi: 10.1007/s11012-019-01040-0.
- Romano, L. (2022) *Advanced Brush Tyre Modeling*. SpringerBriefs in Applied Sciences.
- Romano, L., Bruzelius, F. and Jacobson, B. (2021) “Unsteady-state brush theory,” *Vehicle System Dynamics*, 59(11), pp. 1643–1671. doi: 10.1080/00423114.2020.1774625.
- Sarma, S., Agrawal, V. K. and Udupa, S. (2008) “Software-based resolver-to-digital conversion using a DSP,” *IEEE Transactions on Industrial Electronics*, 55(1), pp. 371–379. doi: 10.1109/TIE.2007.903952.
- Shabana, A. A. (2020) *Dynamics of Multibody Systems*. Cambridge University Press. doi: 10.1017/9781108757553.
- Shampine, L. F. (1994) *Numerical Solution of Ordinary Differential Equations*. 1st Editio. New York: Routledge. doi: <https://doi.org/10.1201/9780203745328>.
- Shampine, L. F. and Gordon, M. K. (1975) *Computer Solution of Ordinary*

Differential Equations: the Initial Value Problem. San Francisco: W.H.Freeman.

Shampine, L. F. and Reichelt, M. W. (1997) *The MATLAB ode suite*, *SIAM Journal of Scientific Computing*. doi: 10.1137/S1064827594276424.

Sharp, R. S. and Limebeer, D. J. N. (2001) "A Motorcycle Model for Stability and Control Analysis," *Multibody System Dynamics*, 6(2), pp. 123–142. doi: 10.1023/A:1017508214101.

Shi, Y. *et al.* (2018) "A practical identifier design of road variations for anti-lock brake system," *Vehicle System Dynamics*, 3114(May 2018), pp. 1–33. doi: 10.1080/00423114.2018.1467018.

Studios, S. M. (2014) *Handling Consultants Feedback Reports*. Available at: <https://wmdportal.com/> (Accessed: June 9, 2022).

Wang, Y. *et al.* (2012) "Finite Element Analysis of the Thermal Characteristics and Parametric Study of Steady Rolling Tires," *Tire Science and Technology*, 40(3), pp. 201–218. doi: 10.2346/TIRE.12.400304.

7 APPENDED PAPERS

The articles that support the dissertation are the following:

- [1] Alcazar, M. et al. (2020) "Motorcycle final drive geometry optimization on uneven roads," *Mechanism and Machine Theory*, 144, p. 103647. doi: 10.1016/j.mechmachtheory.2019.103647.
- [2] Alcázar Vargas, M. et al. (2021) "A novel method for determining angular speed and acceleration using sin-cos encoders," *Sensors (Switzerland)*, 21(2), pp. 1–21. doi: 10.3390/s21020577.
- [3] Alcázar Vargas, M. et al. (2022) "Modeling of the Influence of Operational Parameters on Tire Lateral Dynamics," *Sensors*, 22(17), p. 6380. doi: 10.3390/s22176380.

All of them are located in the first third of the list of their specialty in the JCR, so they add up to 3 points according to ANECA criteria. This satisfies the requirement of the University of Malaga, which demands at least 1 point according to ANECA criteria. The articles and their quality indicators are attached below.

7.1 PAPER #1

7.1.1 Journal article identification:

Title: Motorcycle final drive geometry optimization on uneven roads

DOI: 10.1016/j.mechmachtheory.2019.103647

Coauthors: J. Perez, J.E. Mata, J.A. Cabrera, J.J. Castillo

7.1.2 Quality indicators:

Editor: Elsevier

Journal: Mechanism and Machine Theory

Date of publication: 30 September 2019

Impact factor: 3.866 (JCR)

Quartile and position in its category: 18/137 (Q1) — Engineering, Mechanical

7.1.3 Published article



Contents lists available at ScienceDirect

Mechanism and Machine Theory

journal homepage: www.elsevier.com/locate/mechmachtheory

Research paper

Motorcycle final drive geometry optimization on uneven roads

M. Alcazar^{a,*}, J. Perez^a, J.E. Mata^b, J.A. Cabrera^a, J.J. Castillo^a^a Department of Mechanical Engineering, University of Málaga, Málaga 29071, Spain^b Department of Mechanical and Mining Engineering, University of Jaén, Jaén 23071, Spain

ARTICLE INFO

Article history:

Received 25 July 2019

Revised 19 September 2019

Accepted 30 September 2019

Keywords:

Motorcycle modeling

Final drive

Genetic algorithm optimization

Transient tire model

ABSTRACT

The design of transmission systems plays an important role in the dynamic performance of motorcycles. It is well known that power delivery and stability in motorcycles is strongly affected by the geometry of the final drive.

This article presents a 2D multibody motorcycle model in which the tire and final drive are considered thoroughly. A nonlinear transient model is used to reproduce forces between the tire and the road. The engine and wheel sprockets, the squat ratio and the chain slack have been taken into account in the final drive kinematic model.

The configuration of the final drive elements and its influence on the distance covered by the motorcycle have been studied. Furthermore, the motorcycle final drive design has been optimized to maximize the distance traveled on different uneven roads.

Simulations show a superior performance of the motorcycle when the configuration of the final drive elements is optimized. This study contributes to demonstrating the importance of the configuration and geometry of the final drive to improve stability and overall behavior of the motorcycle on uneven roads.

© 2019 Elsevier Ltd. All rights reserved.

1. Introduction

It is well known that the motorcycle final drive design plays an important role in engine-to-slip dynamics. There are at least four parameters involved in this phenomenon [1], namely:

1. Longitudinal velocity
2. Tire radial compliance
3. Swingarm motion
4. Slip due to wheel rotation

Nowadays, different final drive technologies coexist. The most important ones are continuously variable transmission (CVT) [2], cardan shaft, V-belt and roller chain [3]. The study of this system is of great importance in the analysis of power transmission and motorcycle stability. Besides, the dynamics of this system are also of great importance in the design of TCS and ABS. For example, in [4,5] the resonance phenomena associated with variations in the longitudinal force in the rear wheel and their influence on the stability of the motorcycle are studied. A study of the final drive is carried out in [6]. The

* Corresponding author.

E-mail addresses: manuel.alcazar@uma.es (M. Alcazar), javierperez@uma.es (J. Perez), jemata@ujaen.es (J.E. Mata), jcabrera@uma.es (J.A. Cabrera), juancas@uma.es (J.J. Castillo).<https://doi.org/10.1016/j.mechmachtheory.2019.103647>

0094-114X/© 2019 Elsevier Ltd. All rights reserved.



Nomenclature

Symbol	Magnitude
x	x -coordinate
y	y -coordinate
a	Angular design parameter
L	Longitudinal design parameter
H_y	Height of the ground
λ	Wavelength of the ground
σ	Width of the bump
μ	x -coordinate of the center of the bump
α	Angular coordinate of the engine sprocket
β	Angular coordinate of the wheel sprocket
γ	Upper chain angle
k	Stiffness coefficient
c	Damping coefficient
s	Unloaded length
Φ	Kinematic set of equations
\mathbf{q}	Coordinate vector
$\dot{\mathbf{q}}$	Velocities vector
$\ddot{\mathbf{q}}$	Accelerations vector
SR	Squat ratio
d	Distance traveled

kinematic relationships of the final drive and the dynamic behavior of the front and rear suspension are studied by varying the vertical position of the engine sprocket. Finally, an analysis of power transmission in motorcycles is carried out in [7]. In this work, three models consider the stiffness of the tire and the final drive is described.

The modeling of in-plane dynamics is required to analyze the acceleration process of a motorcycle. To the best of our knowledge, there are basically two complete motorcycle models described in literature. The first one was published by Sharp in 2001. It makes use of independent coordinates to study motorcycle dynamics [8]. This model, with slight modifications, is currently used by the BikeSim commercial simulation package. The second model was published by Cossalter and Lot in 2002. In this case, natural coordinates are used to reproduce the dynamics of the motorcycle [9]. The FastBike commercial simulation package is based on this model.

Furthermore, the tire model is of great importance in the modeling of the motorcycle. There are several contact force models, such as: the restitution coefficient [10], spring-shock absorber systems and the Hertz contact theory [11], among others. Besides, there are also several friction force models [12], for example: Coulomb, Stribeck, Threlfall and LuGre, among others. The most widely used formulation for modeling tire-road friction was established by Pacejka, using the well-known «magic formula» [13]. This model describes both stationary and transient tire behavior. Transient behavior is modeled using a parameter known as relaxation length. Other authors, although they resort to Pacejka's stationary model, propose an alternative transient model. In this approach, they consider the stiffness of the tire instead of a relaxation length [9]. This model allows the slip and contact force to be delayed, modeling the relationship between them by means of a first-order system. Both Pacejka's transient model [13] as well as Cossalter's model [9] are equivalent, as shown in [7], the latter having a more physical sense than the former.

Four-wheeled vehicles have received great attention from research groups. However, research studies focused on two-wheeled vehicles are less common. Although lateral relaxation lengths for various motorcycle tires have been published in literature [14], no studies related to longitudinal relaxation lengths have been found.

The modeling of the final drive can be performed from several perspectives and with different simplifications. The relationships between the engine sprocket, wheel and swingarm can be modeled using kinematic constraints [7,15], dynamical constraints [6] or a combination of both [7]. Dynamic models consider chain stiffness and damping as well as the elastic coupling that exists between the sprocket and the rim. However, these parameters are difficult to measure. Furthermore, incorrect estimates affect the performance and accuracy of the simulations. In this work, these relationships are kinematic, which makes the modeling process less complex and computationally more efficient.

This paper proposes a methodology for the optimal design of motorcycle final drives by means of multibody simulation and genetic algorithms. As found in [16,17], genetic algorithms are an extensively used tool to optimize multiple physical processes, offering an optimal solution in complex multi-variable systems.

In this work, an in-plane motorcycle model with the following features is proposed:

- The final drive has been modeled in detail, analyzing the kinematic relationships between the wheel, the swingarm and the engine sprocket.

- The road-tire contact has been modeled using the Pacejka transient model [13], considering a constant tire relaxation length. The variable effective radius is modeled by considering the radial deformation of the tire.
- Three different road profiles have been simulated: flat, bumpy and sinusoidal.
- Aerodynamics have not been considered.
- The dynamic problem has been formulated by using the augmented Lagrangian formulation [18].
- Multi-step integrators (Adams-Bashforth and Adams-Moulton) have been used [19].
- The modeling of the system has been carried out by means of natural coordinates [18,20].

Real time performance has been achieved thanks to dynamic formulation and the solver used. In addition, due to the tire model considered, the simulation can start from a singularity, such as standstill as well as moving forwards or backwards.

Once the model simulations have been carried out, the parameters that influence the behavior of the motorcycle on an uneven road are studied. These parameters have been optimized by means of genetic algorithms, obtaining the final drive design that maximizes the distance traveled in the test.

This work is organized as follows: in Section 2 the model of the motorcycle is described, including the coordinates and constraints used. Section 3 is devoted to the description of the numerical algorithm employed, both for the formulation of the Differential-Algebraic set of Equations (DAE) and for its solution. In Section 4, the optimization of the problem under consideration is performed, which is the maximization of the distance traveled by the motorcycle. The results obtained are shown and commented in Section 5. Finally, in Section 6, the conclusions of the work are presented.

2. System definition and modeling

2.1. Motorcycle description

In this paper, the motorcycle has been modeled as a system composed of six bodies: chassis, swingarm, engine sprocket, lower front suspension, rear wheel and front wheel. Both the rider and the upper part of the front suspension are assumed to be rigidly attached to the chassis. This simplification has been made because only the in-plane dynamics of the motorbike are studied. A fork and a spring-shock absorber are used in the front and rear suspension respectively. The coordinate system used is the following: horizontal x axis increasing to the right while the y axis is vertical, increasing to the top. The number of degrees of freedom (DoF) of the system is 6 (Fig. 1). These DoF are associated with the bounce (1) and longitudinal translation (2) of the motorcycle chassis, the pitch (3), the rotation of the rear wheel and engine sprocket (4) and the rear and front hop (5 and 6). The rotation of the front wheel is not considered due to the computational cost of solving the tire-road interaction twice. Thus, the convergence of the simulation has been increased as only a pure traction scenario is considered. Neither aerodynamic forces nor rolling resistance have been considered in order to be able to analyse the phenomena under study independently.

A total of 39 coordinates are used to model the motorcycle (Table 1). 30 natural coordinates describe the movement of the 15 points shown in Fig. 3. The remaining 9 coordinates are grouped into two types: lengths associated with the four damper-spring systems considered and five angles. Three angles are associated with the transmission and the other two with the pitch of the chassis and swingarm.

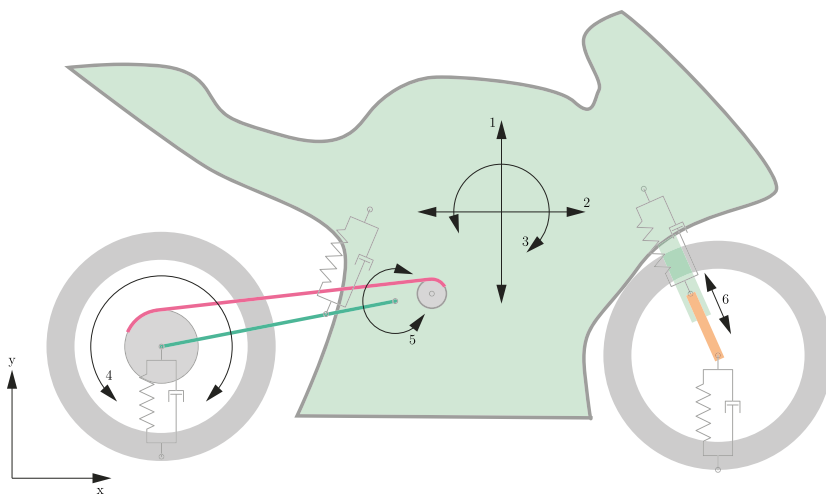


Fig. 1. Dynamic model of the motorcycle.

Table 1
Coordinates.

Coordinate	Description	Coordinate	Description
x_1	Swingarm axis	x_{11}	Wheel sprocket tangential point
y_1		y_{11}	
x_2	Engine axis	x_{12}	Upper point fork suspension
y_2		y_{12}	
x_3	Upper damper pin	x_{13}	Front wheel axis
y_3		y_{13}	
x_4	Upper triple clamp	x_{14}	Rear tire contact point
y_4		y_{14}	
x_5	Lower triple clamp	x_{15}	Front tire contact point
y_5		y_{15}	
x_6	Rear wheel axis	rs	Rear suspension length
y_6		fs	Front suspension length
x_7	Lower damper pin	rt	Rear tire radii
y_7		ft	Front tire radii
x_8	Engine reference point	θ	Chassis angle
y_8		α	Engine sprocket angle
x_9	Rear wheel reference point	β	Wheel sprocket angle
y_9		γ	Upper chain angle + $\pi/2$
x_{10}	Engine sprocket tangential point	ϕ	Swingarm angle
y_{10}			

Table 2
Inertial properties of each body.

Body No.	Ref.	m [kg]	I_{CoG} [kg m ²]
I	Chassis + rider	223.0	26.20
II	Swingarm	10.0	0.80
III	Engine sprocket	1.0	0.50
IV	Rear wheel	16.2	0.66
V	Lower part front fork	7.0	0.18
VI	Front wheel	12.0	0.47

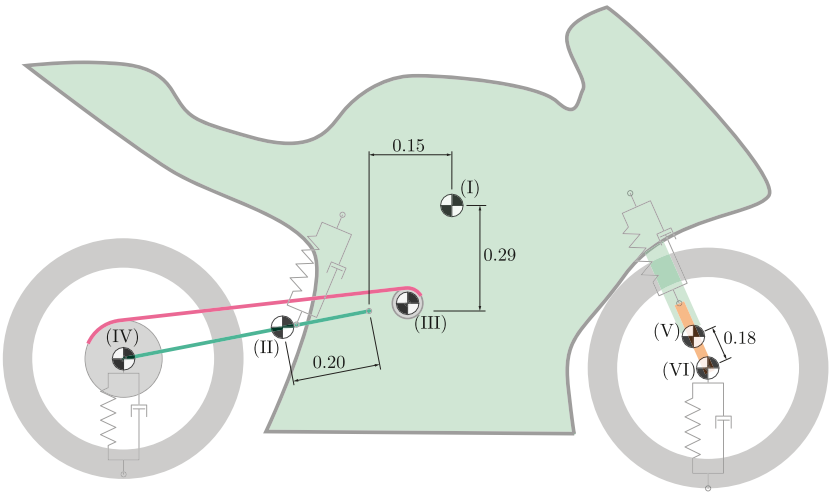


Fig. 2. Locations of the centers of mass of the motorcycle bodies.

The masses and moments of inertia of the bodies that constitute the system have been extracted from [9,21]. They are shown in Table 2 and Fig. 2. The geometry of the motorcycle as well as the parameters of the spring-shock absorber systems which have been obtained from [9,21] are shown in Table 3.

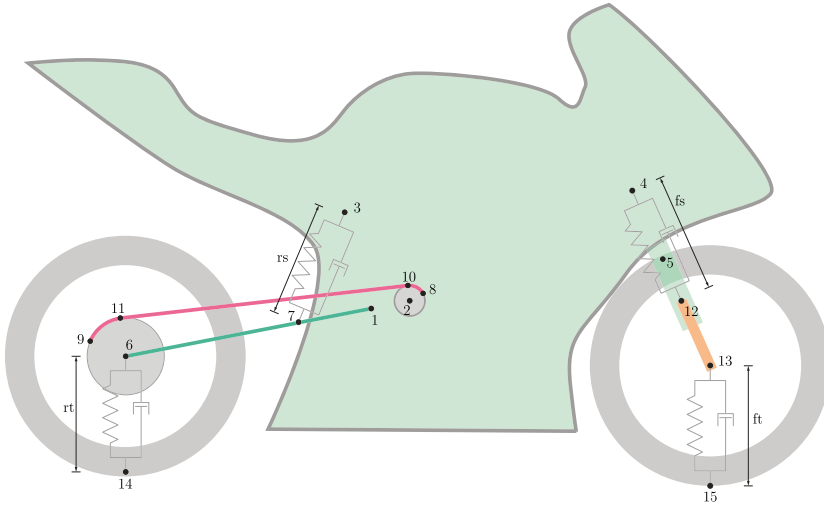


Fig. 3. Motorcycle coordinates.

Table 3
The most important parameters of the motorcycle.

Parameter	Value	Units
Rear equivalent stiffness	19,900	N/m
Rear equivalent damping coef.	3960	Ns/m
Rear unsprung mass	24.5	kg
Front equivalent stiffness	20,800	N/m
Front equivalent damping coef.	1750	Ns/m
Front unsprung mass	19.9	kg
Rear weight distribution	50.7	%
Front weight distribution	49.3	%
Center of gravity height	623	mm
Total mass	272	kg
Wheelbase	1424	mm
Caster angle	24	deg

2.2. Kinematics

Kinematic constraints are grouped into three blocks, namely: motorcycle, transmission and tire-road contact (road profile).

2.2.1. Kinematic model of the motorcycle

The «kinematic model of the motorcycle» refers to the set of equations that governs the kinematics of the chassis, rear axle, front axle and wheels. The kinematic relationships that model transmission as well as tire-road interaction are described in an independent Section.

Five points are used to model the chassis. Points 1 and 2 represent the axle of the swingarm and engine sprocket respectively. Point 3 is the upper anchorage of the rear shock absorber. Points 4 and 5 are used to define the front suspension slider. In addition, the lengths and angles listed in Table 4 are also defined. Eqs. (1)–(8) are the kinematic constraints of the chassis.

$$x_1 + L_2 \cos(\theta + a_2) - x_2 = 0 \quad (1)$$

$$y_1 + L_2 \sin(\theta + a_2) - y_2 = 0 \quad (2)$$

$$x_1 + L_3 \cos(\theta + a_3) - x_3 = 0 \quad (3)$$

$$y_1 + L_3 \sin(\theta + a_3) - y_3 = 0 \quad (4)$$

Table 4
Motorcycle design parameters.

Design Parameter	Description	Value	Units
L_2	$\ \mathbf{r}_{1 \rightarrow 2}\ $	variable	m
L_3	$\ \mathbf{r}_{1 \rightarrow 3}\ $	0.260	m
L_4	$\ \mathbf{r}_{1 \rightarrow 4}\ $	0.767	m
L_5	$\ \mathbf{r}_{1 \rightarrow 5}\ $	0.786	m
a_2	$\angle \mathbf{r}_{1 \rightarrow 2}$	variable	rad
a_3	$\angle \mathbf{r}_{1 \rightarrow 3}$	1.850	rad
a_4	$\angle \mathbf{r}_{1 \rightarrow 4}$	0.785	rad
a_5	$\angle \mathbf{r}_{1 \rightarrow 5}$	0.000	rad
L_7	$\ \mathbf{r}_{1 \rightarrow 7}\ $	0.200	m
L_{SA}	$\ \mathbf{r}_{1 \rightarrow 6}\ $	0.560	m
θ_0	Chassis pitch angle	0.000	rad
φ_0	Swingarm angle	3.316	rad
r_{t0}	Unloaded rear tire radius	0.300	m
f_{t0}	Unloaded front tire radius	0.300	m
R_{WS}	Wheel sprocket radius	variable	m
R_{ES}	Engine sprocket radius	variable	m
L	Fixed chain length	variable	m
H_y	Height of ground irregularities	variable	m
μ	Bump center x-coordinate	variable	m
λ	Wavelength of ground irregularities	variable	m
σ	Bump width	variable	m
L_8	$\ \mathbf{r}_{12 \rightarrow 13}\ $	0.350	m

$$x_1 + L_4 \cos(\theta + a_4) - x_4 = 0 \quad (5)$$

$$y_1 + L_4 \sin(\theta + a_4) - y_4 = 0 \quad (6)$$

$$x_1 + L_5 \cos(\theta + a_5) - x_5 = 0 \quad (7)$$

$$y_1 + L_5 \sin(\theta + a_5) - y_5 = 0 \quad (8)$$

The rear train kinematics are defined by points 6 and 7. The first point is the rear wheel axis and the second one is the lower anchorage of the shock absorber. It is important to note that φ is the angle that forms the swingarm with the horizontal and not with the chassis. The length of the rear shock-absorber is determined by coordinate rs .

$$x_1 + L_{SA} \cos \varphi - x_6 = 0 \quad (9)$$

$$y_1 + L_{SA} \sin \varphi - y_6 = 0 \quad (10)$$

$$x_1 + L_7 \cos \varphi - x_7 = 0 \quad (11)$$

$$y_1 + L_7 \sin \varphi - y_7 = 0 \quad (12)$$

$$(x_3 - x_7)^2 + (y_3 - y_7)^2 - rs^2 = 0 \quad (13)$$

The kinematic constraints of the front fork suspension slider mechanism are defined by Eqs. (14)–(15). The length of the lower part of the front suspension is determined by parameter L_8 . Coordinate fs is the front spring-shock absorber length.

The length of the lower part of the front suspension and the front spring-shock absorber is given by parameter L_8 and coordinate fs , respectively.

$$(x_5 - x_4)(y_{13} - y_{12}) - (y_5 - y_4)(x_{13} - x_{12}) = 0 \quad (14)$$

$$(x_5 - x_4)(y_{13} - y_4) - (y_5 - y_4)(x_{13} - x_4) = 0 \quad (15)$$

$$(x_{13} - x_{12})^2 + (y_{13} - y_{12})^2 - L_8^2 = 0 \quad (16)$$

$$(x_4 - x_{12})^2 + (y_4 - y_{12})^2 - fs^2 = 0 \quad (17)$$

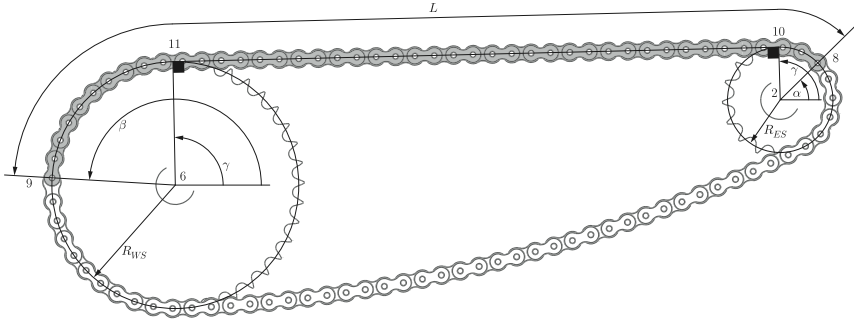


Fig. 4. Coordinates and parameters of transmission kinematics.

The wheel equations are (18)–(21):

$$x_6 - x_{14} = 0 \quad (18)$$

$$x_{13} - x_{15} = 0 \quad (19)$$

$$y_6 - y_{14} - rt = 0 \quad (20)$$

$$y_{13} - y_{15} - ft = 0 \quad (21)$$

2.2.2. Kinematic model of the transmission

Four points (8)–(11) and three additional angles (α , β , γ) are used to model transmission kinematics. The pitch radii of the engine and wheel sprockets are R_{ES} and R_{WS} respectively. Parameter L is the length of the section of the chain between points 8 and 9 (Fig. 4). This length is constant throughout the simulation. Neither the 'polygonal action' that takes place in chain transmissions [22,23] nor the efficiency of the transmission are modeled.

Eqs. (22)–(29) locate points 8 – 11 with respect to the sprocket's axes. Eq. (30) defines length L , while Eq. (31) determines the orthogonality condition of vectors $\mathbf{r}_{6 \rightarrow 11}$ and $\mathbf{r}_{11 \rightarrow 10}$.

$$x_2 + R_{ES} \cos \alpha - x_8 = 0 \quad (22)$$

$$y_2 + R_{ES} \sin \alpha - y_8 = 0 \quad (23)$$

$$x_2 + R_{ES} \cos \gamma - x_{10} = 0 \quad (24)$$

$$y_2 + R_{ES} \sin \gamma - y_{10} = 0 \quad (25)$$

$$x_6 + R_{WS} \cos \beta - x_9 = 0 \quad (26)$$

$$y_6 + R_{WS} \sin \beta - y_9 = 0 \quad (27)$$

$$x_6 + R_{WS} \cos \gamma - x_{11} = 0 \quad (28)$$

$$y_6 + R_{WS} \sin \gamma - y_{11} = 0 \quad (29)$$

$$(\gamma - \alpha)R_{ES} + \sqrt{(x_{10} - x_{11})^2 + (y_{10} - y_{11})^2} + (\beta - \gamma)R_{WS} - L = 0 \quad (30)$$

$$(x_6 - x_{11})(x_{11} - x_{10}) + (y_6 - y_{11})(y_{11} - y_{10}) = 0 \quad (31)$$

Fig. 5 is used to illustrate the kinematic relationship between the two sprockets. In this Figure, it can be seen how an angular movement appears in the wheel when the swingarm moves keeping the engine sprocket locked. This movement

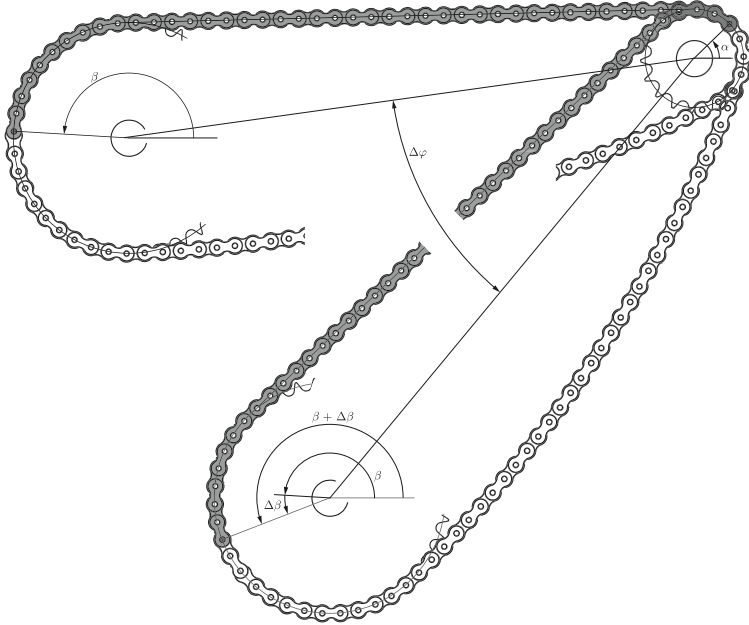


Fig. 5. Graphical demonstration of the movement induced in the wheel when the swingarm moves.

is common in a motorcycle riding on uneven roads. This way, the relationship between the angular speeds of the engine sprocket and the wheel are not determined only by the ratio between the number of teeth of the sprockets. Therefore, the previously described angular movement has to be taken into account to properly model the whole system. This statement is of great importance in the present work because it shows that, as angular accelerations appear in the drivetrain, power transmission from the engine to the wheel is strongly influenced by the design of the final drive.

2.2.3. Test surface profiles

Three different road profiles are simulated in this work, namely:

1. Sinusoidal profile
2. Gaussian profile (bumpy)
3. Flat profile

The coordinates of points 14 and 15 (Fig. 3) are given by equations (32) and (33) according to the type of road: sinusoidal, Gaussian and flat.

$$y_{14} - H_y \sin\left(\frac{2\pi}{\lambda} x_{14}\right) = 0 \quad (32a)$$

$$y_{14} - H_y \exp\left(-\frac{(x_{14} - \mu)^2}{2\sigma^2}\right) = 0 \quad (32b)$$

$$y_{14} = 0 \quad (32c)$$

$$y_{15} - H_y \sin\left(\frac{2\pi}{\lambda} x_{15}\right) = 0 \quad (33a)$$

$$y_{15} - H_y \exp\left(-\frac{(x_{15} - \mu)^2}{2\sigma^2}\right) = 0 \quad (33b)$$

$$y_{15} = 0 \quad (33c)$$

Table 5
Parameters of spring-shock absorber systems.

No.	Suspension parameter	Description	Initial Value	Units
1	k_{rs}	Rear suspension stiffness	251,400	N/m
2	c_{rs}	Rear suspension damping coefficient	50,000	Ns/m
3	s_{rs}	Unloaded rear suspension length	0.327	m
4	k_{fs}	Front suspension stiffness	25,000	N/m
5	c_{fs}	Front suspension damping coefficient	2100	Ns/m
6	s_{fs}	Unloaded front suspension length	0.395	m
7	k_{rt}	Rear tire stiffness	141,000	N/m
8	c_{rt}	Rear tire damping coefficient	50	Ns/m
9	s_{rt}	Unloaded rear tire length	0.300	m
10	k_{ft}	Front tire stiffness	130,000	N/m
11	c_{ft}	Front tire damping coefficient	50	Ns/m
12	s_{ft}	Unloaded front tire length	0.300	m

2.3. Dynamics

The forces that govern the dynamics of the system are grouped into three distinct blocks: front and rear suspensions, vertical forces on the front and rear tires and longitudinal forces on the rear tire. The parameters of the spring-shock absorber systems for both suspensions and tires can be found in Table 5:

The front and rear suspension parameters have been selected so that the equivalent stiffness and damping coefficients on the wheels are similar to those used in [24].

2.3.1. Dynamic model of the suspensions

For the suspensions, it has been decided to use a linear model for both the spring and shock absorber. The equations that reproduce front and rear suspension forces are the following:

$$F_{fs} = -k_{fs}(fs - s_{fs}) - c_{fs}\dot{f}s \quad (34)$$

$$F_{rs} = -k_{rs}(rs - s_{rs}) - c_{rs}\dot{r}s \quad (35)$$

2.3.2. Vertical dynamics of the tires

The following model of a spring-shock absorber has been considered (36),(37). In this model, the vertical force is zero when there is no contact between the tire and the road:

$$F_{rt} = \begin{cases} -k_{rt}(rt - rt_0) - c_{rt} \dot{r}t & \text{if } rt < rt_0 \\ 0 & \text{if } rt \geq rt_0 \end{cases} \quad (36)$$

$$F_{ft} = \begin{cases} -k_{ft}(ft - ft_0) - c_{ft} \dot{f}t & \text{if } ft < ft_0 \\ 0 & \text{if } ft \geq ft_0 \end{cases} \quad (37)$$

2.3.3. Longitudinal dynamics of the tires

The Magic-formula «fully nonlinear transient model» [13] is used to model the longitudinal force. This model, despite its computational cost, is considered to be the most suitable one for this work. The reasons are the following:

- There are fluctuations in the vertical loads due mainly to road surface irregularities and the load transfer that takes place in acceleration processes of motorcycles.
- In pure acceleration processes, due to the power-to-weight ratio of motorcycles, the longitudinal acceleration is important and, consequently, the slip is also high.
- There are important angular accelerations in the powertrain due to the geometry of the transmission system. This causes high slip fluctuations, which makes the slip oscillate from the stable to the unstable zone of the longitudinal force curve.

It is important to define both the effective rolling radius, R_e , and the linear velocity, V_x . The effective rolling radius is defined in [25] and is given by Eq. (38):

$$R_e = \frac{2}{3}rt_0 + \frac{1}{3}rt \quad (38)$$

The speed of the rear wheel axle, V_x , has to be taken into account to calculate the real wheel slip. The difference between considering the speed of the wheel axle or the speed of the chassis is important, as demonstrated further ahead.

$$V_x = \dot{x}_6 \quad (39)$$

Finally, the longitudinal slip speed, V_{sx} , is defined in [13] according to expression (40), in which $\omega = -\dot{\beta}$ due to the sign criteria used:

$$V_{sx} = V_x - R_e \omega \quad (40)$$

Due to the reasons stated before, it is required to resort to the fully nonlinear transient model to properly reproduce tire-road interaction. This model (Eqs. (41)–(52)) is developed in [13]. In this model, a first-order differential equation has to be solved (42). In addition, at very low velocities ($|V_x| \leq V_{low}$) it is necessary to introduce an additional parameter ($k_{v,low}$) to ensure the convergence of the method.

$$\sigma_k^* = \max \left(\frac{\sigma_{k0}}{K_{kk}} \cdot \frac{|F_x| + K_{kk} \varepsilon_F}{|k'| + \varepsilon_F}; \sigma_{\min} \right) \quad (41)$$

$$\frac{du}{dt} + \frac{1}{\sigma_k^*} |V_x| u = -V_{sx} \quad (42)$$

$$k' = \frac{u}{\sigma_k^*} - \frac{K_{V,low}}{K_{kk} V_{sx}} \quad (43)$$

$$K_{V,low} = \begin{cases} \frac{1}{2} K_{V,low0} (1 + \cos(\pi \frac{|V_x|}{V_{low}})) & \text{if } |V_x| \leq V_{low} \\ 0 & \text{if } |V_x| > V_{low} \end{cases} \quad (44)$$

$$F_x = D_x \sin (C_x \arctan (B_x k' - E_x (B_x k' - \arctan (B_x k')))) \quad (45)$$

$$C_x = p_{Cx1} \quad (46)$$

$$D_x = \mu_x F_z \quad (47)$$

$$\mu_x = p_{Dx1} + p_{Dx2} df_z \quad (48)$$

$$E_x = (p_{Ex1} + p_{Ex2} df_z + p_{Ex3} df_z^2) \cdot (1 - p_{Ex4} \operatorname{sgn}(k')) \quad (49)$$

$$K_{kk} = F_z (p_{Kx1} + p_{Kx2} df_z) \cdot \exp(p_{Kx3} df_z) \quad (50)$$

$$B_x = K_{kk} / (C_x D_x) \quad (51)$$

$$df_z = (F_z - F_{z0}) / F_{z0} \quad (52)$$

The parameters related to the stationary Pacejka tire model have been extracted from [24], while the parameters related to the relaxation length (Table 7) have been obtained from [13]. Among the three tires available in literature (Table 6), the 160/70 rear tire is chosen in this paper.

Table 6
Magic formula pure longitudinal parameters of 120/70, 180/55 and 160/70 tires. [24].

	Front tire 120/70	Rear tire 180/55	Rear tire 160/70
p_{Cx1}	1.6064	1.6064	1.6064
p_{Dx1}	1.3806	1.3548	1.2017
p_{Dx2}	-0.041429	-0.060295	-0.092206
p_{Ex1}	0.0263	0.0263	0.0263
p_{Ex2}	0.27056	0.27056	0.27056
p_{Ex3}	-0.076882	-0.076882	-0.076882
p_{Ex4}	1.1268	1.1268	1.1268
p_{Kx1}	25,939	25,939	25,939
p_{Kx2}	-4.2327	-4.2327	-4.2327
p_{Kx3}	0.33686	0.33686	0.33686

Table 7
Relaxation length parameter values. [13].

Parameter	Description	Value	Units
$\kappa_{V,low0}$	Artificial damping parameter	770	Ns/m
$\sigma_{\kappa 0}$	Relaxation length at $\kappa' = 0$	0.2	m
σ_{min}	Minimum relaxation length	0.02	m
ϵ_F	Regularization parameter (Eq. (41))	0.01	–
V_{low}	Speed beyond which the additional damping disappears	2.5	m/s

3. Numerical algorithm

3.1. Kinematic-dynamic formulation: augmented Lagrangian

Lagrange equations in dependent coordinates [18] are given by expression (53):

$$\frac{d}{dt} \left(\frac{\partial T}{\partial \dot{\mathbf{q}}} \right) - \frac{\partial T}{\partial \mathbf{q}} + \Phi_{\mathbf{q}}^T \Phi_{\mathbf{q}} = \mathbf{Q} \quad (53)$$

The kinetic energy, T , can be written as (54):

$$T = \frac{1}{2} \dot{\mathbf{q}}^T \mathbf{M} \dot{\mathbf{q}} \quad (54)$$

The combination of expressions (53) and (54) yields the following system of differential Eqs. (55):

$$\mathbf{M} \ddot{\mathbf{q}} + \Phi_{\mathbf{q}}^T \lambda = \mathbf{Q} \quad (55)$$

Kinematic constraint Eq. (1)–(33) can be grouped into the following system of algebraic equations:

$$\Phi = 0 \quad (56)$$

where \mathbf{q} is the coordinate vector, \mathbf{M} is the mass matrix of the system, \mathbf{Q} is the vector of external forces, $\Phi_{\mathbf{q}}$ is the Jacobian matrix of the constraint equations and λ is the vector of the Lagrange multipliers.

The system of equations to be solved is given by expressions (55) and (56), which constitute a Differential-Algebraic system of Equations (DAE). To transform this DAE into a system of ODEs, the augmented Lagrangian method is used [18,26]:

As stated in [18], the augmented Lagrangian method leads to a simpler set of equations compared to a projection scheme method. Furthermore, the augmented Lagrangian formulation allows a straightforward calculation of the chain force. This force has to be obtained to guarantee that the upper section of the chain is always taut.

$$(\mathbf{M} + \alpha \Phi_{\mathbf{q}}^T \Phi_{\mathbf{q}}) \ddot{\mathbf{q}} = \mathbf{Q} - \Phi_{\mathbf{q}}^T [\lambda_i + \alpha (\Phi_{\mathbf{q}} \dot{\mathbf{q}} + 2\xi \omega \dot{\Phi} + \omega^2 \Phi)] \quad (57)$$

$$\lambda_{i+1} = \lambda_i + \alpha (\ddot{\Phi} + 2\xi \omega \dot{\Phi} + \omega^2 \Phi) \quad (58)$$

where the following parameters of the Baumgarte stabilization [27] are chosen:

$$\alpha = 10^5$$

$$\xi = 1$$

$$\omega = 10$$

The penalty parameter α takes a value of several orders of magnitude lower than if the penalty method were used. This is one of the advantages of the augmented Lagrangian formulation over the penalty method [18].

3.2. Integrator: Adams Bashforth Moulton + Trapezoidal

An Adams-Bashforth and Adams-Moulton solver was selected to solve this ODE system because of the stiffness of the problem. This stiffness is mainly due to the slip calculation, especially at the initial stages of the simulations, where sudden changes in the slip value were observed. Besides, sharp variations of F_z and F_x also occur when the wheels bounce and hit the ground.

Two types of integrators are used for the integration of the dynamic equations. The trapezoidal integrator is used to find the static equilibrium and the first four time steps of the simulation. The Adams-Bashforth and Adams-Moulton multi-step linear integrators are used for the rest of the simulation. The former is explicit and acts as a predictor, while the latter is implicit and acts as a corrector. This predictor-corrector strategy allows increasing the time steps and, consequently, accelerates the calculation process.

These mathematical tools have been developed to solve systems of first-order differential equations of the following form (59):

$$\dot{\mathbf{y}} = \mathbf{f}(\mathbf{y}, t) \quad (59)$$

Therefore, it is necessary to reduce the system of second order differential equations to a system of first order differential equations. To do so, the following transformations have been carried out:

$$\mathbf{y} = \begin{bmatrix} \mathbf{q} \\ \dot{\mathbf{q}} \end{bmatrix} \quad (60)$$

$$\dot{\mathbf{y}} = \begin{bmatrix} \dot{\mathbf{q}} \\ \ddot{\mathbf{q}} \end{bmatrix} \quad (61)$$

Once the transformations have been made, the trapezoidal integrator is used (62):

$$\mathbf{y}_{n+1} = \mathbf{y}_n + \frac{\Delta t}{2} (\dot{\mathbf{y}}_n + \dot{\mathbf{y}}_{n+1}) \quad (62)$$

While the Adams-Bashforth and Adams-Moulton integrators are defined by Eqs. (63) and (64) respectively:

$$\mathbf{p} = \mathbf{y}_{n+1} = \mathbf{y}_n + \frac{\Delta t}{24} (55\dot{\mathbf{y}}_n - 59\dot{\mathbf{y}}_{n-1} + 37\dot{\mathbf{y}}_{n-2} - 9\dot{\mathbf{y}}_{n-3}) \quad (63)$$

$$\mathbf{c}^* = \mathbf{y}_{n+1} = \mathbf{y}_n + \frac{\Delta t}{24} (9\dot{\mathbf{y}}_{n+1} + 19\dot{\mathbf{y}}_n - 5\dot{\mathbf{y}}_{n-1} + \dot{\mathbf{y}}_{n-2}) \quad (64)$$

Where \mathbf{p} is the predictor (Adams-Bashforth) and \mathbf{c}^* is the corrector (Adams-Moulton). A parameter commonly used in CFD integrators, known as «under-relaxation factor» [28,29], has been used. This factor, ν , reduces integrator oscillations and improves method stability, especially with stiff problems. On the other hand, it reduces the convergence of the simulation. This parameter takes the value of 0.7 for all simulations in this work.

$$\mathbf{c} = \mathbf{y}_{n+1} = \begin{cases} \nu \mathbf{c}^* + (1 - \nu) \mathbf{p} & \text{if } 1^{\text{st}} \text{ iteration} \\ \nu \mathbf{c}_{\text{new}}^* + (1 - \nu) \mathbf{c}_{\text{old}} & \text{else} \end{cases} \quad (65)$$

This way, coordinate vector (\mathbf{q}) is obtained from vector \mathbf{c} (65). The error is calculated according to Eq. (66).

$$\text{error} = \sqrt{\sum (\mathbf{q}_{n+1}^{\text{new}} - \mathbf{q}_{n+1}^{\text{old}})^2} \quad (66)$$

3.3. Initialization process: static equilibrium

The algorithm used to perform simulations is described below:

1. It starts by initializing the parameters of the simulation: time step, simulation time, geometry, suspension and tire parameters of the motorcycle.
2. A single-step trapezoidal solver is used to calculate the static equilibrium for the first time step.
3. The same single-step trapezoidal solver is used for the next four time steps.
4. During the rest of the simulation, the Adams Bashfort-Moulton's predictor-corrector multistep solver of the fourth order is used [30].

The static equilibrium position can be determined by means of different methods [18]. A trapezoidal solver from an approximate solution has been used in this work.

4. Optimization process

This Section describes the procedure followed in the optimization process by means of genetic algorithms. To perform this optimization, an objective function has to be defined. In this work, the objective function or fitness function takes into account the distance traveled by the motorcycle during 3.5 s of simulation and two penalties (67):

$$\text{Fitness Function} \equiv d \cdot \max \left\{ \left(\frac{1}{\epsilon_1 |SR - SR_{\text{optimum}}| + 1} \right), \left(\frac{1}{\epsilon_2 |\text{slack}| + 1} \right); 0.95 \right\} \quad (67)$$

The penalties are forced to be greater than 0.95. The nature of the penalties is described next. The first one, associated with the Squat Ratio (SR) [25], affects those solutions in which this parameter deviates from the optimum. According to [1,6,25,31], the optimal value of the SR should be close to 1. It is necessary to consider this phenomenon because an SR away from the unit causes the rear train to extend or to compress during an acceleration while exiting a curve, which is an unfavorable situation. This penalty prevents the swingarm from extending or compressing excessively when the motorcycle accelerates. The penalty factor ϵ_1 takes the value of 0.01.

The second parameter is associated with the length variation of the taut stretch of the chain throughout the simulation. This extension has to be guaranteed, so the lower stretch of the chain has to be left with the appropriate slack. Too much

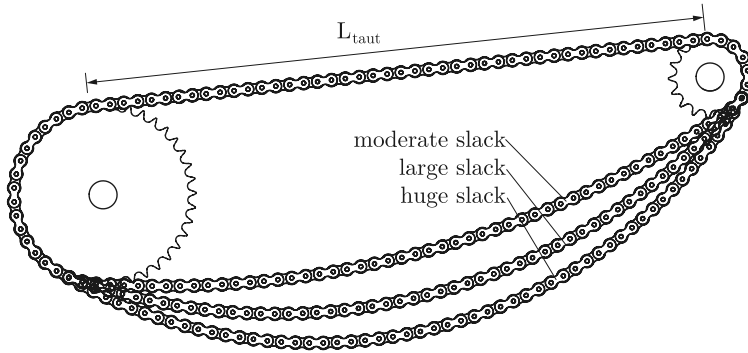


Fig. 6. Chain slack.

slack is not desirable, as it may even cause the chain to escape. The penalty factor ϵ_2 takes the value of 0.1 m^{-1} . Slack is defined by expression (68):

$$\text{slack} = 2[\max(L_{\text{taut}}) - \min(L_{\text{taut}})]. \quad (68)$$

Therefore, the slack is the extra length that the loose part of the chain has in the most unfavorable situation (Fig. 6).

One of the reasons to carry out this work was to contribute to improving motorcycle models by taking into account the influence of swingarm movement in the slip of the rear wheel. Traction and braking control system performance is affected by the changes in the slip of the rear wheel. In this kind of system, the performance is commonly evaluated by minimizing the distance travelled by the motorcycle during the braking process or by maximizing the distance during the acceleration process. Thus, the distance travelled by the motorbike during a pre-determined period of time has been selected as the main factor in the fitness function.

Next, the optimization method used in this work is described. Among the different evolutionary optimization strategies, an algorithm known as differential evolution has been used. This method was described by Storn and Price in [32].

This algorithm has been used in a number of optimization problems applied to mechanical engineering, such as in the determination of the parameters of the Pacejka magic-formula [33] and in the synthesis of mechanisms [34]. The procedure can be summarized as follows (Fig. 7):

1. Initialization of the population through the generation of random individuals.
2. Evaluation of each individual and determination of the optimal one.
3. Generation of the new population through differential evolution:

$$\text{Parent}_2 = \text{Best Individual} + F \cdot (\text{Random Individual}_1 - \text{Random Individual}_2)$$

4. The new population is composed of a fraction of individuals from the previous generation. The remaining members of the new population come from the offspring of the differential evolution process.
5. From the new population, a fraction of individuals of the new population mutate.
6. The population resulting from this iteration is constituted by the best individuals from the population of parents and offspring. The best individual of this iteration is the best individual of the resulting population.
7. Steps 3 to 6 are repeated until the maximum number of iterations is reached.
8. The best individual of the last population is the solution to the optimization problem.

The lower and upper limits of the search space are listed in Table 8:

The rest of the design parameters (Table 4) as well as the suspension system parameters (Table 5) remain constant in all simulations, with the following exceptions:

Table 8
Search space. Genetic algorithm optimization.

Design Parameter	Description	Lower limit	Upper limit	Units
L_2	$\ \mathbf{r}_{1 \rightarrow 2}\ $	0	0.2	m
a_2	$\angle \mathbf{r}_{1 \rightarrow 2}$	0	2π	rad
R_{WS}	Wheel sprocket radius	0.05	0.15	m

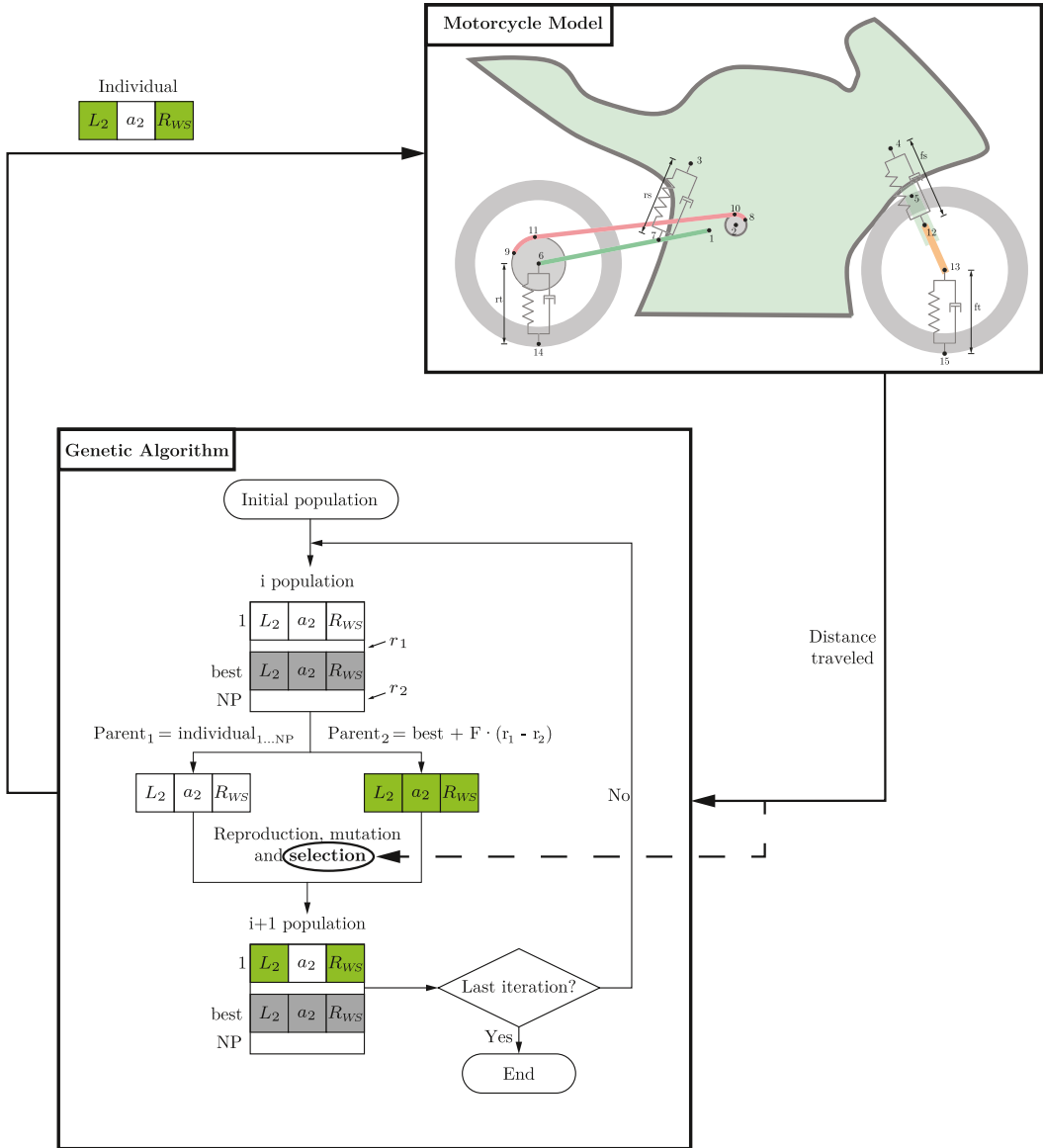


Fig. 7. Optimization algorithm.

- The ratio between the sprocket radii (R_{WS}/R_{ES}) is set at 2.0.
- The chain length is calculated from the geometry of the final drive (69), where subscript 0 indicates the first time step of the simulation.

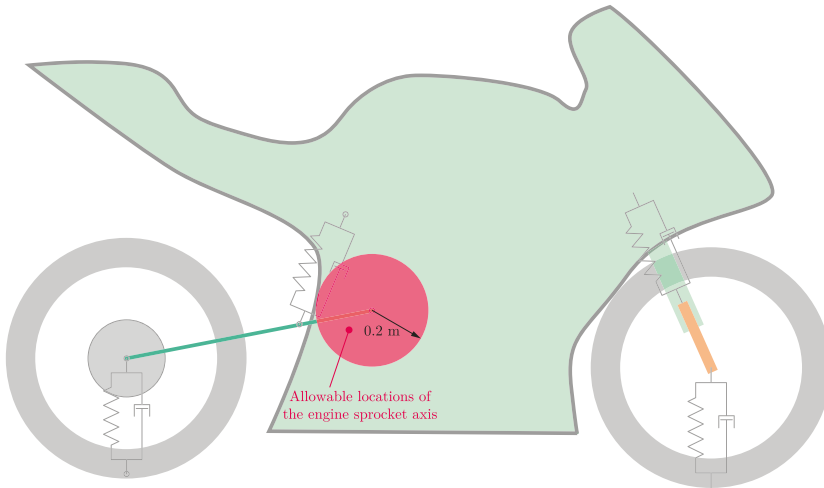
$$L = (\gamma_0 - \alpha_0)R_{ES} + \sqrt{(x_{10,0} - x_{11,0})^2 + (y_{10,0} - y_{11,0})^2} + (\beta_0 - \gamma_0)R_{WS} \quad (69)$$

- The wavelength of the road, (λ), ranges from 2.0 to 5.0 m and the amplitude between 1 and 4 cm, in the case of the road with a sinusoidal profile.
- In the case of the road with a bump, the width, (σ), ranges from 0.2 to 1.0 m and the height between 2 and 4 cm.

Table 9

Search space. Sweep of variables .

Design Parameter	Description	Lower limit	Upper limit	Step size	Units
L_2	$\ \mathbf{r}_1 \rightarrow 2\ $	0	0.2	0.02	m
a_2	$\angle \mathbf{r}_1 \rightarrow 2$	0	360	2	deg

**Fig. 8.** Allowable locations of the center of the engine sprocket.

5. Results

The results of this study are grouped in two blocks. In the first block, a simulation has been carried out by sweeping parameters L_2 and a_2 . In the second block, genetic algorithms have been used to optimize, in addition to the two parameters previously mentioned, the radius of the wheel sprocket (R_{WS}).

It is important to remark that a computational time ratio of 2.2 has been achieved. This is understood as the ratio between the simulation time and the time used for its calculation in a single core. Therefore, real time simulations have been achieved, with an average of 1.6 s to calculate 3.5 s of simulation in an Intel® Core™ i7-7700 CPU @ 3.60 GHz.

5.1. Case #1.- Sweep of variables

In this case, the variables are swept within the range set in Table 9 and Fig. 8:

The sweep has been made for a total of 23 different roads:

- Flat road.
- Sinusoidal road with four different wavelengths (2, 3, 4, and 5 m) and four amplitudes (1, 2, 3, and 4 cm).
- Gaussian (bumpy) road with three different widths (0.2, 0.5 and 1.0 m) and two heights (2 and 4 cm).

For each one of the 23 cases, the fitness function was evaluated by varying parameter a_2 in intervals of 2° from 0° to 360° and parameter L_2 in intervals of 0.02 m from 0 to 0.2 m. Therefore, a total of 45 540 simulations were carried out. The results are shown in Figs. 9–11.

5.2. Case #2.- Genetic algorithm optimization

In the case of the optimization using genetic algorithms, in addition to the two parameters indicated above (a_2 and L_2), the size of the wheel sprocket (R_{WS}) has also been optimized. As far as the road is concerned, the same 23 roads have been considered. The parameters that have been used for the genetic algorithm optimization are shown in Table 10.

The results are presented in Table 11, 12 and 13, which includes the optimal values of the design variables for all road types.

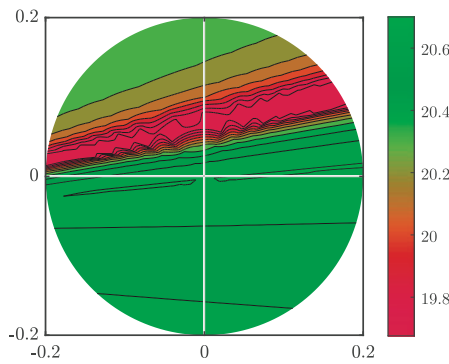


Fig. 9. Distance traveled by the motorcycle depending on the relative position of the engine sprocket axis with respect to the swingarm axis. Flat road.

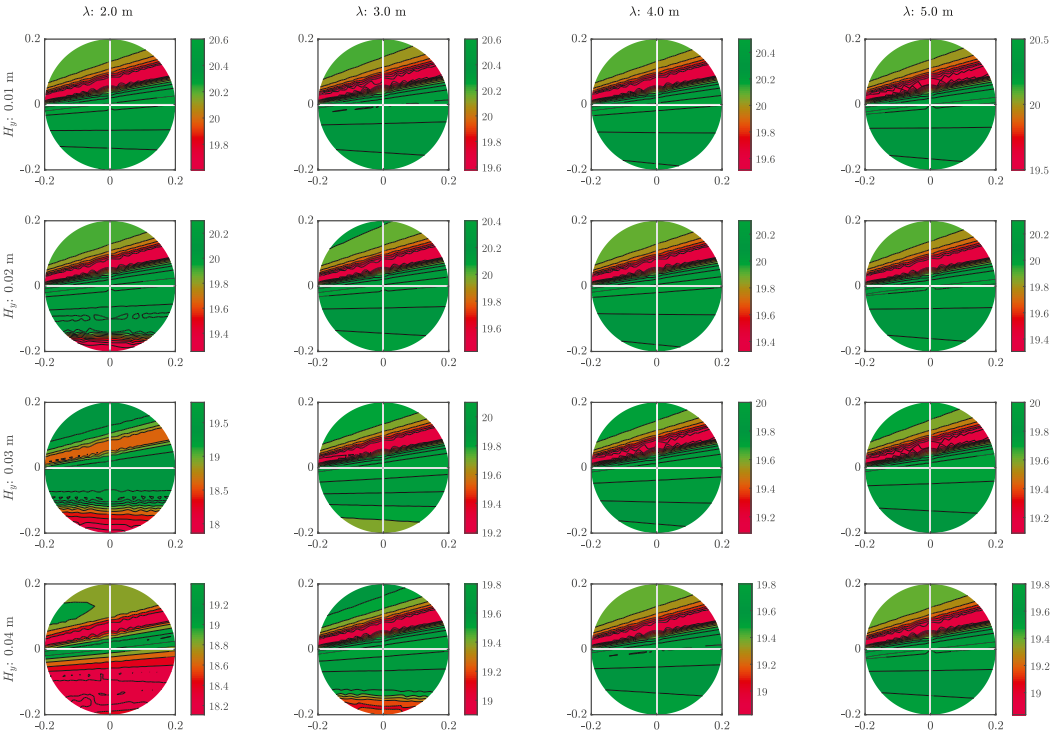


Fig. 10. Distance traveled by the motorcycle depending on the relative position of the engine sprocket axis with respect to the swingarm axis. Different wavelengths and heights of road.

Table 10
Genetic Algorithm optimization parameters.

Parameter	Description	Value
NP	Population size	50
F	Differential evolution F parameter	0.6
CP	Crossover probability	0.6
MP	Mutation probability	0.1
MR	Mutation range	0.2 · (Upper Limit - Lower Limit)
IterMax	Maximum number of iterations	50

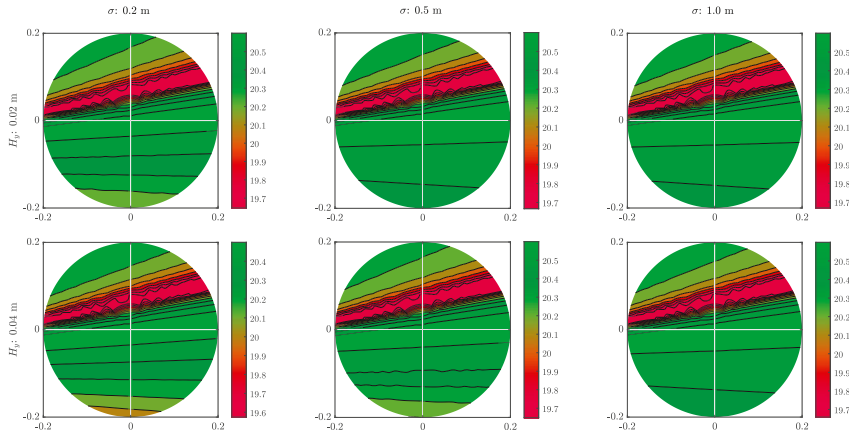


Fig. 11. Distance traveled by the motorcycle depending on the relative position of the engine sprocket axis with respect to the swingarm axis. Different bump sizes.

Table 11

Optimized parameters to maximize the fitness function. Road profile: Flat.

Best					
a_2 deg	L_2 m	R_{WS} m	Slack mm	SR .	fitness fun m
195.3	0.037	0.088	0.132	1.000	20.708

Table 12

Optimized parameters to maximize the fitness function. Road profile: Sinusoidal.

		Best					
H_y	λ	a_2	L_2	R_{WS}	Slack	SR	fitness fun
m	m	deg	m	m	mm	.	m
0.01	2.0	306.0	0.007	0.081	0.554	1.000	20.632
	3.0	263.0	0.009	0.115	0.532	1.000	20.604
	4.0	195.2	0.040	0.100	0.189	1.000	20.536
	5.0	211.7	0.017	0.106	0.354	1.000	20.520
0.02	2.0	199.8	0.027	0.091	0.553	1.000	20.329
	3.0	261.3	0.007	0.087	0.529	1.000	20.432
	4.0	325.5	0.011	0.092	0.606	1.000	20.338
	5.0	290.4	0.007	0.091	0.502	1.000	20.317
0.03	2.0	329.5	0.110	0.050	15.437	0.456	19.846
	3.0	296.6	0.005	0.062	0.742	1.000	20.184
	4.0	191.0	0.067	0.150	0.065	1.000	20.080
	5.0	191.3	0.063	0.121	0.046	1.000	20.092
0.04	2.0	371.0	0.200	0.050	0.503	1.397	19.410
	3.0	192.2	0.048	0.068	0.275	1.000	19.861
	4.0	294.5	0.006	0.074	0.698	1.000	19.804
	5.0	191.9	0.061	0.150	0.104	1.000	19.820

5.3. Discussion of results

From the results shown in Section 5.1, it can be seen that there are huge differences in the fitness function depending on the relative position of the engine sprocket axis with respect to the swingarm axis. The higher the road irregularities, the higher the difference in the results. In addition, the results of the optimizations lead to the following conclusion: the optimal position of the engine sprocket is aligned with the swingarm and very close to its axis (Fig. 12).

In this work, three parameters have been optimized: L_2 , a_2 and R_{WS} . The swingarm length, (L_{SA}), and the swingarm design angle, (φ_0), have not been considered because they strongly affect the wheelbase and the equivalent stiffness of the rear suspension. This way, the optimization is not affected by the suspension system. Optimizing the value of the transmission

Table 13
Optimized parameters to maximize the fitness function. Road profile: Gaussian.

Best					
a_2	L_2	R_{WS}	Slack	SR	fitness fun
deg	m	m	mm	.	m
235.0	0.011	0.118	0.536	1.000	20.674
354.7	0.034	0.081	0.543	1.000	20.698
273.6	0.006	0.082	0.311	1.003	20.699
343.7	0.021	0.099	0.942	1.001	20.584
350.4	0.036	0.108	0.924	1.001	20.677
308.3	0.007	0.071	0.361	0.999	20.689

Table 14
Geometry parameters.

	Geometry 1	Geometry 2	Units
a_2	0	270	deg
L_2	0.00	0.15	m
R_{WS}	0.093	0.150	m
SR	1.092	0.239	–
Slack	0.000	67.270	mm
d	19.868	19.497	m

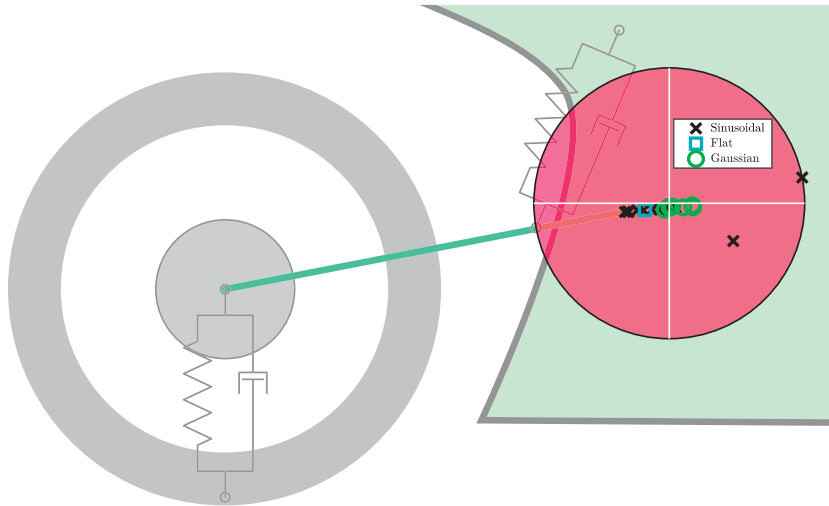


Fig. 12. Solutions from genetic algorithms.

ratio has not been considered either, since the objective is to determine the optimal position of the engine sprocket with respect to the swingarm axis.

On the other hand, it has been observed that it is necessary to model the entire motorcycle, allowing pitch and bounce vibration modes and not only the rear train. Previous simulations carried out with a simplified model showed that optimizations converged to a final drive geometry with the engine sprocket placed in the lowest positions if pitch and bounce movements were restricted. If the engine sprocket is placed very low, the force of the chain compresses the rear wheel. This increases its vertical load and reduces the effective radius, which maximizes the longitudinal force and, thus, the distance traveled. However, this simplification of studying only the rear axle is not valid since the load on the rear wheel cannot grow indefinitely. These phenomena have been eliminated by modeling the front train and allowing these two additional movements.

Fig. 13 shows the values of traveled distance, chain tension, squat ratio, vertical force, longitudinal slip and longitudinal force for the two geometries given in Table 14.

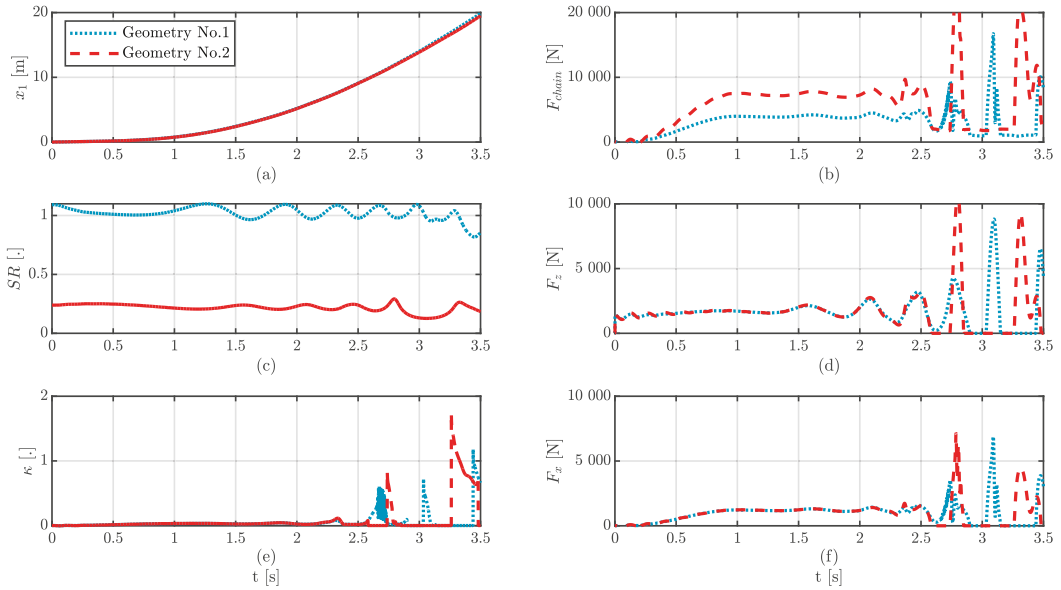


Fig. 13. Traveled distance, chain tension, squat ratio, vertical force, longitudinal slip and longitudinal force against time for two different geometries. Sinusoidal road: $H_y = 4$ cm, $\lambda = 3$ m.

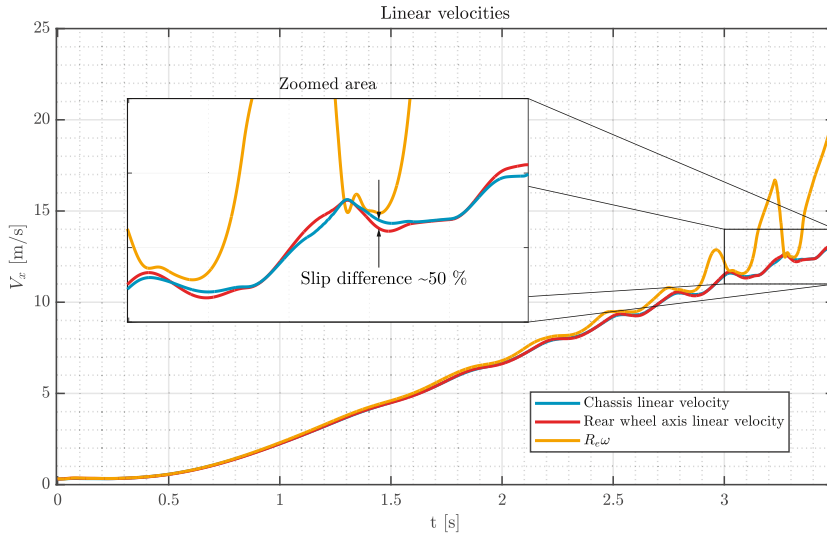


Fig. 14. Different linear velocities.

The first geometry (geometry 1) has been provided by the optimization algorithm. These results propose a configuration with concentric axes ($L_2 = 0$). The radius of the wheel sprocket is the average value provided by the 23 optimizations: $R_{W5} = 93$ mm.

For comparison purposes, a second geometry has been simulated. In this case, the sprocket is placed just below the swingarm axis at a distance of 150 mm, ($L_2 = 0.15$ m and $a_2 = 270^\circ$), and the radius of the wheel sprocket is 50 mm.

In this simulation, a sinusoidal road with an amplitude of 4 cm and a wavelength of 3.0 m was used. Differences up to 2% were observed in the distance traveled between both geometries (Fig. 13(a)). Fig. 13(e) also shows that the optimized

geometry leads to fewer slip fluctuations, which improves the stability of the motorcycle. Besides, the rear wheel of the optimized geometry stays in contact with the ground longer compared to the second geometry, which contributes to traveling a greater distance.

From the results shown in Fig. 13, it can be seen that it is necessary to consider a tire model that takes into account both the non-linearities that relate to the longitudinal slip and longitudinal force as well as the delay that exists in the generation of the longitudinal slip. This result implies that the interaction of the tire and the road with a simple tire model is not reproduced with sufficient accuracy for extreme conditions, such as the conditions analyzed in this paper, where sudden variations in vertical load and longitudinal slip occur.

It is also necessary to emphasize the importance of the proper selection of longitudinal velocity for the calculation of longitudinal slip (Eq. 39). Fig. 14 shows that the longitudinal slip velocity (V_{sx}), and therefore slip (κ), can be doubled depending on whether the linear velocity of the chassis or wheel axle is considered.

The video attached to this paper shows the simultaneous behavior of both configurations during 3.5 s of simulation, showing the results of this study.

6. Conclusions

In this work, an in-plane dynamic model of a motorcycle has been developed. Special attention has been given to the modeling of the transmission system and its influence on the power delivery.

A non-linear tire transient model has been used to reproduce the generation of contact forces between the tire and road. This model makes it possible to start the simulation from standstill, where slip calculation usually presents singularities and numerical errors. In addition, this model takes into account the delay that exists between the slip changes and the subsequent generation of contact forces. This characteristic of the proposed methodology is of particular interest in situations where sudden changes in the longitudinal slip take place, such as riding on irregular roads and during ABS and TCS operation.

The modeling of the motorcycle has been carried out by using 30 natural and 9 mixed coordinates respectively. This way, the mass matrix is constant and no Coriolis or centrifugal forces appear in the model equations. Consequently, a simplified formulation and easier programming of the dynamic equations are achieved.

An augmented Lagrangian formulation has been used. Implicit integrators have also been programmed, both single-step: trapezoidal, and multi-step: Adams-Bashforth (predictor) and Adams-Moulton (corrector). In addition, an under-relaxation factor has been employed to improve the stability of the integrator, which allows solving stiff problems. As a result, real time simulations have been achieved.

The model developed has been used to simulate the longitudinal dynamics of a motorcycle riding on uneven roads. In order to study the optimal configuration of the final drive elements, an optimization process of the relative position and size of the sprocket axis has been carried out. In this process, the transmission ratio is kept constant.

The results of this work show that, in order to maximize power transmission from the engine to the road, the optimal position of the engine sprocket axis relative to the swingarm axis should be virtually concentric or aligned with the swingarm. This conclusion is consistent with the usual configuration observed in sports motorcycles, in which power transmission has to be maximized.

Future works will include the optimization of the suspension system, including their non-linearities as well as the angle and length of the swingarm. Furthermore, the proposed model will be used to develop improved traction and braking control systems.

Declaration of Competing interest

The authors declare that they have no conflict of interest.

Acknowledgements

This work was partly supported by the Ministry of Economy, Industry and Competitiveness under grant TRA2015-67920-R, partly by the Ministry of Education, Culture and Sport under grant FPU17/03161.

Supplementary material

Supplementary material associated with this article can be found, in the online version, at doi:10.1016/j.mechmachtheory.2019.103647.

References

- [1] V. Cossalter, R. Lot, M. Massaro, Modelling, Simulation and Control of Two-wheeled Vehicles, John Wiley & Sons Ltd, 2014, doi:10.1002/9781118536391.
- [2] N. Srivastava, I. Haque, A review on belt and chain continuously variable transmissions (CVT): dynamics and control, Mech. Mach. Theory 44 (1) (2009) 19–41, doi:10.1016/j.mechmachtheory.2008.06.007.
- [3] S. Burgess, C. Lodge, Optimisation of the chain drive system on sports motorcycles, Sports Eng. 7 (2) (2004) 65–73, doi:10.1007/bf02915918.

- [4] V. Cossalter, R. Lot, M. Massaro, The chatter of racing motorcycles, *Veh. Syst. Dyn.* 46 (4) (2008) 339–353, doi:[10.1080/00423110701416501](https://doi.org/10.1080/00423110701416501).
- [5] Y. Tezuka, Y. Shiomi, S. Kokubu, S. Kiyota, *Vibration characteristics analysis in vehicle body vertical plane of motorcycle during turning*, in: *Annual Congress, JSAE Paper*, 2004, pp. 219–224.
- [6] R.S. Sharp, S. Evangelou, D.J.N. Limebeer, Multibody aspects of motorcycle modelling with special reference to autosim, in: J. Ambrósio (Ed.), *Advances in Computational Multibody Systems*, Springer Netherlands, 2005, pp. 45–68, doi:[10.1007/1-4020-3393-1](https://doi.org/10.1007/1-4020-3393-1).
- [7] M. Massaro, R. Lot, V. Cossalter, On engine-to-slip modelling for motorcycle traction control design, *Proc. Inst. Mech.Eng. Part D* 225 (1) (2011) 15–27, doi:[10.1243/09544070/JAUTO1575](https://doi.org/10.1243/09544070/JAUTO1575).
- [8] R.S. Sharp, D.J. Limebeer, A motorcycle model for stability and control analysis, *Multibody Syst. Dyn.* 6 (2) (2001) 123–142, doi:[10.1023/A:1017508214101](https://doi.org/10.1023/A:1017508214101).
- [9] V. Cossalter, R. Lot, A motorcycle multi-body model for real time simulations based on the natural coordinates approach, *Veh. Syst. Dyn.* 37 (6) (2002) 423–447, doi:[10.1076/vesd.37.6.423.3523](https://doi.org/10.1076/vesd.37.6.423.3523).
- [10] R.L. Jackson, I. Green, D.B. Marghitu, Predicting the coefficient of restitution of impacting elastic-perfectly plastic spheres, *Nonlinear Dyn.* 60 (3) (2010) 217–229, doi:[10.1007/s11071-009-9591-z](https://doi.org/10.1007/s11071-009-9591-z).
- [11] M. Machado, P. Moreira, P. Flores, H.M. Lankarani, Compliant contact force models in multibody dynamics: evolution of the hertz contact theory, *Mech. Mach. Theory* 53 (2012) 99–121, doi:[10.1016/j.mechmachtheory.2012.02.010](https://doi.org/10.1016/j.mechmachtheory.2012.02.010).
- [12] F. Marques, P. Flores, J.C. Pimenta Claro, H.M. Lankarani, A survey and comparison of several friction force models for dynamic analysis of multibody mechanical systems, *Nonlinear Dyn.* 86 (3) (2016) 1407–1443, doi:[10.1007/s11071-016-2999-3](https://doi.org/10.1007/s11071-016-2999-3).
- [13] H.B. Pacejka, *Tire and Vehicle Dynamics*, 3, Elsevier, Oxford, 2012, doi:[10.1016/C2010-0-68548-8](https://doi.org/10.1016/C2010-0-68548-8).
- [14] E. de Vries, H. Pacejka, Motorcycle tyre measurements and models, *Veh. Syst. Dyn.* 28 (1) (1998) 280–298, doi:[10.1080/00423119708969565](https://doi.org/10.1080/00423119708969565).
- [15] D. Moreno Giner, *Symbolic-Numeric Tools for the Analysis of Motorcycle Dynamics. Development of a Virtual Rider for Motorcycles based on Model Predictive*, Universidad Miguel Hernández, 2016 Ph.D. thesis.
- [16] A. Robison, A. Vacca, Multi-objective optimization of circular-toothed gerotors for kinematics and wear by genetic algorithm, *Mech. Mach. Theory* 128 (2018) 150–168, doi:[10.1016/j.mechmachtheory.2018.05.011](https://doi.org/10.1016/j.mechmachtheory.2018.05.011).
- [17] F. Silva, M.A. Andrianoely, L. Manin, S. Ayasamy, C. Santini, E. Besnier, D. Remond, Optimization of power losses in poly-V belt transmissions via genetic algorithm and dynamic programming, *Mech. Mach. Theory* 128 (2018) 169–190, doi:[10.1016/j.mechmachtheory.2018.05.016](https://doi.org/10.1016/j.mechmachtheory.2018.05.016).
- [18] J. Garcia de Jalón, E. Bayo, *Kinematic and Dynamic Simulation of Multibody Systems*, Springer New York, New York, 1994, doi:[10.1007/978-1-4612-2600-0](https://doi.org/10.1007/978-1-4612-2600-0).
- [19] L. Shampine, I. Gladwell, S. Thompson, *Solving ODEs with MATLAB* - Shampine Gladwell Thompson, Cambridge University Press, 1st edition.
- [20] J.G. De Jalón, Twenty-five years of natural coordinates, *Multibody Syst. Dyn.* 18 (1) (2007) 15–33, doi:[10.1007/s11044-007-9068-0](https://doi.org/10.1007/s11044-007-9068-0).
- [21] R.S. Sharp, S. Evangelou, D.J. Limebeer, Advances in the modelling of motorcycle dynamics, *Multibody Syst. Dyn.* 12 (3) (2004) 251–283, doi:[10.1023/B:MUBO.0000049195.60868.a2](https://doi.org/10.1023/B:MUBO.0000049195.60868.a2).
- [22] S. Mahalingam, Polygonal action in chain drives, *J. Frankl. Inst.* 265 (1) (1958) 23–28, doi:[10.1016/0016-0032\(58\)90665-3](https://doi.org/10.1016/0016-0032(58)90665-3).
- [23] N. Fuglede, J.J. Thomsen, Kinematics of roller chain drives - Exact and approximate analysis, *Mech. Mach. Theory* 100 (2016) 17–32, doi:[10.1016/j.mechmachtheory.2016.01.009](https://doi.org/10.1016/j.mechmachtheory.2016.01.009).
- [24] S. Evangelou, *The Control and Stability analysis of Two Wheeled Road Vehicles*, 2003 Ph.D. thesis.
- [25] V. Cossalter, *Motorcycle Dynamics*, 2nd, LuLu, 2006, doi:[10.1002/9781118536391.ch1](https://doi.org/10.1002/9781118536391.ch1).
- [26] J. Nocedal, S. Wright, *Numerical Optimization*, 2nd, Springer, 2006.
- [27] J. Baumgarte, Stabilization of constraints and integrals of motion in dynamical systems, *Comput. Methods Appl. Mech.Eng.* 1 (1) (1972) 1–16, doi:[10.1016/0045-7825\(72\)90018-7](https://doi.org/10.1016/0045-7825(72)90018-7).
- [28] N. Fueyo, J.A. Blasco, Relaxation control in the solution of CFD problems, *Int. J. Comput. Fluid Dyn.* 13 (1) (1999) 43–63, doi:[10.1080/10618569908940889](https://doi.org/10.1080/10618569908940889).
- [29] H. Versteeg, W. Malalasekera, *An Introduction to Computational Fluid Dynamics*, 2, Pearson Education, London, 2007.
- [30] J. Cardenal, J. Cuadrado, P. Morer, E. Bayo, A multi-index variable time step method for the dynamic simulation of multibody systems, *Int. J. Numer. Methods Eng.* 44 (11) (1999) 1579–1598, doi:[10.1002/\(SICI\)1097-0207\(19990420\)44:11<1579::AID-NME551>3.0.CO;2-5](https://doi.org/10.1002/(SICI)1097-0207(19990420)44:11<1579::AID-NME551>3.0.CO;2-5).
- [31] T. Foale, *Motorcycle Handling and Chassis Design the Art and Science*, 1, 2002.
- [32] K.S. Rainer, Prince, Differential evolution - a simple and efficient heuristic for global optimization over continuous spaces, *J. Global Optim.* 11 (1) (1997) 341–359, doi:[10.1023/A:1008202821328](https://doi.org/10.1023/A:1008202821328).
- [33] J. Cabrera, A. Ortiz, E. Carabias, A. Simon, An alternative method to determine the magic tyre model parameters using genetic algorithms, *Veh. Syst. Dyn.* 41 (2) (2004) 109–127, doi:[10.1076/vesd.41.2.109.26496](https://doi.org/10.1076/vesd.41.2.109.26496).
- [34] J.A. Cabrera, A. Ortiz, F. Nadal, J.J. Castillo, An evolutionary algorithm for path synthesis of mechanisms, *Mech. Mach. Theory* 46 (2) (2011) 127–141, doi:[10.1016/j.mechmachtheory.2010.10.003](https://doi.org/10.1016/j.mechmachtheory.2010.10.003).

7.2 PAPER #2

7.2.1 Journal article identification:

Title: A Novel Method for Determining Angular Speed and Acceleration Using Sin-Cos Encoders

DOI: 10.3390/s21020577

Coauthors: Pérez Fernández, J.; Velasco García, J.M.; Cabrera Carrillo, J.A.; Castillo Aguilar, J.J.

7.2.2 Quality indicators:

Editor: MDPI

Journal: Sensors

Date of publication: 15 January 2021

Impact factor: 3.576 (JCR)

Quartile and position in its category: 14/64 (Q1) — Instruments & Instrumentation

7.2.3 Published article



Article

A Novel Method for Determining Angular Speed and Acceleration Using Sin-Cos Encoders

Manuel Alcázar Vargas , Javier Pérez Fernández , Juan M. Velasco García, Juan A. Cabrera Carrillo and Juan J. Castillo Aguilar *

Department of Mechanical Engineering, University of Málaga, 29071 Málaga, Spain; manuel.alcazar@uma.es (M.A.V.); javierperez@uma.es (J.P.F.); juanmav@uma.es (J.M.V.G.); jcabrera@uma.es (J.A.C.C.)

* Correspondence: juancas@uma.es

Abstract: The performance of vehicle safety systems depends very much on the accuracy of the signals coming from vehicle sensors. Among them, the wheel speed is of vital importance. This paper describes a new method to obtain the wheel speed by using Sin-Cos encoders. The methodology is based on the use of the Savitzky–Golay filters to optimally determine the coefficients of the polynomials that best fit the measured signals and their time derivatives. The whole process requires a low computational cost, which makes it suitable for real-time applications. This way it is possible to provide the safety system with an accurate measurement of both the angular speed and acceleration of the wheels. The proposed method has been compared to other conventional approaches. The results obtained in simulations and real tests show the superior performance of the proposed method, particularly for medium and low wheel angular speeds.

Keywords: Sin-Cos encoder; ABS encoder; wheel angular speed; Savitzky–Golay filter; vehicle control systems; vehicle sensors



Citation: Alcázar Vargas, M.; Pérez Fernández, J.; Velasco García, J.M.; Cabrera Carrillo, J.A.; Castillo Aguilar, J.J. A Novel Method for Determining Angular Speed and Acceleration Using Sin-Cos Encoders. *Sensors* **2021**, *21*, 577. <https://doi.org/10.3390/s21020577>

Received: 16 October 2020

Accepted: 13 January 2021

Published: 15 January 2021

Publisher's Note: MDPI stays neutral with regard to jurisdictional claims in published maps and institutional affiliations.



Copyright: © 2021 by the authors. Licensee MDPI, Basel, Switzerland. This article is an open access article distributed under the terms and conditions of the Creative Commons Attribution (CC BY) license (<https://creativecommons.org/licenses/by/4.0/>).

1. Introduction

The proper determination of the angular speed of vehicle wheels is of particular importance for active safety systems: Anti-lock Braking Systems (ABS), Traction Control System (TCS), Electronic Stability Program (ESP), etc. [1]. The information from the wheel speed sensors is used as an input parameter to traction and braking control systems [2–4]. Tire longitudinal traction and braking forces depend essentially on the slip ratio, which is the relationship between wheel peripheral speed and the linear speed of the vehicle [5–7]. In the field of brake control systems, it is crucial to determine the angular speed of the wheels in medium and low-speed conditions [6,8,9]. This is because ABS prevents the wheels from locking, so it is required to determine whether the wheel is moving slowly or if it is already locked.

Currently, most of the sensors used to determine the angular speed of the wheels are of the incremental encoder type [1,9]. These provide one or more rectangular signals whose frequency increases as does the angular speed of the wheel. Basically, there are three methods: *M-type*, *T-type*, and a combination of both: *MT-type* to process the output of wheel sensors to estimate the angular speed of the wheels [10]. The first one is more appropriate for high speeds. The computational cost of this method is very low which makes it suitable for real-time systems. However, the main drawback is that the measurement error is high at low speeds. On the contrary, the second one provides highly accurate measurements at low speed but the performance is poor at high speeds. In addition, the computational cost is higher because it is required to perform a division [11]. The third method is based on a combination of the other two. It provides better measurements at medium-low speed, but the computational cost is also higher.

Consequently, all three methods mentioned above have drawbacks that make them inappropriate for some conditions. The main problem is related to the fact that they are based on the use of pulses. When the speed is medium or low, the number of pulses per unit of time can be low or null. This way, none of the previous methods can update the estimated velocity unless a pulse is detected. However, as far as braking control algorithms are concerned, it is of vital importance to make use of reliable wheel angular speed and acceleration measurements. Several modifications of the M/T method have been proposed to cope with the previously mentioned drawbacks. The goals of these proposals are varied, but, in general, they try to improve accuracy and/or computational cost. Thus, the time stamping concept was used to capture the encoder transitions and their time instants at a high clock frequency in [12]. These data were used to estimate position, velocity, and acceleration by means of polynomial interpolation of the encoder events and polynomial extrapolation at the time of interest. Experiments showed improvement of the velocity and acceleration estimations. Similarly, a method to estimate angular velocity by removing the periodical disturbances introduced by sensor imperfections was presented in [13]. To do so, a number of harmonic components of the disturbance were identified and used to improve the velocity estimation. The authors claimed that the proposed scheme represented an improvement over the time stamping algorithm since better estimates were obtained without using a large number of events or introducing a long delay. Similarly, a Single-Phase Self-Adaptive M/T method was proposed in [14] to suppress measurement error and extend speed measurement. The use of a compensation routine was proposed to reduce measurement errors and bias in [15]. These methods improved the estimation accuracy but they required a higher computational cost compared to the conventional M/T method. On the contrary, improvements of the M/T were described in [16–18] to reduce the computational cost by avoiding performing the division operations that the conventional M/T method requires. This way, a so-called Divisionless MT-type velocity estimation algorithm was proposed. The main advantage of this method was that it only required addition and multiplication operations, allowing a cost-effective implementation. Finally, the use of a Kalman filter [19,20] was proposed to increase the accuracy of the calculation of the wheel angular speed and acceleration in ABS systems by removing measurement noise and improving the differentiation method.

Another type of sensor used to measure absolute mechanical angles are resolvers. These devices are abundantly used in industrial applications thanks to their high accuracy, resolution and robustness [21]. Resolvers produce quadrature sinusoidal electrical signals representative of the angular position of the shaft. These signals have to be processed with a suitable converter to determine the angular position. On one hand, open-loop conversion methods have been proposed in the literature to carry out this task. Thus, linearization-based techniques, in which the sinusoidal signals were converted into a linear output signal from which displacement can be determined, were described in [22–24]. Trigonometric methods yield the angular position directly and have a good dynamic response. However, they generally resort to lookup tables to perform the arctangent computation, which increases memory requirements. In addition, differentiation and filtering to remove high frequency noise, which cause phase delay, are required to obtain angular speed and acceleration [25–27]. Further less-common open-loop methods can be found in [28–31].

On the other hand, most closed-loop converters are based on the use of the Phase-Locked Loop (PLL) technique [32–34]. These methods track the angular position and speed smoothly and accurately, but the filter gains have to be properly tuned and it may have problems for high angular acceleration rates. Kalman filter-based closed-loop converters have also been described in [35].

With the massive introduction of electric vehicles, more and more permanent magnet synchronous motors (PMSM) are being used. These electric motors make use of Sin-Cos type encoders. These encoders allow the determination of the relative position between a rotor and a stator with high accuracy, which is decisive for the control of this type of motors.

They provide two analog outputs: the sine and the cosine of the relative angle between the rotor and the stator [36,37]. Commonly, the operation principles of resolver converters are applicable to Sin-Cos type encoders. Hence, open-loop and closed-loop converters can be used to provide the angular position from signals provided by this type of sensor.

Regarding the estimation of angular acceleration from resolvers and Sin-Cos encoders, to the best of our knowledge, only modifications of the PLL described above are found in literature, building another loop at the output of the speed estimator to obtain angular acceleration [38,39]. These systems must be tuned for each application, and it is necessary to consider the bandwidth. In commercial chips, this adjustment is usually done in an analogical way, since they consist of capacitors and resistors [40,41].

On the other hand, when the speed of the rotating element equipped with Sin-Cos encoders is high, counting zero-crossings gives a sufficiently approximate measurement of the angular speed. However, in the automotive field, and more specifically within traction control and braking algorithms, it is interesting to measure low angular speeds. Therefore, it is necessary to address this problem to find an appropriate strategy for all wheel speed conditions.

In this work, a novel open-loop method for the determination of speed and angular acceleration from the signals provided by a Sin-Cos encoder is proposed. The proposed approach is based on the use of Savitzky-Golay (S-G) filters. The S-G filter has been described to be used in chemical analysis, image processing fields, signal processing and biomedical data processing [42–44]. However, to the best of our knowledge, the use of this method with Sin-Cos encoders and resolvers has not been proposed up to now.

The main advantages of this method are related to a fast and direct calculation of time derivatives, its low computational cost, and that the delay introduced in the filtered signal is known in advance. A further advantage of the proposed method is that the matrix defined in the calculations is composed of only integer numbers. In addition, the mathematical operations required to obtain the filtered data involve mainly integer numbers. Noninteger numbers are only required in the last stage of the filter. Finally, a remarkable advantage of the developed method is that angular speed and acceleration can be obtained as continuous signals by using only additions and multiplications. These advantages simplify the implementation of this method in FPGA-based systems since less computational effort and fewer logic blocks are required. Thus, it properly measures high, medium, and very low speeds. On the other hand, the main drawback is that the order and number of side-points of the filter have to be properly determined. The method developed for the determination of speed and angular acceleration is described. The performance of the proposed method has been evaluated by means of simulations. Finally, a validation of the method from experimental data has been carried out. In automotive applications, wheel angular speeds can be low in some cases (i.e., traction and braking control systems). This way, the use of these sensors in low-speed conditions requires new methods to provide accurate measurements. This paper is intended to serve as an approach to the use of S-G filters in this kind of applications.

This work is structured as follows: first, the mathematical development of the algorithm presented in the work is exposed in Section 2. Next, the results obtained in simulations and real tests are included in Section 3. Results are divided into two subsections. In the first one, the method is validated and its performance is verified by means of simulations. In the second one, the algorithm developed is implemented in a real system and its performance is evaluated. The advantages of the proposed method and the conclusions of this work and are drawn in Section 4.

2. Materials and Methods

Sin-Cos encoders provide two analog signals: the sine and the cosine of the relative angle between the rotor and the stator [36,37]. The following novel method is proposed to determine the rotor angular speed and acceleration, which is the fundamental contribution of this work. This method resorts to the Savitzky-Golay filter to calculate the time deriva-

tives of the output signals. This way, the angular speed and acceleration are computed requiring only sums and multiplications. The mathematics of this method is described next.

Be the encoder outputs x and y (Equations (1) and (2)):

$$x = A \cos(\omega t + \varphi), \quad (1)$$

$$y = A \sin(\omega t + \varphi), \quad (2)$$

where A is the amplitude, ω is the angular speed, and φ is the phase shift. The relative angle between the rotor and the stator is given by expression Equation (3):

$$\theta = \operatorname{atan}\left(\frac{y}{x}\right), \quad (3)$$

The angular speed of the rotor is given by the time derivative of the angular coordinate Equation (4):

$$\frac{d\theta}{dt} = \dot{\theta} = \frac{\frac{d}{dt}\left(\frac{y}{x}\right)}{1 + \left(\frac{y}{x}\right)^2}, \quad (4)$$

Operating:

$$\dot{\theta} = \frac{\frac{x\dot{y} - \dot{x}y}{x^2}}{\frac{x^2 + y^2}{x^2}}, \quad (5)$$

$$\dot{\theta} = \frac{x\dot{y} - \dot{x}y}{x^2 + y^2}, \quad (6)$$

where $x^2 + y^2 = A^2 \sin^2(\omega t + \varphi) + A^2 \cos^2(\omega t + \varphi) = A^2$, is constant. It is rewritten:

$$\dot{\theta} = \frac{1}{A^2} (x\dot{y} - \dot{x}y), \quad (7)$$

Differentiating again with respect to time and rearranging, the expression for angular acceleration can be obtained Equation (8):

$$\frac{d^2\theta}{dt^2} = \ddot{\theta} = \frac{1}{A^2} (x\ddot{y} - \ddot{x}y), \quad (8)$$

Therefore, it is necessary to differentiate the sensor signals to obtain both the angular rotor speed and acceleration. To do so, the Savitzky-Golay (SG) filters [45,46] are used to filter the signals and determine their time derivatives. These filters optimally fit a set of data points to polynomials of different orders. In order to use this tool, the points have to be equispaced in time and cannot have discontinuities. Some of the advantages of this method include the following:

- It allows the direct calculation of the time derivatives.
- The delay of all time derivatives, including the zeroth derivative is identical.
- Once the filter parameters are determined, the computational cost is very small since only additions and multiplications are required. This allows it to be used in real-time applications with very high sampling and processing frequencies.
- The Savitzky-Golay filter optimally fits a set of data points to a polynomial using least-squares regression.

To use the SG filter, it is necessary to set the order of the interpolation polynomial and the number of side points. Once defined, the matrix of coefficients \mathbf{g} is calculated. Each of the columns of this matrix constitutes the convolution vector used to determine the time derivatives. The way to proceed with the mathematics is different if the angular speed is calculated in real-time or if it is obtained through postprocessing computation. Thus, in real-time, the convolution operation is replaced by the dot product of the corresponding column of the matrix \mathbf{g} by the last m elements of the data vector (\mathbf{x}) , where m is the number

of rows of the matrix \mathbf{g} ($m = 2 \cdot \text{sidepoints} + 1$). In this case, the delay of the output signal is equal to the number of side points.

On the contrary, for data postprocessing applications, a single convolution of the whole data vector and the corresponding column of the matrix \mathbf{g} is performed. In the latter case, the signal is not delayed.

This way, and for real-time applications such as braking control systems, the filtered value of the signal for the point k (\hat{x}_k) is the dot product of the first column of the convolution matrix (\mathbf{g}_0) by the last values of the data vector (\mathbf{x}) by the term $(-\Delta t)^{-p}$ and by $p!$, where p is the order of the time derivative (see Equations (9)–(11)).

$$\hat{x}_k = 0! \cdot \mathbf{g}_0^T \cdot \mathbf{x} \cdot (-\Delta t)^{-0} = \mathbf{g}_0^T \cdot \mathbf{x} \quad (9)$$

$$\hat{x}_k = 1! \cdot \mathbf{g}_1^T \cdot \mathbf{x} \cdot (-\Delta t)^{-1} = -\mathbf{g}_1^T \cdot \mathbf{x} \cdot \Delta t^{-1} \quad (10)$$

$$\hat{x}_k = 2! \cdot \mathbf{g}_2^T \cdot \mathbf{x} \cdot (-\Delta t)^{-2} = 2 \cdot \mathbf{g}_2^T \cdot \mathbf{x} \cdot \Delta t^{-2} \quad (11)$$

It is important to note that the delay is equal to the number of side points if the angular speed is calculated in real-time. Consequently, it is interesting to reduce the number of points used. On the other hand, the results obtained with a low-order polynomial (two or three) are satisfactory in the case of filtering a sinusoidal signal for some applications (i.e., estimating relative position). However, the order of the polynomial, as well as the number of points to be used, has to be determined if the goal is to accurately calculate the angular speed and acceleration. Therefore, the optimal polynomial order and the number of points have been studied for this application. Figure 1 shows different polynomials fitting the output signal of a Sin-Cos encoder. Figure 2 shows the errors of these fittings. Figures 3 and 4 show the calculation of the angular speed and the angular acceleration respectively using different polynomials.

The procedure consists of the following. First, for comparison purposes, the data points are fitted by means of a sine, obtaining the fundamental parameters of the wave, namely: amplitude, frequency, and phase shift. In this case, the R-squared (R^2) reached is greater than 0.999. These parameters determine the signal named “Fitted signal” or “Best-fit”. It is important to highlight the fact that this fitting operation cannot be performed in real-time. Despite being not appropriate for real system applications, it has been used to select the best filter configuration in this problem. Knowing the frequency of the sine wave, the angular speed of the wheel can be determined ($\omega = 2 \cdot \pi \cdot f$). In this case, there is no angular acceleration. These fitted values are the reference to estimate the errors of the process.

Then, the sine is fitted to polynomials of different orders and number of side points. This way, polynomials of order 2, 3, and 4; and 3, 5, and 7 side points are represented in Figures 1 and 2. It is important to point out that matrix \mathbf{g} has some interesting characteristics depending on the order of the polynomial. The convolution coefficients for the zeroth and second-time derivatives are identical in the case of polynomials of order 2 and 3, as well as 4 and 5. Similarly, in the case of the first and third-time derivative, the polynomials of orders 1 and 2 are the same, and those of orders 3 and 4 are equal too. Therefore, polynomial fitting of order 2 is not shown in Figures 1 and 2 for the zeroth and second time derivative (it is identical to third order) and the fourth-order polynomial is not shown for the first time derivative (identical to third order). In the case of Figure 3, all orders of the polynomials are shown since time derivatives zero, one, and two are combined.

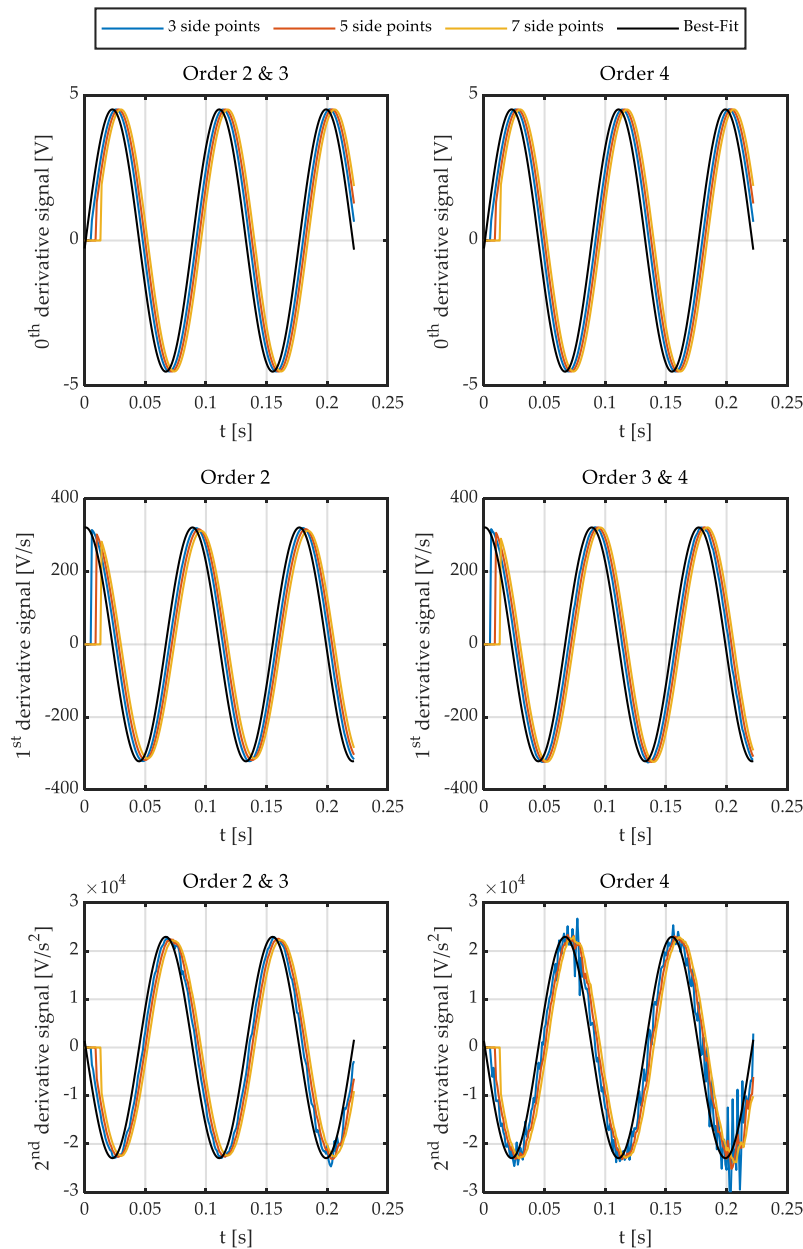


Figure 1. Signals fitted by a sine (black) and signals fitted by polynomials using the Savitzky-Golay method. (top) zeroth derivative. (center) first derivative. (bottom) second derivative.

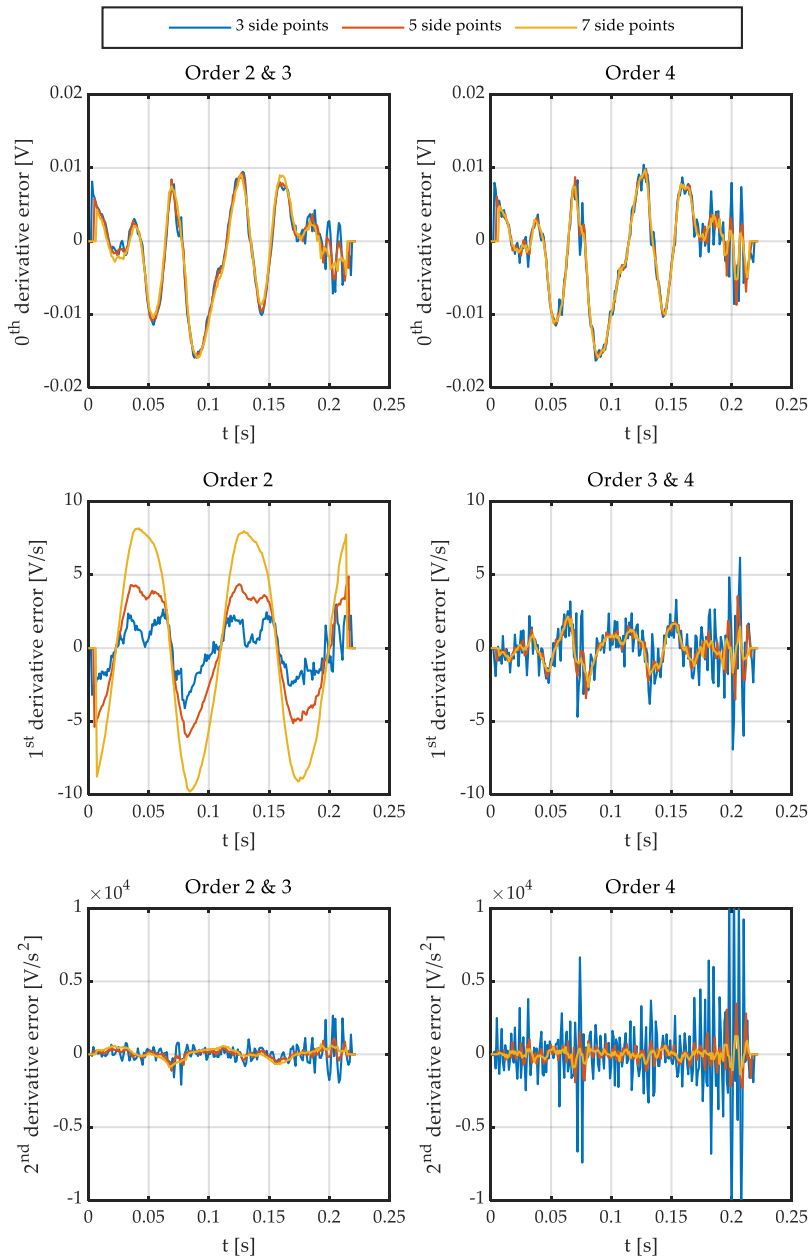


Figure 2. Errors of the signals fitted by polynomials using the Savitzky-Golay method. (**top**) zeroth derivative. (**center**) first derivative. (**bottom**) second derivative.

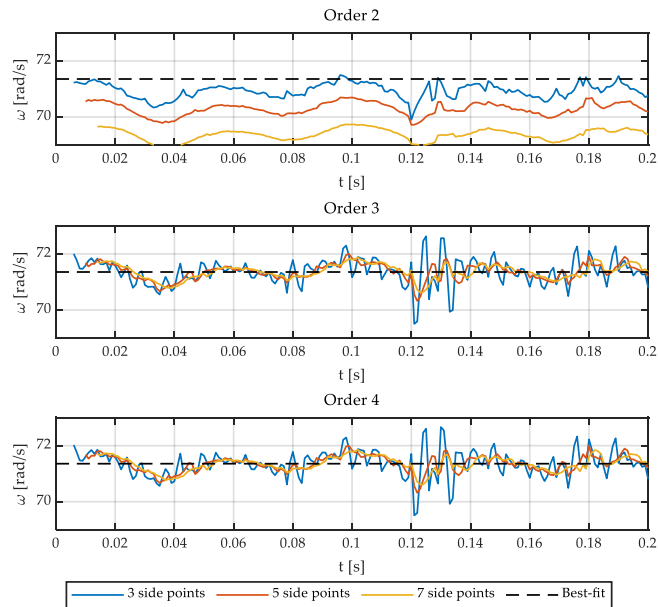


Figure 3. Angular speed fitted to polynomials of order 2, 3, and 4 with 3, 5, and 7 side points.

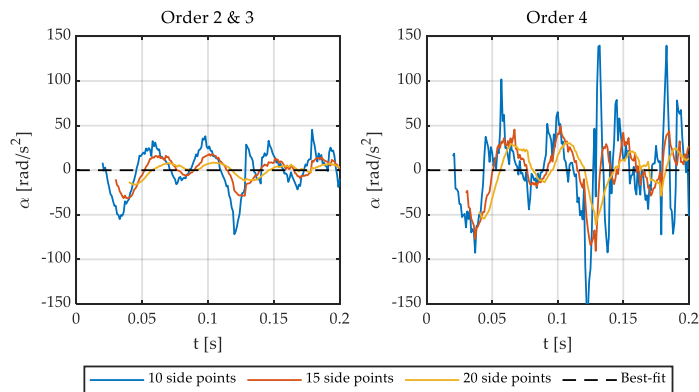


Figure 4. Angular acceleration fitted to polynomials of order 2, 3, and 4 with 10, 15, and 20 side points.

Figure 1 also shows that the delay increases as the number of side points does. In addition, it can be seen that a parabola is not able to fit the sine properly, slightly reducing the amplitude of the first derivative. As a result, the use of polynomials of at least order three for the calculation of angular speeds is required.

Finally, it can be seen that it is necessary to significantly increase the number of side points (and therefore the delay) in the case of polynomials of order 4 since the noise of these is considerably higher than those of order 3 (see Figures 1 and 2).

In this work, it has been decided to use a cubic polynomial and 5 side points for the system under study. Once the number of side points has been decided, the delay can be precisely calculated. Moreover, the delay is the same whatever the frequency of the input signal. Furthermore, the delay of all time derivatives is identical provided that the same S-G filter parameters are used. These parameters are related to the computational

cost, phase lag, and filtering effect. This way, the higher the number of side-points, the higher the delay but also the filtering effect. Conversely, the higher the order, the lower the filtering effect. The acquisition and processing of the analog signals are carried out at a frequency of 1 kHz. This way, the delay in the determination of the signals (position, speed, and acceleration) is 5 ms. This configuration allows an accurate calculation of speeds of up to 250 km/h for a medium-sized wheel (car, motorcycle, etc.).

Table 1 shows the **g** matrix for the case previously mentioned. The table has been reproduced similarly as it was published in [45] so that only integers are written. Actually, these are fractional numbers, so it is necessary to divide each g_k by the divisor of its corresponding column. The procedure to calculate the **g** matrix for different cases can be found in [45,46], among others. In the case of using MATLAB® (R2019b, Natick, MA, USA), the `sgolay` function directly returns the **g** matrix.

Table 1. Matrix **g** for 5 side points and order 3.

g	Filter/ 0th Derivative	1st Derivative	2nd Derivative
g_{k-10}	−36	300	30
g_{k-9}	9	−294	12
g_{k-8}	44	−532	−2
g_{k-7}	69	−503	−12
g_{k-6}	84	−296	−18
g_{k-5}	89	0	−20
g_{k-4}	84	296	−18
g_{k-3}	69	503	−12
g_{k-2}	44	532	−2
g_{k-1}	9	294	12
g_k	−36	−300	30
Divisor	429	5148	858

3. Results

The results of the described method are presented in this section. To do this, first, simulations with the most common methods used in commercial ABS encoders and Sin-Cos encoders were carried out. Then, the method proposed in this work is compared to the methods mentioned above. Next, real tests were conducted on the bench to evaluate the performance of these methods in a real system.

3.1. Simulations

Simulations were carried out to validate the proposed method, called *SinCos-method*. The ABS encoder used in the vehicle model MINI Cooper has been reproduced. This encoder is the same one that will be later used in the real test. Figure 5 shows the measured variables for each of the four methods: *M-type*, *T-type*, *MT-type*, and *Divisionless-MT-type*.

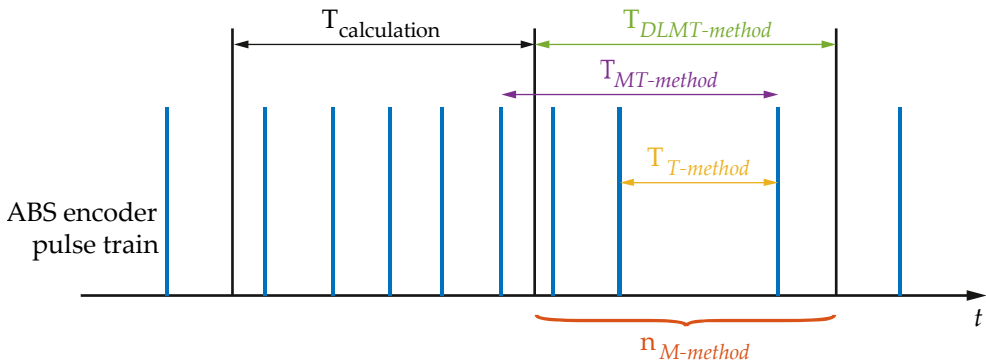


Figure 5. Measured variables for the four different methods mentioned.

Where $T_{\text{calculation}}$ is the calculation period, $T_{\text{MT-method}}$ is the time interval between the last pulse of the current period and the last pulse of the period in which at least one pulse was detected, $T_{\text{T-method}}$ is the time interval between the last two pulses of the current interval, and $n_{\text{M-method}}$ is the number of pulses in the current interval.

First, the following analysis has been made to determine the calculation frequency ($f_{\text{calculation}}$) of the angular speed from the ABS encoder. To do so, the angular speed given by the linear function $\omega(t) = 100 - 100t$, $t \in [0, 1]$ has been simulated. The digital signal of the ABS encoder was sampled at $f_{\text{sample,ABS}} = 1$ MHz. The angular speed was calculated at six different frequencies, namely: $f_{\text{calculation,ABS}} = 20, 50, 100, 200, 500, 1000$ Hz. The angular speed has been determined for each of these six frequencies using four aforementioned methods. The term “Ideal” is used in the following figures to define the reference magnitude. The results are shown in Figure 6.

The following conclusions can be drawn from these results. The noise of the signals is small at low frequencies (Figure 6a,b) with greater delay as the calculation frequency decreases. *M* and *T* methods provide noisy signals for higher frequencies (Figure 6e,f). In both cases, the calculation frequency cannot be very high because a minimum number of pulses have to be counted within the calculation period. If no pulses are detected in the current period, the output of both methods (*M* and *T*) is equal to zero.

It is important to note that the *T-method* performs well above a determined angular speed. Provided that at least two flanks of the encoder signal enter within a calculation period, the results yielded by this method are accurate ($f_{\text{ABS}} \geq 2 f_{\text{calculation}}$). On the other hand, the performance of the *MT-method* is fairly good regardless of the calculation frequency but for very low angular speeds. This is because this method resorts to previous calculation periods before the current one if no pulses enter in the current period. This way, it goes back to previous periods until it finds the last pulse that entered and the speed is obtained from data measured prior to the current calculation period. The disadvantage of the *MT-method* is that the computational cost is the highest of the three. Finally, the performance of the *Divisionless-MT-type* method is similar to the one provided by the *MT-type* method except for low speed, where high fluctuations are observed.

Based on these previous results, an intermediate calculation frequency of 100 Hz has been chosen for the simulations and the experimental tests. This frequency is considered appropriate for traction and braking control applications since it shows a good balance between accuracy and measurement delay. Next, the comparison between the aforementioned methods is shown. To do so, simulations were carried out reproducing a braking process. Figure 7 shows the results obtained for an input angular speed given by the linear function $\omega(t) = 100 - 100t$. The following default parameters were set: $f_{\text{sample,ABS}} = 1$ MHz, $f_{\text{calculation,ABS}} = 100$ Hz, $f_{\text{sample,Sin-Cos}} = f_{\text{calculation,Sin-Cos}} = 1$ kHz. The number of pole pairs (i.e., pulses per revolution) of the ABS encoder is 176.

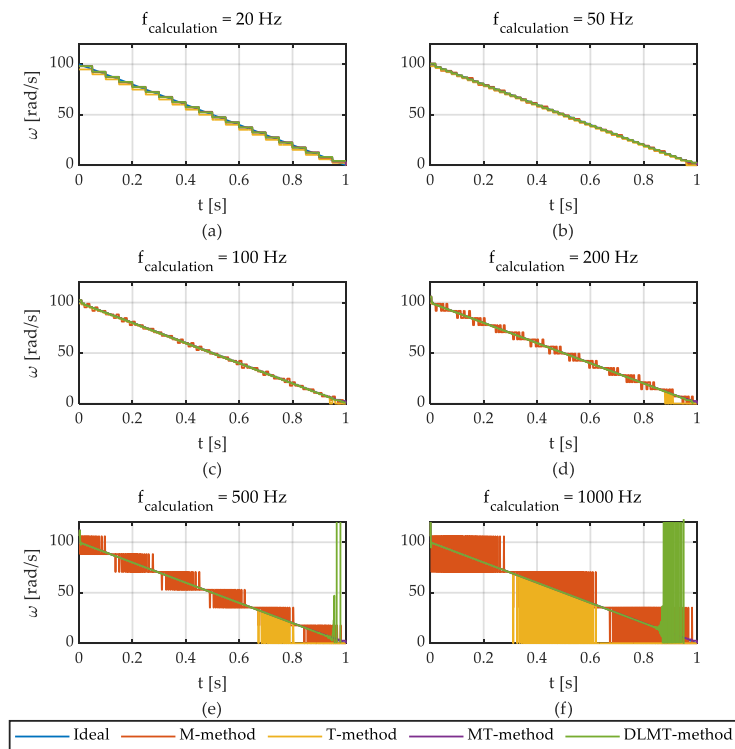


Figure 6. Angular speed estimation for different calculation frequencies.

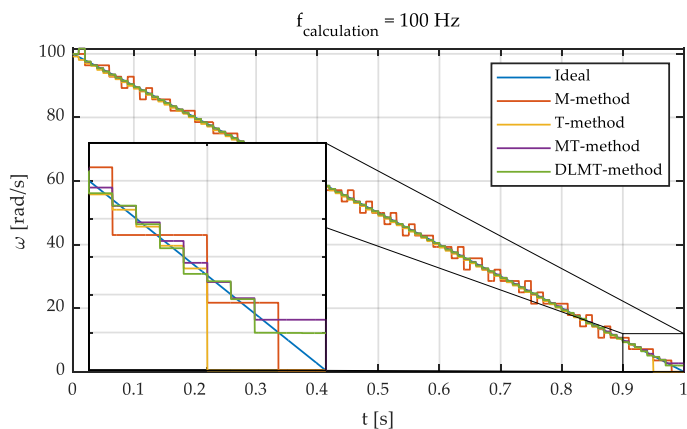


Figure 7. Simulation with different methods. $d\omega/dt = -100 \text{ rad/s}^2$. $\omega_0 = 100 \text{ rad/s}$.

It can be seen that the performance of the DLMT method is similar to the MT when the angular velocity is high. Conversely, the main disadvantage is that it is not able to provide adequate measures at low angular speeds. The following steps can be carried out to cope with this problem. The first one is to store the number of elapsed intervals without any

input pulse. Next, it becomes necessary to make a division or store in memory the value of $[(n - 1) \cdot T_s]^{-1}$, where n is the number of intervals that have elapsed without arriving pulses. Thus, these steps greatly increase the computational cost of this approach. Consequently, this method is discarded since a fast and accurate measurement of low angular speeds is required in traction control and braking algorithms, the MT being considered the most appropriate one for this type of applications.

On the other hand, speed and angular acceleration with sinusoidal transducers can also be determined using a closed-loop dual-PLL configuration [38,39]. Figure 8 shows an outline of this approach. It consists of a first loop to determine angular velocity ($\hat{\omega}$) and position ($\hat{\theta}$) and a second loop, with a similar structure, to determine angular acceleration (\hat{a}). This second loop includes a first-order low-pass filter with time constant (τ). Five parameters have to be set, namely: $K_{p,1}$, $K_{i,1}$, $K_{p,2}$, $K_{i,2}$, τ . These parameters should be tuned, taking into account the noise of the signals coming from the Sin-Cos encoder, the maximum allowable delay and the sampling frequency, among others.

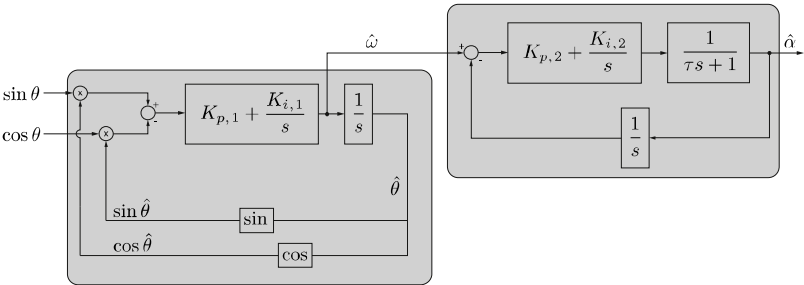


Figure 8. Dual-Phase-Locked Loop (PLL) scheme for estimation of angular speed and acceleration.

Next, a comparison between the MT-method, PLL, and the proposed method (SinCos. RT) is carried out. To do so, a braking process given by the parabolic function $\omega(t) = 100 - 100 t^2$ with the same default parameters used in the previous simulation was reproduced. Figure 9 shows the estimated angular speeds with the three methods.

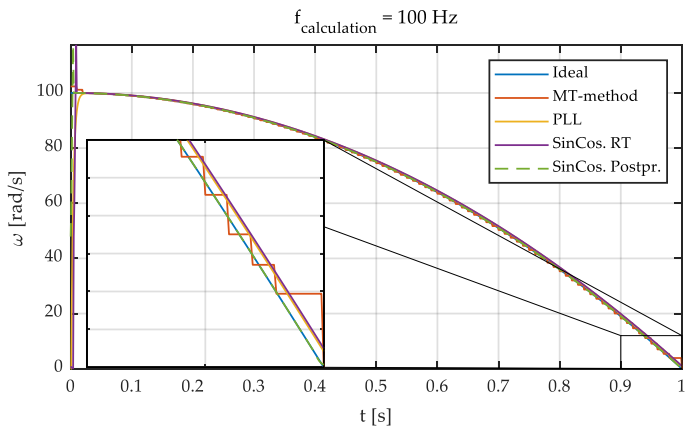


Figure 9. Simulation with different methods. $d\omega/dt = -200 \cdot t \text{ rad/s}^2$. $\omega_0 = 100 \text{ rad/s}$.

As expected, the noise in the signals is greatly reduced with the selected calculation frequency of 100 Hz. Furthermore, the speed determined according to MT-method almost converges to the true value. Finally, it is observed that the PLL and SinCos-methods also

perform satisfactorily. In this last case, the delay is constant being determined by the number of points chosen for the calculation of the speed. It has also been plotted the angular speed calculated using the SinCos-method replacing the dot product by a convolution operation. In this case, 15 side points have been selected and no delay exists between the calculated wheel speed and actual wheel speed. This demonstrates that this method can be used to obtain the angular speed for postprocessing applications. This output can also be considered as the reference wheel speed.

Next, a braking process with an ABS is simulated. The initial linear velocity is 30 m/s. The wheel radius is 0.30 m. This way, angular speed is 100 rad/s for the first second. Then, a severe braking maneuver takes place. The following parameters were imposed: linear deceleration 10 m/s², maximum angular deceleration 500 rad/s², and maximum angular acceleration 1500 rad/s². The slip ratio, that is, the ratio between peripheral wheel speed and vehicle speed, is kept between 20 and 80%. The vehicle fully stops after 3 s of braking. Figure 10 shows the angular velocity and acceleration (α) of the wheels. These magnitudes have been calculated using the three methods previously described. In the case of the acceleration estimation using the S-G Filter, as a second time derivative is required, it is recommended to increase the number of side points used. Therefore, a total of 6 side points have been considered for acceleration estimation. Figure 10 shows a simulation in which the sine and cosine signals have an amplitude of 4.5 V and white noise of $\mu = 0$ and $\sigma = 6$ mV. These noise parameters have been considered to reproduce the measured noise of the real signals from the Sin Cos encoder.

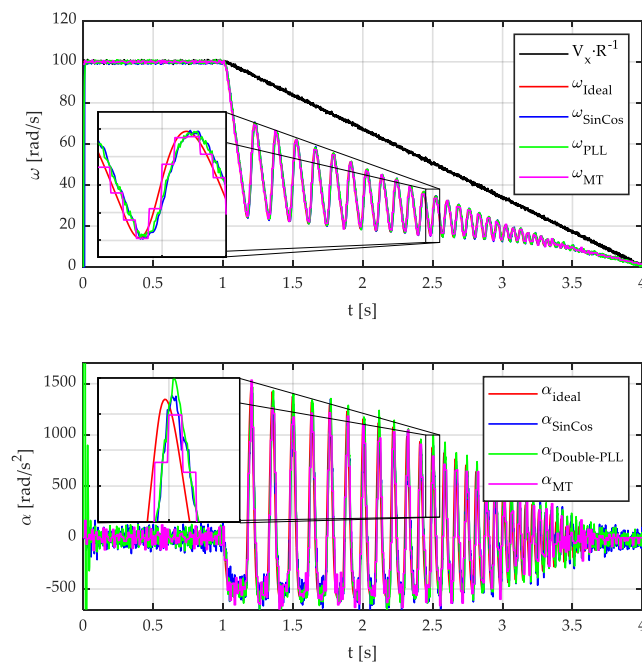


Figure 10. Simulated angular acceleration with noise. Sin-Cos amplitude: 4.5 V. Sin-Cos standard deviation noise: 6 mV.

To obtain angular acceleration from the incremental encoder, a simple two-point estimator has been considered (Equation (12)). Some other approaches could have been considered, such as Kalman filters [47], but at the expense of a high increase in the computational cost.

$$\alpha_k^{MT} = \left(\omega_k^{MT} - \omega_{k-1}^{MT} \right) \cdot f, \tag{12}$$

With regards to the double PLL algorithm (Figure 8), five parameters have been properly tuned. The PI parameters of the first loop are $K_{p,1} = 60$ and $K_{i,1} = 0.1$. For the second loop, the value of these parameters are $K_{p,2} = 400$ and $K_{i,3} = 0.1$. The time constant of the first-order filter, τ , is set to 5 ms. It can also be noted that the contribution of the integral part of the PI is almost negligible.

It can be seen that the PLL-based and S-G filter methods provide similar results. In both cases, the angular speed and acceleration match to real values adequately. Similar delays are obtained in both cases. On the contrary, the *MT-type method* provides discontinuous values due to discrete pulses from the incremental encoder and the calculation frequency.

To evaluate the computational cost of each method, the time required to measure the speed in the previous simulation at the selected frequency of 100 Hz was recorded. An Intel(R) Core™ i7-7700HQ CPU, 2.80 GHz, 16 GB RAM machine using MATLAB was used in this test. Simulations were repeated 1000 times and the average execution time was obtained. Results are listed in Table 2. It can be seen that the computation cost of the proposed methods is considerably lower compared to its competitors.

Table 2. Computational cost of the different methods.

Method	M	T	MT	DLMT	PLL	SinCos
Time (ms)	2.3531	4.8033	4.7263	3.4798	0.0251	0.0237

3.2. Bench Tests

For comparison purposes, the proposed *SinCos-method* and the *MT-method* were programmed in the IMMa (*Ingeniería Mecánica Málaga—Mechanical Engineering Málaga*) Flat Track tire test bench [47]. In this test bench, both the angular wheel speed (ω) and the linear belt speed (V_x) can be measured (Figure 11). *M-method*, *T-method*, and *Divisionless-MT-type* were not included in this comparison because their performances are inferior compared to the *MT-method*, as it was shown in the previous subsection.

These comparative tests require the use of two sensors of different technologies: incremental magnetic encoder also called in the automotive field “ABS encoder” (Figure 12), and absolute encoder Sin-Cos. The former was placed beside the brake disk while the latter was already installed on a Kistler RoaDyn P625 wheel force transducer used in this test bench (Figure 11). Finally, A 5th wheel equipped with a high-end incremental magnetic encoder with 4000 pulses per revolution was used to measure the linear speed of the belt.

A sbRIO-9637 Single-Board Controller by National Instruments™ was used to perform data acquisition. This device includes an FPGA and a real-time operating system. To avoid possible asymmetries in the output signal of the Hall effect sensor, the rising edges provided by the incremental encoder were used to measure the angular speed. Equation (13) was used to determine the angular speed from the ABS sensor:

$$\omega_{ABS} = \frac{2 \pi x}{p T_{ABS}^{MT}}, \tag{13}$$

where ω_{ABS} is the measured angular speed, x is the number of pulses that entered during T_{ABS}^{MT} , p is the number of pulses of the ABS encoder, T_{ABS}^{MT} is the time gap between the last pulse of the previous calculation period and the last flank (see Figure 5). This time is measured by counting ticks within two pulses with a 1 MHz clock. The subscripts “ABS” and “Sin-Cos” are used to indicate that the signals come from the ABS encoder and Sin-Cos encoder respectively.

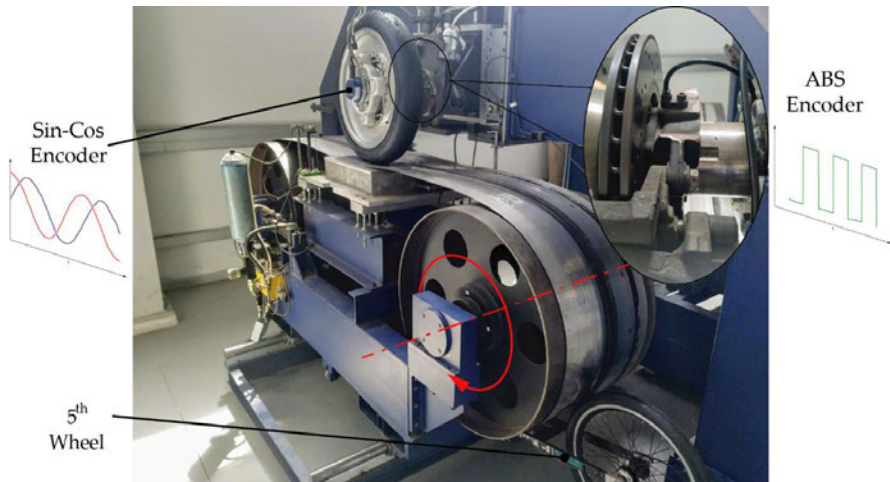


Figure 11. IMMA Flat track with speed sensors depicted.

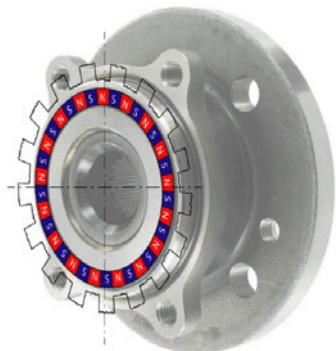


Figure 12. Incremental magnetic encoder, also known as ABS encoder (SKF VKBA 6634).

Regarding the errors in the signals coming from the Sin-Cos encoder, three error sources can be identified [36], namely: offset between the magnet and the sensor (Figure 13a), different gain for each signal (Figure 13b), and delay in the acquisition of the signals (Figure 13c).

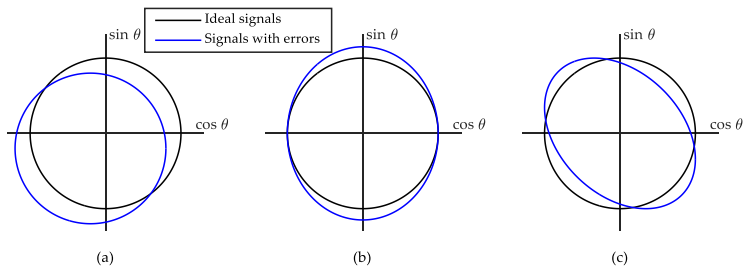


Figure 13. Three possible errors in the output signal of the Sin-Cos encoder. (a) Offset. (b) Different gains. (c) Acquisition delay.

None of the previously mentioned errors were observed when the Kistler RoaDyn P625 and sbRIO-9637 acquisition system were used (Figure 14). In any case, errors of type (a) and type (b) can be corrected by adding an offset and modifying the gain of one of the signals respectively. Both measurement corrections require a very low computational cost.

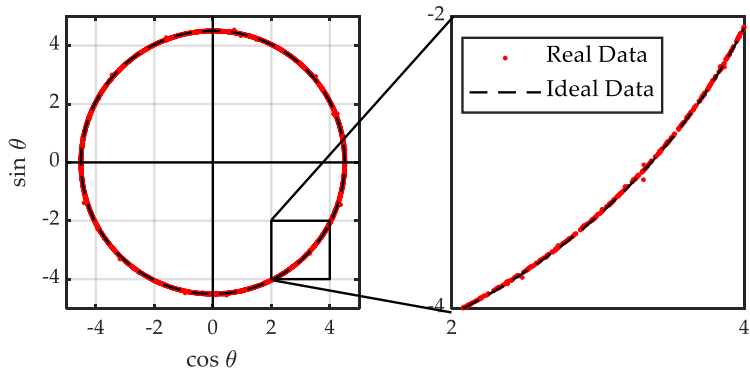


Figure 14. Sin-Cos sensor output signals.

The results of the measurement of the wheel’s angular speed while braking at different linear speeds are shown below. Figures 15 and 16 show a braking process with an initial speed of 60 km/h (205/55 R15 tire). In these tests, the speed was kept constant for 0.3 s. Next, wheel angular speed was reduced by applying high pressure to the brake pads until the wheel locks. Belt speed was kept constant.

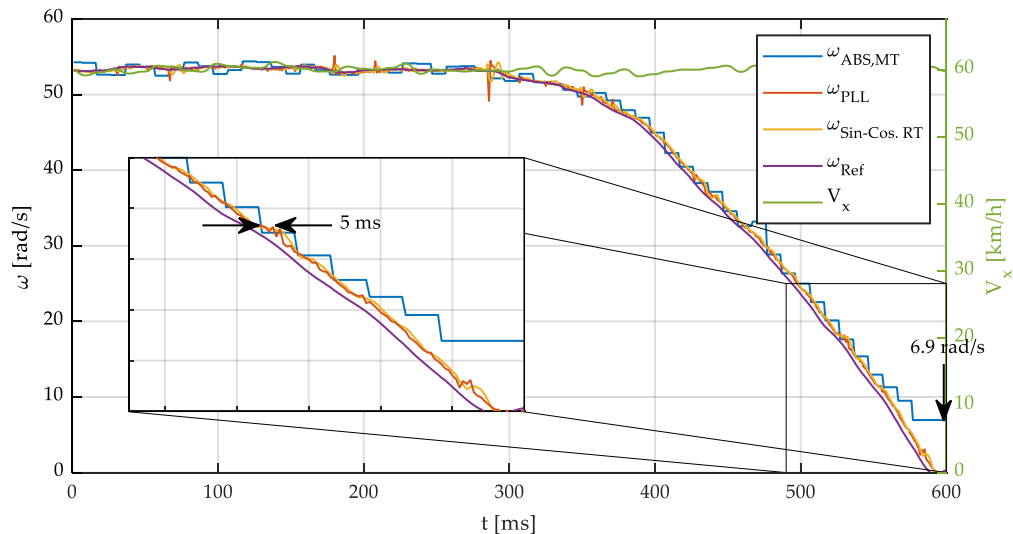


Figure 15. Wheel angular speed and linear speed vs. time. Vehicle speed 60 km/h.

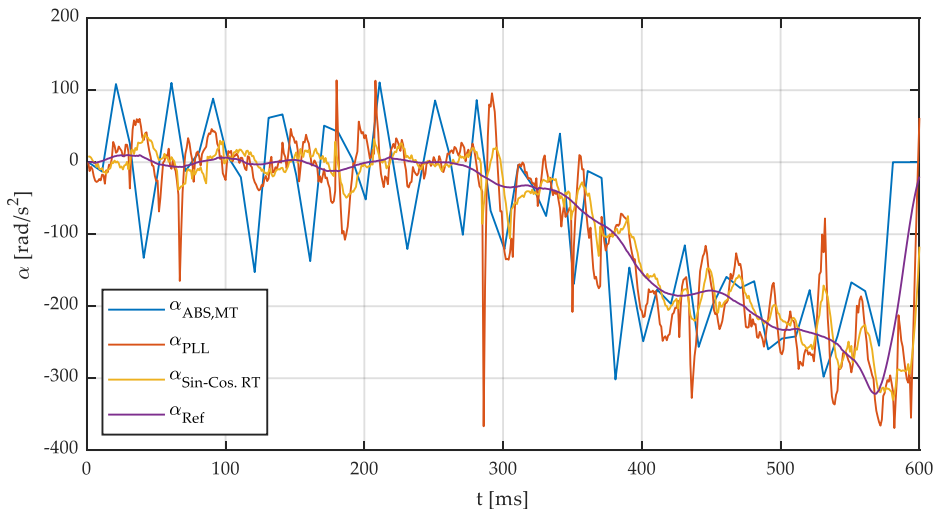


Figure 16. Wheel angular speed and linear speed vs. time. Vehicle speed 60 km/h.

Figure 15 shows both the angular speed of the wheel and the linear speed of the belt while Figure 16 shows the angular acceleration of the wheel. Both magnitudes have been calculated through the three different methods previously described: MT, PLL, and SinCos. For verification purposes, the angular speed obtained using 15 side points and a polynomial of order 3 will be used as a reference in the experimental tests (ω_{ref} and α_{ref}). This reference angular speed is obtained by postprocessing the measured signal with the parameters previously described. As shown previously in Figures 7 and 9, the nondelayed angular speed and acceleration calculated by a convolution and more side points can be considered the reference angular speed since the error in the simulations is negligible. The following conclusions can be drawn from the observation of these results:

- The method proposed here is valid for both very low and high speeds. However, with an incremental encoder, even if the *MT-method* is used, errors are observed when measuring low speeds. This is of particular interest in the application of these sensors to brake control systems, where the wheels operate near the locking condition.
- Very low speeds and even wheel locking can be accurately calculated with the PLL and the proposed method. This is because Sin-Cos signals are continuous, as opposed to those of ABS encoders that are discontinuous.
- A low noise signal is obtained with the proposed method.
- If the signal from the ABS encoder is filtered to smooth the output, the filter will add a delay to this signal, which may be even longer than the delay of the signal from the Sin-Cos encoder.

It can be seen that wheel locking takes place at 600 ms. However, the *MT-method* does not detect this fact, producing a constant low value of angular speed in the last stage of the braking process. This behavior is due to the fact the angular speed is not updated because the sensor does not generate new pulses while the wheel is locked. On the other side, the proposed method provides an accurate measurement even at very low angular speed.

Figure 17 shows braking tests at $V_x = 40, 50, 70$, and 80 km/h, showing similar results.

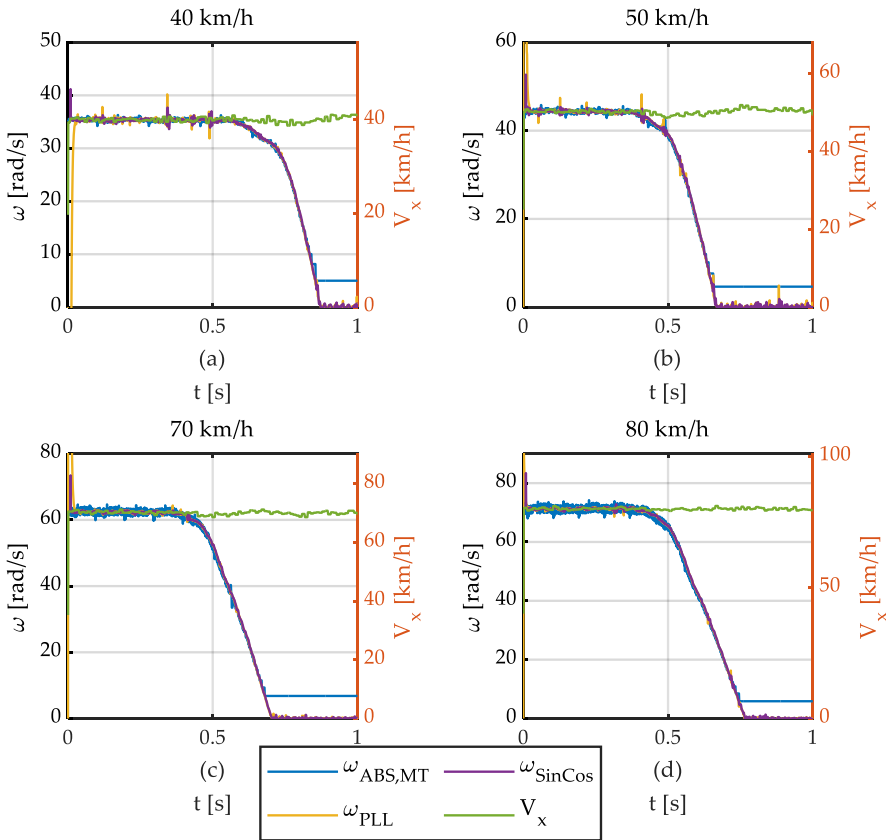


Figure 17. Wheel speed and linear speed vs. time. Different vehicle speeds. (a) 40 km/h. (b) 50 km/h. (c) 70 km/h. (d) 80 km/h.

It can be seen that experimental results confirm the results obtained in simulations. This way, the MT method does not provide accurate measurements at low speed. Furthermore, highly noisy accelerations have been obtained. The PLL-based method and the S-G filter provide low-noise robust speed estimates. In addition, angular accelerations provided by both methods show a reasonably good correlation with real values.

4. Conclusions

Nowadays, most cars and motorcycles measure the angular speed of the wheels with incremental encoders. This work proposes a novel method for determining angular speeds using absolute encoders Sin-Cos. These are being increasingly used, especially in electric vehicles, although its implementation has not been extended to measure speeds but to determine the relative position of the rotor and stator in PMSM motors.

In this paper, the methods commonly used to determine wheel angular speeds have been described and a new method has been proposed. This method has been compared both in simulation and experimentally against commercial algorithms.

The advantages of the method presented are diverse. On the one hand, it makes it possible to measure very low speeds, close to wheel locking with a known and controlled delay. On the other hand, the computational cost is reduced, making it possible to be implemented in real-time applications. In addition, the noise from the signals is minimized

through a least-squares fitting, providing accurate estimates of the position, speed, and angular acceleration signals.

As a summary and as an innovative contribution, it is important to note the following: the signals from a Sin-Cos encoder are time differentiated through the Savitzky–Golay filter. This way, the angular speed can be obtained in real-time with a reduced computational cost. Results show that improved estimates can be obtained with the proposed method. The performance of the Sin-Cos Method exceeds that of the most widely used commercial methods. Thus, it provides robust and accurate results from very low to high speeds. Current ABS encoders are not able to accurately measure or estimate wheel velocity in low speed conditions, which leads to poor wheel slip calculation. Consequently, the ABS is deactivated for speeds below 10–15 km/h, jeopardizing vehicle safety in braking maneuvers. The improved performance of the proposed method contributes to a better calculation of the wheel slip at low speed, thus enhancing ABS performance. This result shows that the use of this method can lead to the control improvement of ABS systems in vehicles.

Author Contributions: M.A.V. and J.P.F. developed the proposed algorithm. M.A.V., J.P.F. and J.M.V.G., performed the simulations and experiments, data acquisition as well as the writing of the manuscript. J.A.C.C. and J.J.C.A. conceived and designed the experiments, helped to analyze the data and provided some useful suggestions in the writing and revision of the text. The work and results have been supervised by J.A.C.C. and J.J.C.A. All authors have read and agreed to the published version of the manuscript.

Funding: This work is partly supported by the partly by the Spanish Ministry of Science and Innovation under grant PID2019-105572RB-I00, partly by the Economy, Knowledge, Enterprise and Universities Council of the Andalusian Regional Government under grant UMA18-FEDERJA-109, partly by the Spanish Ministry of Education, Culture and Sport under grants FPU17/03161 and FPU18/00450, and partly by the University of Málaga.

Institutional Review Board Statement: Not applicable.

Informed Consent Statement: Not applicable.

Data Availability Statement: The data presented in this study are available on request from the corresponding author.

Conflicts of Interest: The authors declare no conflict of interest.

References

1. Robert Bosch GmbH. *Bosch Automotive Electrics and Automotive Electronics*, 5th ed.; Springer: Berlin/Heidelberg, Germany, 2007.
2. Park, J.H.; Kim, C.Y. Wheel Slip Control in Traction Control System for Vehicle Stability. *Veh. Syst. Dyn.* **1999**, *31*, 263–278. [\[CrossRef\]](#)
3. Pusch, S. New Generation of Intelligent Wheel Speed Sensors for ABS Application. In Proceedings of the SAE 2000 World Congress, Detroit, MI, USA, 6–9 March 2000; SAE Technical Paper Series. [\[CrossRef\]](#)
4. Song, C.K.; Uchanski, M.; Hedrick, J.K. Vehicle Speed Estimation Using Accelerometer and Wheel Speed Measurements. In Proceedings of the International Body Engineering Conference & Exhibition and Automotive & Transportation Technology Congress, Paris, France, 9–11 July 2002; SAE Technical Paper Series. [\[CrossRef\]](#)
5. Societe de Technologie Michelin SAS. *The Tire-Grip*; Societe de Technologie Michelin SAS: Clermont Ferrand, France, 2001; p. 92.
6. Pacejka, H.B. *Tire and Vehicle Dynamics*, 3rd ed.; Elsevier: Amsterdam, The Netherlands, 2012.
7. Ricciardi, V.; Savitski, D.; Augsburg, K.; Ivanov, V. Estimation of Brake Friction Coefficient for Blending Function of Base Braking Control. *SAE Int. J. Passeng. Cars Mech. Syst.* **2017**, *10*, 774–785. [\[CrossRef\]](#)
8. Capra, D.; D’Alfio, N.; Morgando, A.; Vigliani, A. Experimental Test of Vehicle Longitudinal Velocity and Road Friction Estimation for ABS System. In Proceedings of the SAE World Congress & Exhibition 2009, Detroit, MI, USA, 20–23 April 2009; SAE Technical Paper Series. [\[CrossRef\]](#)
9. Reif, K. *Brakes, Brake Control and Driver Assistance Systems-Bosch Professional Automotive Information*; Springer: Berlin/Heidelberg, Germany, 2014.
10. Ohmae, T.; Matsuda, T.; Kamiyama, K.; Tachikawa, M. A Microprocessor-Controlled High-Accuracy Wide-Range Speed Regulator for Motor Drives. *IEEE Trans. Ind. Electron.* **1982**, *29*, 207–211. [\[CrossRef\]](#)
11. Li, Y.; Gu, F.; Harris, G.; Ball, A.D.; Bennett, N.; Travis, K. The measurement of instantaneous angular speed. *Mech. Syst. Signal Process.* **2005**, *19*, 786–805. [\[CrossRef\]](#)

12. Merry, R.J.E.; van de Molengraft, M.J.G.; Steinbuch, M. Velocity and Acceleration Estimation for Optical Incremental Encoders. *IFAC Proc. Vol.* **2008**, *41*, 7570–7575. [\[CrossRef\]](#)
13. Aguado-Rojas, M.; Pasillas-Lépine, W.; Loria, A.; De Bernardinis, A. Angular velocity estimation from incremental encoder measurements in the presence of sensor. *IFAC-PapersOnLine* **2017**, *50*, 5979–5984. [\[CrossRef\]](#)
14. Chen, Y.; Yang, M.; Long, J.; Xu, D.; Blaabjerg, F. M/T method based incremental encoder velocity measurement error analysis and self-adaptive error elimination algorithm. In Proceedings of the IECON 2017–43rd Annual Conference of the IEEE Industrial Electronics Society, Beijing, China, 29 October–1 November 2017. [\[CrossRef\]](#)
15. Kavanagh, R.C. Performance analysis and compensation of M/T-type digital tachometers. *IEEE Trans. Instrum. Meas.* **2001**, *50*, 965–970. [\[CrossRef\]](#)
16. Hacı, A.; Curkovic, M. A Novel Divisionless MT-Type Velocity Estimation Algorithm for Efficient FPGA Implementation. *IEEE Access* **2018**, *6*, 48074–48087. [\[CrossRef\]](#)
17. Hacı, A.; Ćurković, M. Accurate FPGA-Based Velocity Measurement with an Incremental Encoder by a Fast Generalized Divisionless MT-Type Algorithm. *Sensors* **2018**, *18*, 3250. [\[CrossRef\]](#)
18. Hacı, A. The Improved Division-Less MT-Type Velocity Estimation Algorithm for Low-Cost FPGAs. *Electronics* **2019**, *8*, 361. [\[CrossRef\]](#)
19. Zhang, Q.; Liu, G.; Wang, Y.; Zhou, T. Study of calculation method of wheel angular acceleration in ABS system. In Proceedings of the International Conference on Information Acquisition, Hefei, China, 21–25 June 2004; pp. 147–150. [\[CrossRef\]](#)
20. Liu, G.; Zhang, Q.; Xiong, J.; Xie, X.; Peng, S. An investigation of calculation method of wheel angular acceleration in anti-lock braking system. In Proceedings of the 2008 International Conference on Information and Automation, Changsha, China, 20–23 June 2008; pp. 840–843. [\[CrossRef\]](#)
21. Alipour-Sarabi, R.; Nasiri-Gheidari, Z.; Tootoonchian, F.; Oraee, H. Performance Analysis of Concentrated Wound-Rotor Resolver for Its Applications in High Pole Number Permanent Magnet Motors. *IEEE Sens. J.* **2017**, *17*, 7877–7885. [\[CrossRef\]](#)
22. Benammar, M. A novel amplitude-to-phase converter for sine/cosine position transducers. *Int. J. Electron.* **2007**, *94*, 353–365. [\[CrossRef\]](#)
23. Ben-Brahim, L.; Benammar, M.; Alhamadi, M.A.; Al-Emadi, N.; Al-Hitmi, M.A. A New Low Cost Linear Resolver Converter. *IEEE Sens. J.* **2008**, *8*, 1620–1627. [\[CrossRef\]](#)
24. Ye, G.; Fan, S.; Liu, H.; Li, X.; Yu, H.; Shi, Y.; Yin, L.; Lu, B. Design of a precise and robust linearized converter for optical encoders using a ratiometric technique. *Meas. Sci. Technol.* **2014**, *25*. [\[CrossRef\]](#)
25. Staebler, M. *TMS320F240 DSP Solution for Obtaining Resolver Angular Position and Speed*; Texas Instruments: Dallas, TX, USA, 2000.
26. Sarma, S.; Agrawal, V.K.; Udupa, S. Software-Based Resolver-to-Digital Conversion Using a DSP. *IEEE Trans. Ind. Electron.* **2008**, *55*, 371–379. [\[CrossRef\]](#)
27. Reddy, S.C.M.; Rau, K.N. Inverse tangent based resolver to digital converter—A software approach. *Int. J. Adv. Eng. Technol.* **2012**, *4*, 228–235.
28. Attaianes, C.; Tomasso, G. Position Measurement in Industrial Drives by Means of Low-Cost Resolver-to-Digital Converter. *IEEE Trans. Instrum. Meas.* **2007**, *56*, 2155–2159. [\[CrossRef\]](#)
29. Sarma, S.; Agrawal, V.; Udupa, S.; Parameswaran, K. Instantaneous angular position and speed measurement using a DSP based resolver-to-digital converter. *Measurement* **2008**, *41*, 788–796. [\[CrossRef\]](#)
30. Wang, Y.; Zhu, Z.; Zuo, S. A Novel Design Method for Resolver-to-Digital Conversion. *IEEE Trans. Ind. Electron.* **2014**, *62*, 1. [\[CrossRef\]](#)
31. Benammar, M.; Ben-Brahim, L.; Alhamadi, M.A.; Al-Naemi, M. A novel method for estimating the angle from analog co-sinusoidal quadrature signals. *Sens. Actuators A Phys.* **2008**, *142*, 225–231. [\[CrossRef\]](#)
32. Petrella, R.; Tursini, M.; Peretti, L.; Zigliotto, M. Speed measurement algorithms for low-resolution incremental encoder equipped drives: A comparative analysis. In Proceedings of the 2007 International Aegean Conference on Electrical Machines and Power Electronics, Bodrum, Turkey, 10–12 September 2007; pp. 780–787. [\[CrossRef\]](#)
33. Al-Emadi, N.; Ben-Brahim, L.; Benammar, M. A new tracking technique for mechanical angle measurement. *Measurement* **2014**, *54*, 58–64. [\[CrossRef\]](#)
34. Liu, H.; Wu, Z. Demodulation of Angular Position and Velocity from Resolver Signals via Chebyshev Filter-Based Type III Phase Locked Loop. *Electronics* **2018**, *7*, 354. [\[CrossRef\]](#)
35. Harnfors, L. Speed estimation from noisy resolver signals. In Proceedings of the 1996 Sixth International Conference on Power Electronics and Variable Speed Drives (Conf. Publ. No. 429), Nottingham, UK, 23–25 September 1996; pp. 279–282. [\[CrossRef\]](#)
36. Albrecht, C.; Klöck, J.; Martens, O.; Schumacher, W. Online Estimation and Correction of Systematic Encoder Line Errors. *Machines* **2017**, *5*, 1. [\[CrossRef\]](#)
37. Benammar, M.; Gonzales, A.S.P. Position Measurement Using Sinusoidal Encoders and All Analog PLL Converter with Improved Dynamic Performance. *IEEE Trans. Ind. Electron.* **2015**, *63*, 1. [\[CrossRef\]](#)
38. Puglisi, L.J.; Pazmiño, S.; Cena, R.J.G.; Elisabet, C. On the Velocity and Acceleration Estimation from Discrete Time-Position Sensors. *J. Control Eng. Appl. Inform.* **2015**, *17*, 30–40.
39. Shaowei, W.; Shanming, W. Velocity and acceleration computations by single-dimensional Kalman filter with adaptive noise variance. *Przegld Elektrotech-Niczn* **2012**, *2*, 283–287.
40. Analog Devices. Variable Resolution, Resolver-to-Digital Converter. AD2S83 Datasheet, Rev. E. 2000. [Online]. Available online: <https://www.analog.com/media/en/technical-documentation/data-sheets/AD2S83.pdf> (accessed on 10 December 2020).

41. Analog Devices. Variable Resolution, 10-Bit to 16-Bit R/D Converter with Reference Oscillator. AD2S1210 Datasheet, Rev. A. 2010. [Online]. Available online: <https://www.analog.com/media/en/technical-documentation/data-sheets/AD2S1210.pdf> (accessed on 10 December 2020).
42. Zimmermann, B.; Kohler, A. Optimizing Savitzky-Golay Parameters for Improving Spectral Resolution and Quantification in Infrared Spectroscopy. *Appl. Spectrosc.* **2013**, *67*, 892–902. [[CrossRef](#)]
43. Serafinczuk, J.; Pietrucha, J.; Schroeder, G.; Gotszalk, T.P. Thin film thickness determination using X-ray reflectivity and Savitzky-Golay algorithm. *Opt. Appl.* **2011**, *41*, 315–322.
44. Staggs, J. Savitzky-Golay smoothing and numerical differentiation of cone calorimeter mass data. *Fire Saf. J.* **2005**, *40*, 493–505. [[CrossRef](#)]
45. Savitzky, A.; Golay, M.J.E. Smoothing and Differentiation of Data by Simplified Least Squares Procedures. *Anal. Chem.* **1964**, *36*, 1627–1639. [[CrossRef](#)]
46. Krishnan, S.R.; Seelamantula, C.S. On the Selection of Optimum Savitzky-Golay Filters. *IEEE Trans. Signal Process.* **2013**, *61*, 380–391. [[CrossRef](#)]
47. Cabrera, J. A Versatile Flat Track Tire Testing Machine. *Veh. Syst. Dyn.* **2003**, *40*, 271–284. [[CrossRef](#)]

7.3 PAPER #3

7.3.1 Journal article identification:

Title:	Modeling of the Influence of Operational Parameters on Tire Lateral Dynamics
DOI:	10.3390/s22176380
Coauthors:	Pérez Fernández J, Sánchez Andrades I, Cabrera Carrillo JA, Castillo Aguilar JJ..

7.3.2 Quality indicators:

Editor:	MDPI
Journal:	Sensors
Date of publication:	24 August 2022
Impact factor:	3.847 (JCR)
Quartile and position in its category:	19/64 (Q2) — Instruments & Instrumentation

7.3.3 Published article



Article

Modeling of the Influence of Operational Parameters on Tire Lateral Dynamics

Manuel Alcázar Vargas , Javier Pérez Fernández , Ignacio Sánchez Andrades , Juan A. Cabrera Carrillo and Juan J. Castillo Aguilar

Department of Mechanical Engineering, University of Malaga, 29071 Malaga, Spain

* Correspondence: manuel.alcazar@uma.es

Abstract: Tires play a critical role in vehicle safety. Proper modeling of tire–road interaction is essential for optimal performance of active safety systems. This work studies the influence of temperature, longitudinal vehicle speed, steering frequency, vertical load, and inflation pressure on lateral tire dynamics. To this end, a tire test bench that allows the accurate control of these parameters and the measurement of the variables of interest was used. The obtained results made it possible to propose a simple model that allowed the determination of relaxation length as a function of tire vertical load and vehicle linear speed, and the determination of a representative tread temperature. Additionally, a model has been proposed to determine the lateral friction coefficient from the aforementioned temperature. Finally, results also showed that some variables had little influence on the parameters that characterize lateral dynamics.

Keywords: vehicle dynamics; tire model; thermal tire model; transient tire model; relaxation length



Citation: Alcázar Vargas, M.; Pérez Fernández, J.; Sánchez Andrades, I.; Cabrera Carrillo, J.A.; Castillo Aguilar, J.J. Modeling of the Influence of Operational Parameters on Tire Lateral Dynamics. *Sensors* **2022**, *22*, 6380. <https://doi.org/10.3390/s22176380>

Academic Editors: Marek Jaśkiewicz, Milos Poliak and Ondrej Stopka

Received: 21 July 2022

Accepted: 23 August 2022

Published: 24 August 2022

Publisher's Note: MDPI stays neutral with regard to jurisdictional claims in published maps and institutional affiliations.



Copyright: © 2022 by the authors. Licensee MDPI, Basel, Switzerland. This article is an open access article distributed under the terms and conditions of the Creative Commons Attribution (CC BY) license (<https://creativecommons.org/licenses/by/4.0/>).

1. Introduction

Vehicle safety is a subject of significant interest in today's society. More and more, efforts are focused on active vehicle safety in the automotive industry. Within active safety, tires play a crucial role. In 2012, the NHTSA reported that tire-related defects were linked to more than 200,000 accidents per year [1]. In 2007, Tire Pressure Monitoring Systems (TPMS) became mandatory in the USA. These systems have also been mandatory in the EU since 2012. These requirements aim to ensure that tires run in optimum operating conditions to improve vehicle safety on one hand and reduce energy consumption and tire wear on the other [2].

In the EU, anti-lock brake systems (ABS) have been mandatory for cars and motorcycles since 2002 and 2016, respectively. In addition, electronic stability programs (ESP) have been mandatory for cars since 2014. All these factors justify the need to research and develop improvements in active security systems that consider tire–road interaction. These systems are arguably the most complex ones to determine and control. Hence, a better understanding of tire dynamics leads to an improvement in active safety systems. Therefore, the objective of this work is to analyze the effect of various parameters on cornering stiffness and tire relaxation dynamics, as well as in the maximum friction coefficient.

The modeling of tire–road interaction has been a subject of great interest over recent decades. These models are usually classified into two non-hermetic categories: empirical and physical models. The state-of-the-art model is the well-known Pacejka's magic formula (MF) [3], which belongs to the first category. This model, valid for quasi-stationary simulations, fits the obtained experimental results reliably on and off the bench. This model has evolved over the years, from the first formulation in 1987 [4] to the current version that belongs to Siemens SimCenter Tire. Since this latest version, it has been included in the Simcenter MF-Tyre/MF-SWIFT package. One of the problems of this current version is that it does not consider any thermal parameters of the road or tire (tread, carcass, air, etc.) and

linear speed of the vehicle is marginally considered in the model. Hence, several authors have modified this model to include these parameters.

Among these modifications, the following can be highlighted. Mizuno [5] proposed a linear dependence of parameter D with temperature. Sorniotti [6] proposed a linear dependence of the maximum lateral and longitudinal friction coefficient on tread temperature and a linear dependence of longitudinal and transverse stiffness on carcass temperature.

Sakhnevych et al. [7,8] proposed a modification of Pacejka's magic formula (MF-evo) that incorporates the influence of temperature and pressure, modifying various coefficients of the MF by adding polynomial terms. The Kelly and Sharp model [9] uses Gaussian functions, modeling the friction coefficient as a function of both temperature and longitudinal velocity. The model of Harsh and Shyrokau [10] slightly modified the Kelly and Sharp model to estimate heat generation due to friction and modified the D and K parameters of the MF. D and K are affected by a quadratic factor for pure longitudinal behavior. D is also affected by a quadratic factor for pure lateral behavior, while K is affected by a more complex expression. Ozerem and Morrey [11] employ the brush model, along with Kelly and Sharp's contact force formulation for a FSAE vehicle. Calabrese et al. [12,13] modified MF parameters λ_μ and λ_k to consider the influence of temperature in the maximum friction coefficient and cornering stiffness. Cabrera et al. [14] proposed a decreasing exponential dependence of the maximum friction coefficient on linear velocity of the vehicle.

Regarding physical models, the brush model [3] discretizes the contact patch into a series of bristles aiming to understand what happens during tire–road interaction. Romano et al. have employed a modified brush model to investigate transient effects of the tire force generation, including non-linearities [15–17]. Semi-physical models have also been used to study the influence of vertical load excitation frequency on the generation of contact forces [18]. Recently, with the development of finite element methods, many simulations have been carried out to study mechanical carcass deformation, pressure distribution in the contact footprint, and the generation of tangential forces [19,20]. The main problem with these methods is their computational cost, which makes it unfeasible to use them for real-time applications. In addition, a deep knowledge of tire construction is required, including: the compounds used, fiber arrangement, amount of wear, etc. Thus, FEM simulations have been relegated to the following applications: tire design by manufacturers, the study of high-frequency behavior (vibration modes) of tires, improving the understanding of mechanical/elastic behavior of tires, and, finally, allowing the generation of simplified finite element models for use in real-time applications: simulation and videogames, mainly.

Based on experimental and FEM results, several software packages analyze tire dynamics in the following ways. The SETA tire model, used in the Project Cars 2 driving simulator, performs three simultaneous simulations: tire deformation, generation of contact forces in the tire tread and contact patch, and heat transfer and generation model [21]. Michelin's TaMeTirE model [22–24] also performs three simulations, virtually identical to the SETA model. For the generation of contact forces, it distinguishes two zones: sliding and adherent. Cosin's FTire model also performs simultaneous simulations: mechanical, thermal, wear, air volume vibration, and the flexible visco-plastic rim one [25,26]. In the iRacing simulator, the tire model currently used is the New Tire Model V7 (NTM V7). It performs the same three simulations simultaneously: carcass deformation, thread force generation, and thermal models [27].

The first methods described, the empirical ones, have the advantage that it is only under certain conditions it is necessary to measure contact forces and to access these data, either in the form of Look-Up-Tables or mathematical expressions. On the other hand, apart from the tested conditions, that is, apart from the conditions of loading, temperatures, slip, velocities, and rolling surface, the results must be extrapolated and their accuracy is not guaranteed.

Alternatively, physical models have several advantages that make them considerably more appropriate according to some authors. On one hand, the parameters that characterize tires are physical properties: stiffnesses in the three directions of space, damping

coefficients, specific heats, etc. This means that modeling a new tire should theoretically be straightforward once a tire has been modeled. In addition, it is not necessary to test tires in all conditions and then interpolate them within that tested range. Nevertheless, it could be extrapolated as it is based on a physical model. The main drawback is that it is necessary to know how the tire carcass will deform according to applied loads (mechanical model) and, more importantly, to understand how the tread compound will generate frictional forces according to operating conditions. This latter point is the one that presents the most uncertainty, as indicated by all authors. The main reason is the highly non-linear viscoelastic behavior of vulcanized polymers [28].

The generation of friction forces between the tire and road is due mainly to molecular adhesion and indentation [9,29]. The first occurs on a microscopic scale due to Van der Waals bondings between the tire and road. The road must be clean and dry for this to take place. The second one, which occurs on a macroscopic scale, depends on the indentation of road roughness on the tread. Viscoelasticity of the compound means that, as roughness penetrates rubber, it is necessary to apply more energy than it releases when it returns to its original shape. This difference causes a resulting force that opposes sliding. Therefore, viscoelasticity generates friction between the tire and road. Hence, the importance of viscoelastic behavior of the compound. What happens is that this viscoelastic behavior is strongly dependent on a multitude of factors, which explains the enormous complexity of determining contact forces. Essentially, this friction depends on the temperature of tires with respect to the vitrification temperature of the compound, the frequency of excitation of these irregularities and the chemical composition of the compound. When excited at low frequencies, the tire behavior is essentially elastic, and the viscous component is of little importance. At the other extreme, the tire is dramatically stiffer at very high excitation frequencies, behaving more like glass (glassy state). In an intermediate frequency range, the viscoelastic component predominates. It is in this frequency range where it is essential to work. Something similar happens with temperature. Below the vitrification temperature (the temperature at which it changes from one kind of behavior to the other), the composite is very rigid and brittle. The behavior is purely elastic above the vitrification temperature, with a much lower stiffness than when it is colder.

The vitrification temperature in winter tires is considerably lower than the one in the case of summer tires, which, in turn, is lower than the one in competition tires (slicks). William, Landel, and Ferry [30] determined an expression to relate these variables (WLF equation) since this vitrification temperature also depends on the excitation frequency. This relationship, which has been known for decades and is applied to polymers, has been adapted to the field of tire dynamics, replacing working temperature with respect to vitrification temperature with a working temperature with respect to a reference temperature, as well as the excitation frequency by sliding velocity or longitudinal velocity. This is the case of the TaMe-TirE model or the Sharp and Kelly model. Other models, such as those used in simulators, being a black box, do not specify which model of tangential force generation they use. However, they consider temperature and time (iRacing, SETA,...). The relationship between the friction coefficient and sliding velocity and the temperature of the TaMe-TirE model has a Gaussian shape, similar to the one described by WLF in their work. Additionally, the Kelly and Sharp model considers a Gaussian shape.

Another area of study that has been investigated and which has garnered significant interest in recent years is the study of transient tire dynamics. Most tire data are obtained under quasi-stationary conditions. Therefore, it is impossible to predict tire behavior apart from low-frequency maneuvers. As Lozia demonstrates [31], not including transient models in vehicle control simulations can lead to inaccurate results. It is, therefore, necessary to use more complex models to consider this specific type of maneuver, such as the operation of an ABS, an ESP, or crash-avoiding maneuvers (lane change maneuver). The first works on this subject date back to the second half of the twentieth century, including those of Segel [32,33] and Schieschke [34,35]. Pacejka's new formulation of the model is called SWIFT, which stands for short wavelength intermediate frequency tire model. Many of

the efforts for this type of transient model have focused on vertical load fluctuations [18], produced by load transfer or road irregularities. Others employ very complex models where it is necessary to solve systems of differential equations, such as in the case of the SWIFT model [3], RMOD-K [36,37], or FTire [25,26]. A comparison of these three methods can be found in [3]. Luty [38] analyzes the influence of relaxation parameters for truck tires on the results of a simulation. Other authors use first [39] or second order models [40] with lower computational costs. These first-order systems are a good compromise between the number of tests needed to characterize them and the accuracy of the model. In addition, the computational cost is meager. These first-order linear models are defined by proportionality and time constants. This time constant is usually expressed as a distance traveled and is referred to as the relaxation length. In this work, a linear first-order model is used, defined by the two parameters described above, which, as it will be seen, are strongly influenced by vertical load and linear velocity.

Two extremes can be distinguished within tire model formulations: pure lateral and pure longitudinal dynamics. Once these two cases have been studied, they can be used together in the so-called combined models. In the former, longitudinal sliding velocity is zero, and so is longitudinal force; in the latter, the opposite occurs: lateral sliding velocity is zero and, hence, lateral force is zero. In this work, we will analyze only the pure lateral model. This is because:

- Lateral dynamics are much more stable: it is much easier to control lateral slip than longitudinal slip. This allows for much better repeatability of tests.
- The generation of lateral forces generates a temperature gradient across the tread that the longitudinal force does not. This allows for studying the influence of temperature distribution along the tread.
- The tire test bench at the research group's facilities cannot impose one speed on the wheel and another on the running belt. Only braking of the wheel is possible. This results in two outcomes. First, the tests requiring longitudinal slippage must be brief, as the brake disc heats up very quickly. Secondly, once the slip corresponding to maximum grip has been reached, the tire locks up almost instantaneously, making it very difficult to work in the non-linear zone of the tire. In addition, measuring angular velocity of the wheels in situations close to lock-up and, therefore, measuring high slip is quite complex in a vehicle not instrumented for this purpose [41].

Therefore, temperature and speed significantly influence the generation of contact forces on the road, being these forces the only ones that enable the vehicle to be driven. To the best of the authors' knowledge, active safety systems in vehicles do not measure tire temperature. Only some TPMS monitor gas temperature inside the tire. This is why the objective of the present work is multiple:

- Designing, coding, and assembling the temperature measuring device using IR sensors to determine temperature distribution of the tire.
- Performing a number of tests to determine the influence of various parameters on the generation of contact forces.
- Analyzing and proposing a novel model to estimate the parameters of interest in the tire.

Regarding the measurement of tire temperature, it is interesting to measure it for the following reasons:

- It is the most easily measurable temperature and the most relevant to generation of contact forces.
- An accurate and inexpensive temperature distribution can be obtained using an infrared sensor, given that the emissivity of dry rubber is known and approximately constant.
- Only tire sidewall temperature is considered for estimating carcass temperature.
- The contributions of the present work are:

- Proposing a model for determining a representative temperature as a function of the temperature of the whole tire.
- Proposing a model for estimating relaxation length as a function of vertical load and linear speed of the vehicle.
- Proposing a model to determine the maximum friction coefficient as a function of the representative tire temperature.
- Ensuring a reduced computational cost to evaluate these models while maintaining a reduced number of tests needed to characterize them.

This work is structured as follows: first, a description of instruments employed, experiments performed, and mathematical methods is provided in the Materials and Methods section. This section and the Results and Discussion section are divided into two subsections: linear and non-linear experiments. In the first subsection, experiments are described. Later, results obtained in real tests are exposed and analyzed in the Results and Discussion section. The conclusions of this work are drawn in the last section, as well as future works.

2. Materials and Methods

This section describes the tests performed. The conditions of tests, the variables that have been studied, and the instrumentation used are also explained here. It is also described how measurements were made. The tests are grouped into two main blocks: linear and non-linear (Figure 1). Linear tests are those where the slip angle, α , remains close to zero.

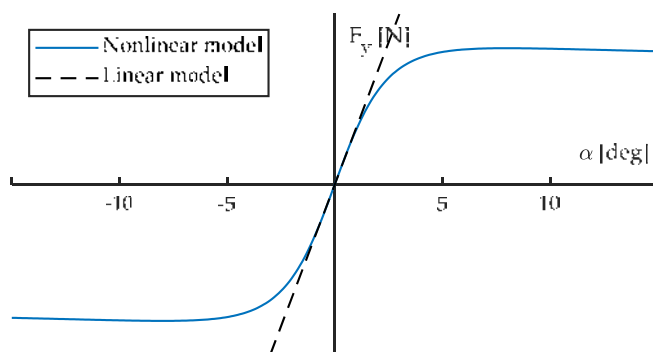


Figure 1. Pure lateral force against slip angle. Linear and non-linear regimes.

To characterize behavior within linear range of the tire, the following parameters are measured:

- Relaxation length for the generation of F_y : L_{Fy} ;
- Cornering stiffness: $C_{\alpha, Fy}$.

Apart from linear range, it is also of interest to determine the maximum lateral friction coefficient, μ_y . The objective of this work is to determine the influence of the following variables on the previous parameters:

- Vertical load: F_z ;
- Longitudinal speed: V_x ;
- Tire pressure: P ;
- Tire temperature: T ;
- Slip angle excitation frequency: f_{SA} .

2.1. Linear Tests

To determine the influence of these variables on linear parameters of the tire, three groups of tests are performed, resulting in a total of 88 experiments. For all of them, unless otherwise stated, the conditions are:

- Vertical load, 4000 N;
- Longitudinal speed, 60 km/h (16.7 m/s);
- Tire pressure, 2.3 bar;
- Tire temperature, 60 °C;
- Slip angle excitation frequency, 1 Hz;
- Slip angle excitation amplitude, 2°.

In these first linear tests, a sinusoidal slip angle of amplitude and frequency, indicated above, is imposed. The amplitude of 2 degrees has been chosen to stay within the linear region. It has been decided to excite the system with a frequency of 1 Hz because it is in the middle of the excitation frequencies considered. The following first-order system is fitted (1):

$$y = \frac{C}{\tau s + 1} u \quad (1)$$

where C is the cornering stiffness, u is the slip angle, and τ is the time constant of the first order system. The output, y, is the lateral force. To determine relaxation length, L, once longitudinal velocity, V_x , and the time constant, τ , are known, it is given by Equation (2):

$$L = \tau V_x \quad (2)$$

Subsequently, the Matlab System Identification Toolbox [42] is used, and the `iddata` test object is created. With this toolbox, these parameters can easily be determined while monitoring the error made in the modeling.

The tests are performed on the research group's tire testing machine at the University of Malaga (Figure 2) [43]. Forces and torques are measured with a Kistler RoaDyn P625 instrumented rim. Control and data acquisition are performed with an sbRio 9637 and LabVIEW software. Data acquisition is performed at 5 kHz and the machine is controlled in closed loop at a frequency of 1000 Hz.

The temperature sensors used are Melexis MLX90614. These infrared sensors provide a digital output through the I2C protocol. Nine of these sensors are arranged on three PCBs (Figure 3). A microcontroller is used to convert transmitted messages by I2C into a CAN message, which is much more common in the automotive industry and has no transmission distance problems. The maximum acquisition frequency of these sensors is 2 Hz. This frequency is limited by the filter of the sensor. Thus, all variables are recorded at a rate of 5 kHz, except tire temperature which is acquired at 2 Hz. Table 1 shows a fragment of the calibration certificate of the instrumented rim.

As for the tests in which the temperature is required to be homogeneous and not to vary throughout the test, the way to achieve these conditions has been as follows. A tire warmer from the manufacturer Thermal Technology with an RC31 II Series controller is mounted and the temperature is set. It is kept at this temperature for 60 min and the pressure is adjusted once the tire is hot. This way, all layers of the tire are at the same temperature. Immediately after removing the heater, the test to determine the relaxation parameters is carried out. These tests have a very short duration as only a few cycles are performed. The measured surface temperature is not shown on the graphs as it is constant.

On the contrary, for tests to determine the maximum lateral friction coefficient as a function of tread temperature, the tire starts at ambient temperature and gradually warms up due to friction. In this case, the surface temperature is continuously heated until the maximum temperature is reached. This leads to a non-homogeneous temperature distribution, where the hardest working part of the tire heats up the most.

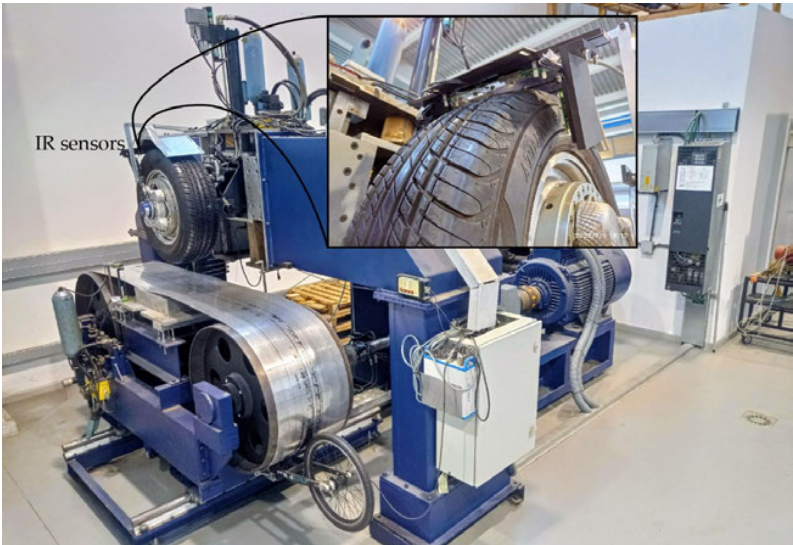


Figure 2. Tire testing machine property of the research group.

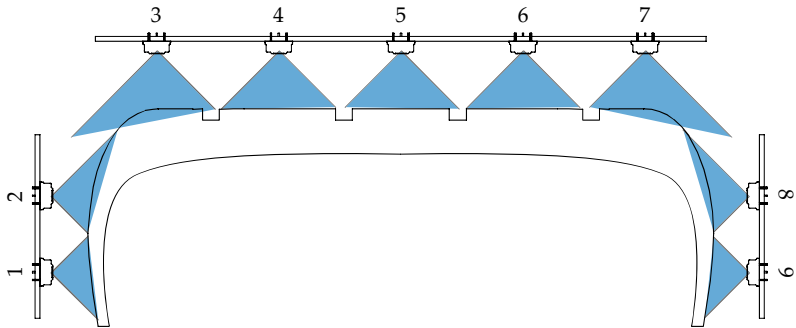


Figure 3. IR sensors layout.

Table 1. Kistler RoaDyn P625 calibration certificate.

	F_y	F_z
Range [N]	± 8000	$\pm 15,000$
Linearity [% FS]	0.4	0.1
Hysteresis [% FS]	0.4	0.2
Sample rate [Hz]	5000	5000

2.1.1. First Group of Tests: Influence of F_z and V_x

Different vertical loads and longitudinal velocities are imposed in the first set of tests. The loads vary from 2000 to 6000 N in 1000 N steps. The speed increases from 30 to 70 km/h in 10 km/h increments. Thus, there are five different loads and five different speeds. Therefore, 25 tests are performed.

2.1.2. Second Group of Tests: Influence of Slip Angle Excitation Frequency

These tests are similar to the previous ones, with the difference that the wheel steering frequency varies from 0.1 Hz to 2.0 Hz, with increments of 0.1 Hz until reaching 1.5 Hz and 0.5 Hz after that. The reason is that a significant change in the relaxation length and stiffness is observed at around 1 Hz. This group consists of 18 tests.

2.1.3. Third Group of Tests: Influence of Temperature and Pressure

The last group of tests in the linear regime is performed by modifying temperature and pressure. Tests are carried out at 30, 60, and 90 °C and 1.8, 2.3, and 2.8 bar. Vertical load is also modified since it is believed that pressure and vertical load are related, as both significantly affect the shape and distribution of the contact patch. Vertical load ranges from 2000 to 6000 N in 1000 N steps. All other parameters remain the same. Thus, three different temperatures and pressures and five vertical loads are tested, resulting in 45 tests.

2.2. Non-Linear Tests

Finally, to determine the influence of temperature on the maximum lateral friction coefficient, it is necessary to perform another approach. It is known that the maximum friction coefficient is outside the linear range of tire behavior [3], so it will be necessary to impose a much higher slip angle. Therefore, the following test is performed. A slip angle of −8 degrees, a longitudinal speed of 60 km/h, and a vertical load of 4000 N are set. The test starts with a cold tire that warms up during the test. After about three minutes, some parts of the tire reach 120 °C and the experiment finishes.

The test results allow determining the influence of tire temperature on lateral force generation. Two issues are addressed:

1. Taking a representative temperature value (scalar) from the reading of the nine sensors. The following Equation (3) is proposed:

$$T_{\text{averaged}} = \sum_{i=1}^n (w_i \cdot T_i) \quad (3)$$

where w_i is the weight corresponding to the reading of each sensor. The expression to calculate it is (4):

$$w_i = \frac{T_i - T_{\text{ambient}}}{\sum_{j=1}^n (T_j - T_{\text{ambient}})} \quad (4)$$

It is proposed to assign a weight to the i -th sensor reading proportional to temperature difference between that reading and ambient temperature. This way, the tire parts at ambient temperature do not contribute to the generation of frictional force. This expression was chosen because convection is the fundamental mechanism of heat dissipation in this process (Newton's law of cooling). The heat dissipated by this mechanism, Q , is proportional to temperature difference between of the tire surface (measured magnitude) and ambient temperature.

Thus, assuming that all the heat is generated by friction and evacuated only by convection, as shown by the experimental results by de la Rosa et al. [44], the following can be written (5):

$$\mu_y \cdot F_z \cdot V_x \cdot \sin \alpha = Q \propto (T - T_{\text{ambient}}) \quad (5)$$

where term $\mu_y \cdot F_z$ is lateral force F_y . It is impossible to know the pressure distribution in the contact patch during the steering process in a vehicle that is not instrumented for this purpose. Therefore, this weighting method assigns more importance to the part of the tire that is more heated since it contributes more to the generation of lateral force. Moreover, computing this operation is highly inexpensive. In this way, these weights (4) take into account the zones of the tire that generate friction. In the extreme case that the temperature of a tire zone coincides with ambient temperature ($T_i = T_{\text{ambient}}$), it must be because this zone does not generate friction. Otherwise, this friction would be converted into heat which increases the temperature of that part of the tire.

- 2. Proposing a model to determine the grip as a function of temperature. In this case, an expression using a hyperbolic cosine is proposed, which will be described in more detail in the Results section.

3. Results and Discussion

The previous section described procedures for performing tests, instruments used, and data processing. This section will show the results and their interpretation. Following the previous section, they are divided into two main groups: linear and non-linear tests. A commercial summer passenger car tire is tested (Austone Athena SP-6) with an overall size of 205/65 R15.

3.1. Linear Tests

The results of the 88 linear tests performed are shown in Figures 4–12.

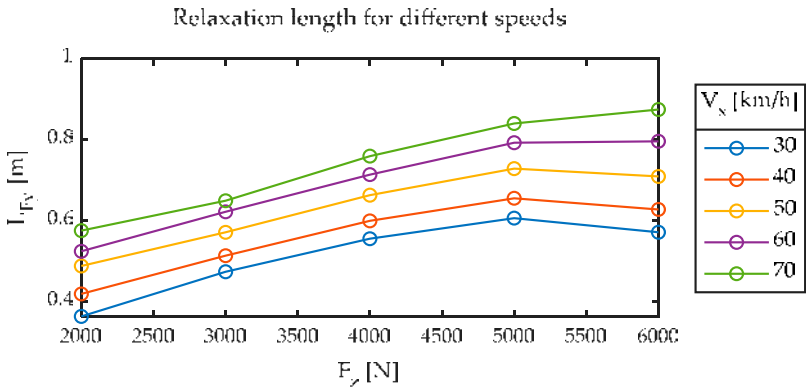


Figure 4. Relaxation length for different longitudinal speeds. Slip angle sweep $\pm 2^\circ$. Frequency 1.0 Hz.

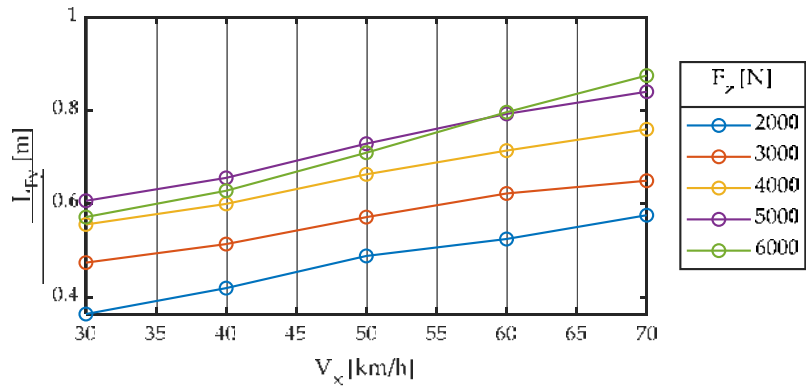


Figure 5. Relaxation length for different vertical loads. Slip angle sweep $\pm 2^\circ$. Frequency 1.0 Hz.

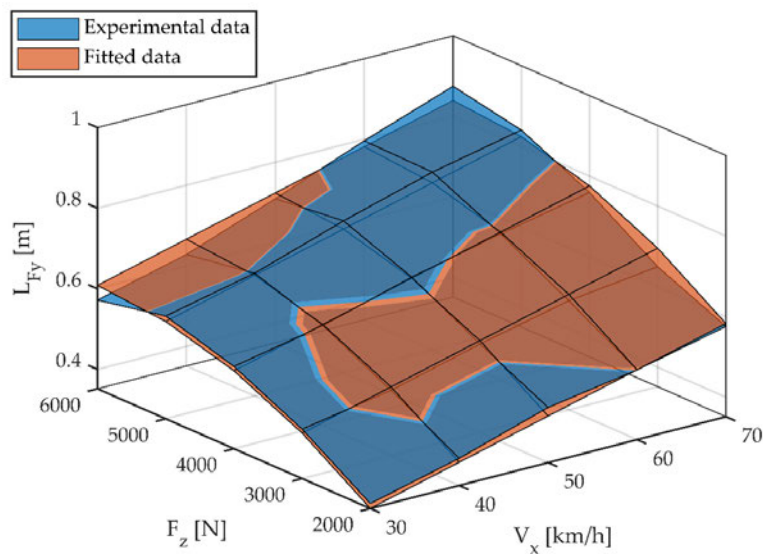


Figure 6. Relaxation length for different vertical loads and longitudinal speeds. Experimental data and fitted data.

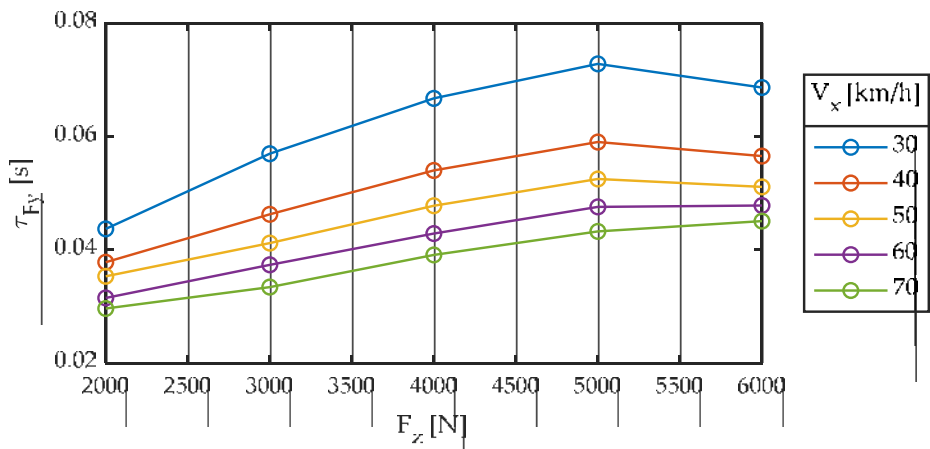


Figure 7. Relaxation time constant for different longitudinal speeds. Slip angle sweep $\pm 2^\circ$. Frequency 1.0 Hz.

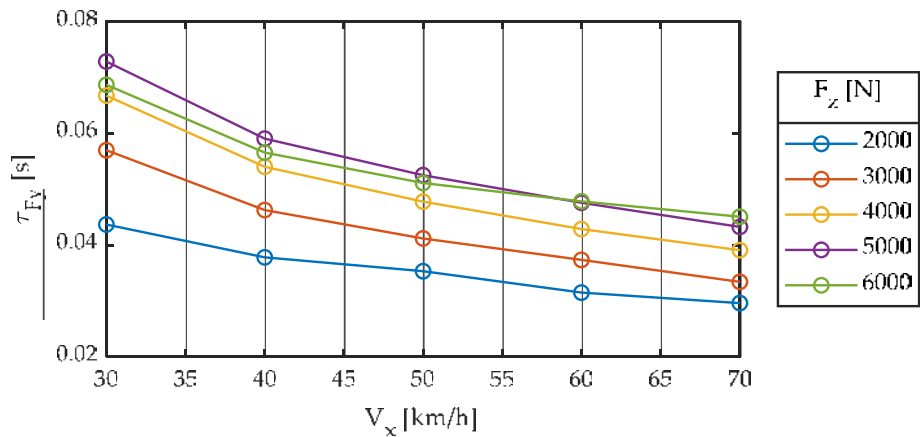


Figure 8. Relaxation time constant for different vertical loads. Slip angle sweep $\pm 2^\circ$. Frequency 1.0 Hz.

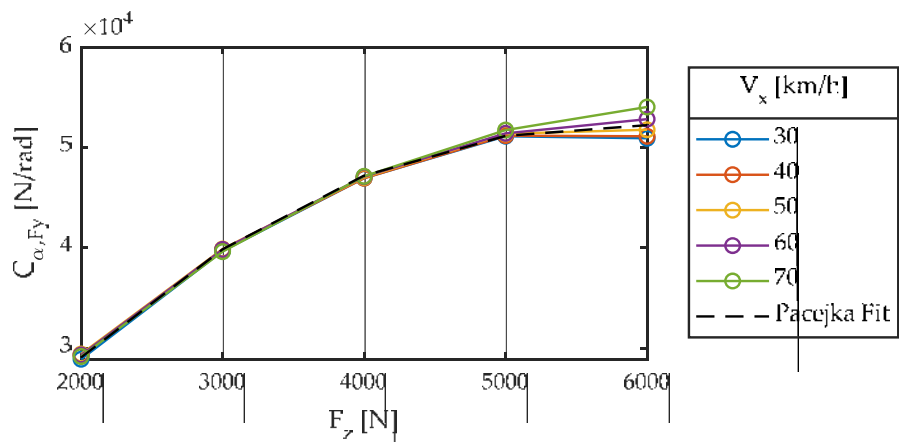


Figure 9. Cornering stiffness for different longitudinal speeds. Slip angle sweep $\pm 2^\circ$. Frequency 1.0 Hz.

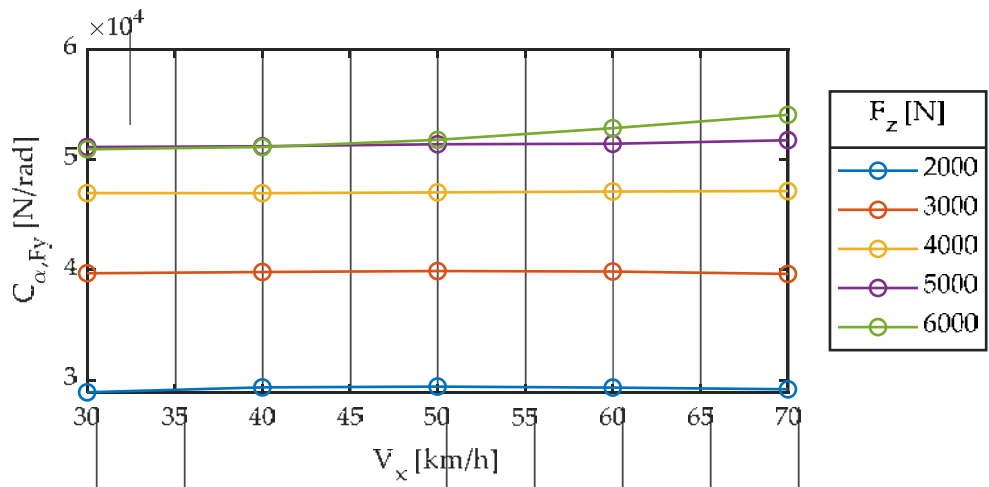


Figure 10. Cornering stiffness for different vertical loads. Slip angle sweep $\pm 2^\circ$. Frequency 1.0 Hz.

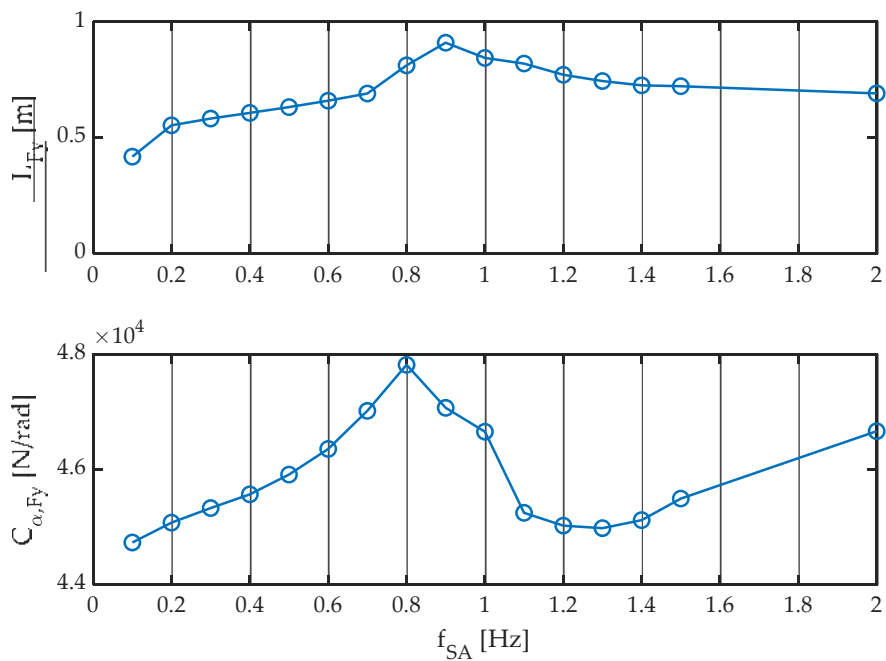


Figure 11. Relaxation length and cornering stiffness for different slip-angle sweep frequencies. Amplitude $\pm 2^\circ$. Longitudinal speed 60 km/h. Vertical load 4000 N. Tire temperature 60°C .

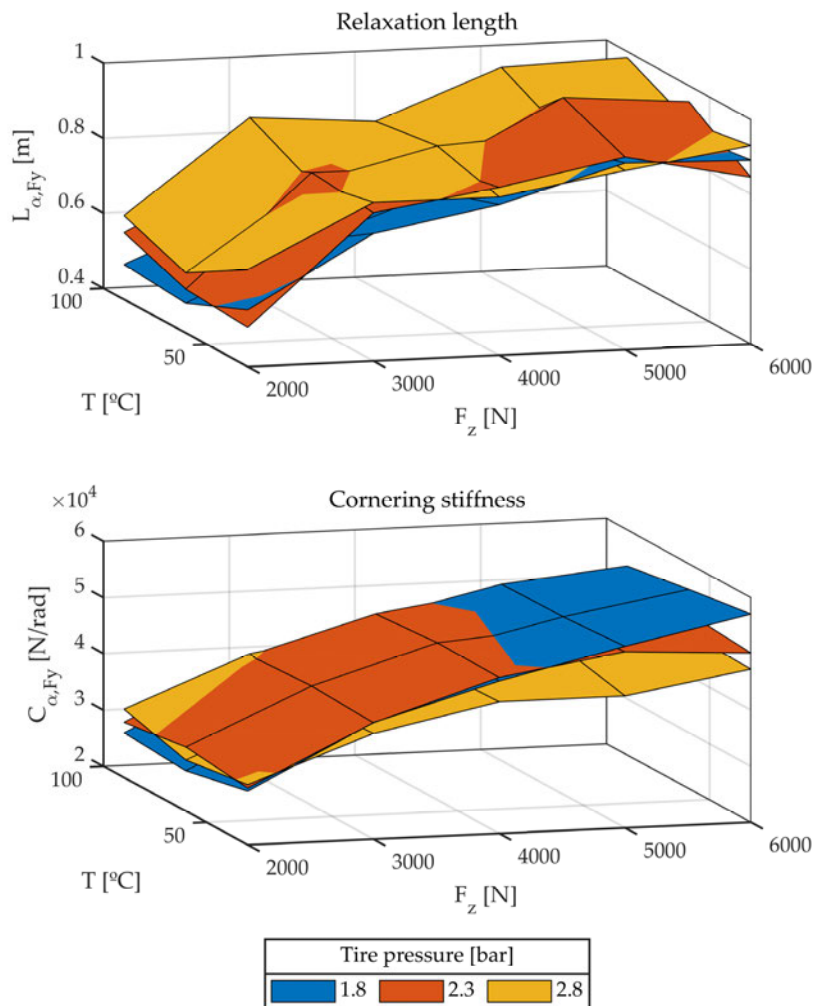


Figure 12. Relaxation length and cornering stiffness. Different temperatures, pressures, and vertical loads.

3.1.1.1. First Group of Tests: Influence of F_z and V_x

In these first tests, the modified variables are vertical load and linear velocity. Figure 4 shows lateral relaxation length. This length is not constant but increases with vertical load and speed.

Figure 5 also shows the same results as in Figure 4, where the x -axis represents longitudinal velocity. Similar conclusions can be drawn as in the previous case, but two phenomena can also be distinguished. First, a linear dependence is observed between relaxation length and longitudinal velocity. Second, a non-linear dependence is observed between relaxation length and vertical load.

Considering the results presented in the previous two figures in this work, we propose the following model (6):

$$L_{Fy} = c_1 + c_2 V_x + c_3 F_z + c_4 F_z^2 \quad (6)$$

which is fitted through least squares [45], yielding the following values (Table 2):

Table 2. Values resulting from a least squares fitting of Equation (6).

Variable	Value	Units
c_1	-1.4×10^{-1}	m
c_2	$+2.1 \times 10^{-2}$	s
c_3	$+1.9 \times 10^{-4}$	$m \cdot N^{-1}$
c_4	-1.6×10^{-8}	$m \cdot N^{-2}$

Figure 6 shows the relaxation length as a function of vertical load and linear velocity. Experimental results and the polynomial function fitted by Equation (6) are shown. A very accurate fit can be observed.

The delay in the generation of forces can be interpreted as distance (relaxation length) or time (time constant). What happens is that neither the first nor the second is constant. Figures 7 and 8 are equivalent to Figures 4 and 5, respectively, where the time constant has replaced relaxation length.

It is observed that the delay between the input to the system (slip angle) and the output (force) is strongly dependent on both vertical load and linear velocity and that it is not constant, whether viewed either in the form of distance traveled or in the form of time. Maximum variations in the order of 200% are observed in time (30–70 ms) and distance (0.3–0.9 m).

The other parameter characterizing a first-order system is the proportionality constant or gain. For the case of no camber angle ($\gamma = 0$) and without taking into account the influence of pressure ($dp_i = 0$), Pacejka [3] proposes the following Equation (7):

$$C_{\alpha,F_y} = d_1 \cdot \sin(d_2 \cdot \text{atan}(d_3 \cdot F_z)) \tag{7}$$

whose nomenclature has been modified according to the one of the present work. This stiffness in literature does not depend on linear velocity but vertical load. Figures 9 and 10 show experimental data, which agree with the Equation (7) proposed by Pacejka (dashed line). The fitted coefficients are summarized in Table 3.

Table 3. Values obtained by means of a least squares fitting of Equation (7).

Variable	Value	Units
d_1	$+5.2 \times 10^4$	N/rad
d_2	$+2.7 \times 10^0$	-
d_3	$+1.1 \times 10^{-4}$	N^{-1}

3.1.2. Second Group of Tests: Influence of Slip Angle Excitation Frequency

The next series of tests seek to determine the influence of the slip angle excitation frequency on the two parameters studied above. The slip angle is related to the steering angle. Hence, it is interesting to determine the delay in lateral force generation depending on steering wheel speed. Figure 11 shows how relaxation length and stiffness vary as a function of excitation frequency. Several remarkable effects can be observed:

- The relaxation length increases from almost zero frequencies (<0.5 m) to a maximum at around 1 Hz, where it almost doubles its value (~ 1.0 m).
- The stiffness also has a maximum value of around 1 Hz, but these values vary much less in percentage terms, around 5%.

Testing was not continued at frequencies higher than 2 Hz since faster maneuvers are rare to occur.

3.1.3. Third Group of Tests: Influence of Temperature and Pressure

The test previously described is then performed, modifying three variables: pressure, temperature, and vertical load. Figure 12 shows the results of these tests.

Little predictable behavior can be observed: temperature seems to have practically no influence on any of the parameters studied, while pressure seems to have a slight effect, although no tendency can be identified. It could be said that all parameters increase slightly with pressure but, as shown in Figure 12, this is not always the case.

3.2. Non-Linear Tests

Non-linear tests are described in this section. These were performed outside the linear range of the tire, in this case, with a slip angle of -8 degrees.

Figure 13 shows time evolution of each of the nine temperature sensor readings. It can be seen how the sidewall of the tire temperature (sensors 1, 2, 8, and 9) remains virtually constant over time. On the other hand, the tread working zone (sensors 5–7) heats up very

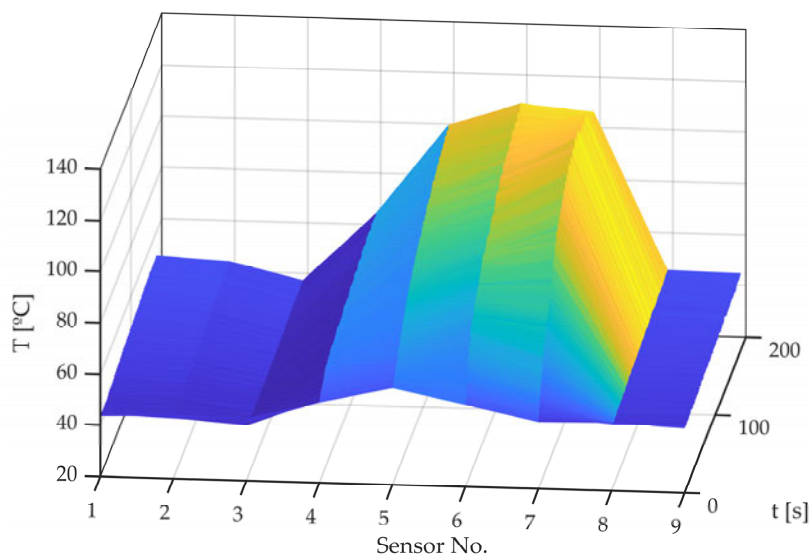


Figure 13. Measured temperatures for each sensor against time.

Figure 14 shows the reading of the five sensors on the tire tread over time. The following can be observed:

- The tread area sensors that barely work (3 and 4) show how tire temperature slightly increases, reaching a stationary value relatively quickly.
- Sensors positioned in the tread area that contribute strongly to lateral force generation (sensors 5–7) show how the temperature in this area increases approximately linearly over time for sensors 5 and 6, while for sensor 7, it increases until it reaches a maximum around 120°C and then it cools down slightly.
- If the temperature behavior of sensor 7 is analyzed, this maximum can be interpreted as follows. Since the friction coefficient increases with temperature up to a reference or optimum temperature and then decreases, this tire area generates less friction when this temperature is exceeded. As it generates less friction, it heats up less and cools down. It would be expected that, when it cools down, it would generate more friction and heat up again. What happens is that the area of the nearest sensors (5 and 6) has already exceeded 100°C , so the total friction and heat generation decreases. As it can

be seen in Figure 15, after approximately 100 s of testing, total friction decreases slightly. This moment occurs at the same time as the hardest working zones (5–7) exceed 100 °C. Consequently, the previously described Equation (3) is proposed to be used to provide a single value that represents the measurements of all the temperature sensors.

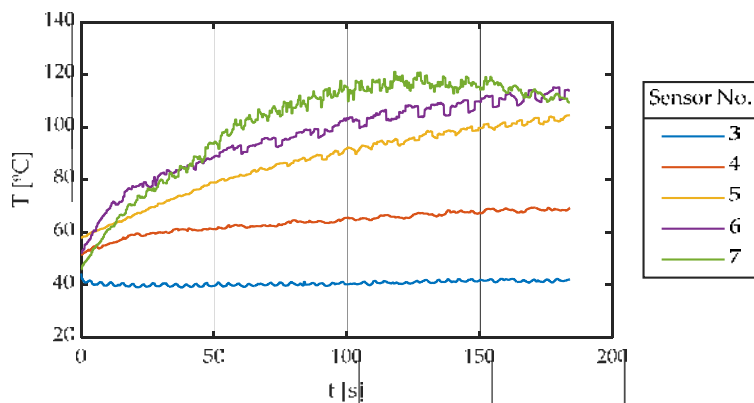


Figure 14. Tread temperatures against time.

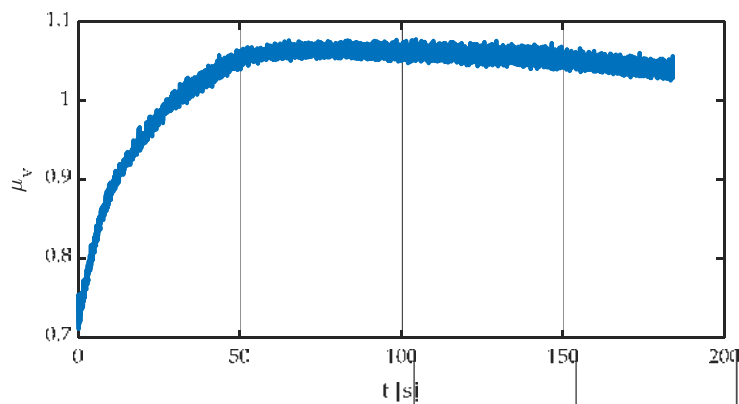


Figure 15. Friction coefficient against time.

Figure 15 shows time evolution of the friction coefficient. This is a very illustrative graph since two main phenomena can be observed:

- The friction coefficient varies enormously with temperature. It starts at about a value of 0.7 and rises to a maximum of 1.05, representing an increase of 50%. This is one of the reasons for studying the influence of temperature on tire grip.
- The friction coefficient shows a maximum (not very sharp), then it decreases slowly.

As a novel contribution, this work includes determining an average temperature (Equation (3)), and a mathematical model that, using this averaged temperature, estimates the maximum friction coefficient. Figure 16 shows the friction coefficient versus the aver-

aged temperature according to Equation (3). The fitting of data is carried out according to the newly proposed Equation (8):

$$\mu_y(T) = \mu_y^{\max} + \left[1 - \cosh\left(\frac{T_{\text{averaged}} - T_{\text{opt}}}{T_{\text{dispersion}}}\right) \right] \tag{8}$$

where the fitted coefficients are shown in Table 4:

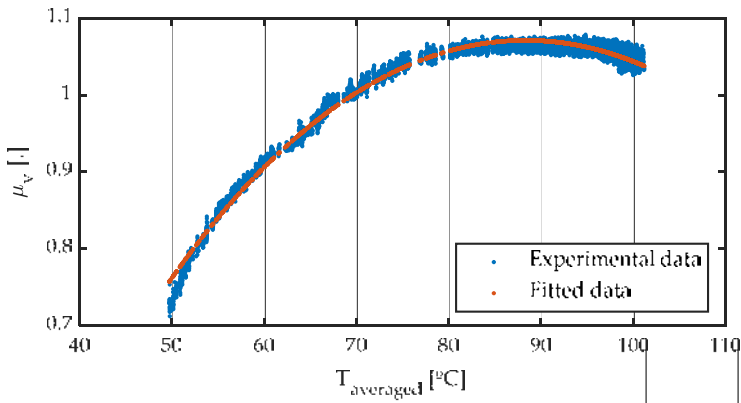


Figure 16. Friction coefficient against temperature. Different averaging methods.

Table 4. Values obtained by means of a least squares fitting of Equation (8).

Variable	Value	Units
μ_y^{\max}	$+1.1 \times 10^0$	-
$T_{\text{dispersion}}$	$+5.0 \times 10^1$	°C
T_{opt}	$+8.8 \times 10^1$	°C

It is important to note that all parameters have a physical meaning: the maximum friction coefficient is given by μ_y^{\max} and occurs at temperature T_{opt} . Additionally, $T_{\text{dispersion}}$ is associated with the shape of the curve: a higher value indicates a flatter curve, whereas a lower one means a sharper one. It is observed that the adjustment is very accurate, allowing to estimate both the optimum working temperature and the value of maximum friction coefficient as a function of temperature.

This expression can be used to modify Pacejka’s magic formula, so that μ_y^{\max} is given by the MF, while the D term is obtained from the proposed Equation (8), resulting in (9):

$$D_y = \left(\mu_y^{\max} + \left[1 - \cosh\left(\frac{T_{\text{averaged}} - T_{\text{opt}}}{T_{\text{dispersion}}}\right) \right] \right) \cdot F_z \tag{9}$$

4. Conclusions and Future Works

This work describes the importance of studying lateral dynamics between the tire and road. Experiments have been carried out on a test bench to determine the influence of temperature, longitudinal speed of the vehicle, steering frequency, vertical load, and tire pressure on lateral dynamics. Linear parameters associated with a first-order system have been studied: relaxation length and time constant. It has been shown how these parameters affect the maximum lateral friction coefficient outside the linear range. As contributions, the following are included:

- A new polynomial model is proposed to determine lateral relaxation length as a function of tire vertical load and longitudinal vehicle speed. It can be evaluated in real-time due to its low computational cost.
- A method is described to obtain a single representative temperature of the entire tread from an inhomogeneous distribution measured with infrared sensors. This method is based on Newton's law of cooling, which is the fundamental heat dissipation mechanism of tires. In addition, the computational cost of determining this averaged temperature is relatively low.
- A new mathematical model to determine the maximum lateral friction coefficient as a function of representative temperature calculated according to the proposed method and its implementation into the MF set of equations.
- It has been indicated how some variables do not influence some of the parameters that characterize lateral dynamics so that they can be obviated for predictive control.
- Future work will include the following:
 - Performing the same tests on different rolling surfaces: different belts on the tire test bench and especially real roads with an instrumented vehicle.
 - Performing tests with different tires to determine the influence of other parameters, such as aspect ratio, tread width, etc.
 - Carrying out longitudinal tests in order to be able to elaborate more complex combined models later.

Author Contributions: M.A.V. and J.P.F. developed the proposed model. M.A.V., J.P.F. and I.S.A. performed the simulations and experiments, data acquisition, as well as the writing of the manuscript. J.A.C.C. and J.J.C.A. conceived and designed the experiments, helped to analyze the data and provided some useful suggestions in the writing and revision of the text. The work and results have been supervised by J.A.C.C. and J.J.C.A. All authors have read and agreed to the published version of the manuscript.

Funding: This work is partly supported partly by the Spanish Ministry of Science and Innovation under grant PID2019-105572RB-I00, partly by the Economy, Knowledge, Enterprise and Universities Council of the Andalusian Regional Government under grant UMA18-FEDERJA-109, partly by the Spanish Ministry of Education, Culture and Sport under grant FPU18/00450, and partly by the University of Malaga.

Institutional Review Board Statement: Not applicable.

Informed Consent Statement: Not applicable.

Data Availability Statement: Not applicable.

Conflicts of Interest: The authors declare no conflict of interest.

References

1. Choi, E.H. *Tire-Related Factors in the Pre-Crash Phase*; NHTSA: Washington, DC, USA, 2012.
2. Reina, G.; Gentile, A.; Messina, A. Tyre Pressure Monitoring Using a Dynamical Model-Based Estimator. *Veh. Syst. Dyn.* **2015**, *53*, 568–586. [\[CrossRef\]](#)
3. Pacejka, H.B. *Tire and Vehicle Dynamics*, 3rd ed.; Elsevier Ltd.: Amsterdam, The Netherlands, 2012.
4. Bakker, E.; Nyborg, L.; Pacejka, H.B. Tyre Modelling for Use in Vehicle Dynamics Studies. *SAE Tech. Pap. Ser.* **1987**, 190–204. [\[CrossRef\]](#)
5. Mizuno, M.; Sakai, H.; Oyama, K.; Isomura, Y. Development of a Tyre Force Model Incorporating the Influence of the Tyre Surface Temperature. *Veh. Syst. Dyn.* **2005**, *43*, 395–402. [\[CrossRef\]](#)
6. Sornioti, A.; Velardocchia, M. Enhanced Tire Brush Model for Vehicle Dynamics Simulation. *SAE Tech. Pap.* **2008**. [\[CrossRef\]](#)
7. Sakhnevych, A. Multiphysical MF-Based Tyre Modelling and Parametrisation for Vehicle Setup and Control Strategies Optimisation. *Veh. Syst. Dyn.* **2021**, 1–22. [\[CrossRef\]](#)
8. Farroni, F.; Sakhnevych, A. Tire Multiphysical Modeling for the Analysis of Thermal and Wear Sensitivity on Vehicle Objective Dynamics and Racing Performances. *Simul. Model. Pract. Theory* **2022**, *117*, 102517. [\[CrossRef\]](#)
9. Kelly, D.P.; Sharp, R.S. Time-Optimal Control of the Race Car: Influence of a Thermodynamic Tyre Model. *Veh. Syst. Dyn.* **2012**, *50*, 641–662. [\[CrossRef\]](#)
10. Harsh, D.; Shyrokau, B. Tire Model with Temperature Effects for Formula SAE Vehicle. *Appl. Sci.* **2019**, *9*, 5328. [\[CrossRef\]](#)

11. Ozerem, O.; Morrey, D. A Brush-Based Thermo-Physical Tyre Model and Its Effectiveness in Handling Simulation of a Formula SAE Vehicle. *Proc. Inst. Mech. Eng. Part D J. Automob. Eng.* **2019**, *233*, 107–120. [\[CrossRef\]](#)
12. Calabrese, F.; Baecker, M.; Galbally, C.; Gallrein, A. A Detailed Thermo-Mechanical Tire Model for Advanced Handling Applications. *SAE Int. J. Passeng. Cars Mech. Syst.* **2015**, *8*, 501–511. [\[CrossRef\]](#)
13. Calabrese, F.; Ludwig, C.; Bäcker, M.; Gallrein, A. A Study of Parameter Identification for a Thermal-Mechanical Tire Model Based on Flat Track Measurements. In *The Dynamics of Vehicles on Roads and Tracks*; CRC Press: Boca Raton, FL, USA, 2017; pp. 169–175. ISBN 9781351057264.
14. Cabrera, J.A.; Castillo, J.J.; Pérez, J.; Velasco, J.M.; Guerra, A.J.; Hernández, P. A Procedure for Determining Tire-Road Friction Characteristics Using a Modification of the Magic Formula Based on Experimental Results. *Sensors* **2018**, *18*, 896. [\[CrossRef\]](#) [\[PubMed\]](#)
15. Romano, L.; Sakhnevych, A.; Strano, S.; Timpone, F. A Novel Brush-Model with Flexible Carcass for Transient Interactions. *Meccanica* **2019**, *54*, 1663–1679. [\[CrossRef\]](#)
16. Romano, L.; Bruzelius, F.; Jacobson, B. Unsteady-State Brush Theory. *Veh. Syst. Dyn.* **2021**, *59*, 1643–1671. [\[CrossRef\]](#)
17. Romano, L. *Advanced Brush Tyre Modeling*; Springer: Berlin/Heidelberg, Germany, 2022; ISBN 9783030984342.
18. Ma, Y.; Lu, D.; Yin, H.; Li, L.; Lv, M.; Wang, W. The Unsteady-State Response of Tires to Slip Angle and Vertical Load Variations. *Machines* **2022**, *10*, 527. [\[CrossRef\]](#)
19. Wang, Y.; Wei, Y.; Feng, X.; Yao, Z. Finite Element Analysis of the Thermal Characteristics and Parametric Study of Steady Rolling Tires. *Tire Sci. Technol.* **2012**, *40*, 201–218. [\[CrossRef\]](#)
20. Ebbott, T.G.; Hohman, R.L.; Jeusette, J.P.; Kerchman, V. Tire Temperature and Rolling Resistance Prediction with Finite Element Analysis. *Tire Sci. Technol.* **1999**, *27*, 2–21. [\[CrossRef\]](#)
21. Studios, S.M. Handling Consultants Feedback Reports. Available online: <https://wmdportal.com/> (accessed on 9 June 2022).
22. Durand-Gasselín, B.; Dailliez, T.; Mossner-Beigel, M.; Knorr, S.; Rauh, J. Assessing the Thermo-Mechanical TaMeTirE Model in Offline Vehicle Simulation and Driving Simulator Tests. *Veh. Syst. Dyn.* **2010**, *48*, 211–229. [\[CrossRef\]](#)
23. Grob, M.; Blanco-Hague, O.; Spetler, F. Tametire's Testing Procedure Outside Michelin. In Proceedings of the 4th International Tyre Colloquium, Guildford, UK, 20–21 April 2015.
24. Fevrier, P.; Fandard, G. Thermal and Mechanical Tyre Modelling. *ATZ Worldw.* **2008**, *110*, 26–31. [\[CrossRef\]](#)
25. Gipser, M. FTire and Puzzling Tyre Physics: Teacher, Not Student. *Veh. Syst. Dyn.* **2016**, *54*, 113–127. [\[CrossRef\]](#)
26. Hofmann, G.; Gipser, M. *FTire-Flexible Structure Tire Model*; Cosin Scientific Software: Munich, Germany, 2017; p. 64.
27. Kaemer, D. Physics Modeling NTM V7. Available online: <https://www.iracing.com/physics-modeling-ntm-v7-info-plus/> (accessed on 9 June 2022).
28. Ward, I.M.; Sweeney, J. *Mechanical Properties of Solid Polymers*, 3rd ed.; John Wiley & Sons Ltd.: Hoboken, NJ, USA, 2013; ISBN 9781444319507.
29. Société de Technologie Michelin. The Tyre Encyclopaedia. Part 1: Grip; 2001. Available online: <http://docenti.ing.unipi.it/guiggiani-m/dinvei.html> (accessed on 9 June 2022).
30. Williams, M.L.; Landel, R.F.; Ferry, J.D. The Temperature Dependence of Relaxation Mechanisms in Amorphous Polymers and Other Glass-Forming Liquids. *J. Am. Chem. Soc.* **1955**, *77*, 3701–3707. [\[CrossRef\]](#)
31. Lozia, Z. Is the Representation of Transient States of Tyres a Matter of Practical Importance in the Simulations of Vehicle Motion. *Arch. Automot. Eng.* **2017**, *77*, 63–84.
32. Segel, L. Force and Moment Response of Pneumatic Tires to Lateral Motion Inputs. *J. Manuf. Sci. Eng. Trans. ASME* **1966**, *88*, 37–44. [\[CrossRef\]](#)
33. Dugoff, H.; Fancher, P.S.; Segel, L. An Analysis of Tire Traction Properties and Their Influence on Vehicle Dynamic Performance. *SAE Tech. Pap.* **1970**, *79*, 1219–1243. [\[CrossRef\]](#)
34. Schieschke, R.; Hiemenz, R. The Relevance of Tire Dynamics in Vehicle Simulation. In Proceedings of the XXIII FISITA Congress, Torino, Italy, 7–11 May 1990.
35. Schieschke, R. The Importance of Tire Dynamics in Vehicle Simulation. In Proceedings of the 9th Annual Meeting and Conference on Tire Science and Technology, Tire Science and Technology, Akron, OH, USA, 20–21 March 1990.
36. Oertel, C.; Fandre, A. RMOD-K Tyre Model System. *ATZ Worldw.* **2001**, *103*, 23–25. [\[CrossRef\]](#)
37. Oertel, C.; Fandre, A. Tire Model RMOD-K 7 and Misuse Load Cases. *SAE Tech. Pap.* **2009**. [\[CrossRef\]](#)
38. Luty, W. Influence of the Tire Relaxation on the Simulation Results of the Vehicle Lateral Dynamics in Aspect of the Vehicle Driving Safety. *J. KONES Powertrain Transp.* **2015**, *22*, 185–192. [\[CrossRef\]](#)
39. Luty, W. Simulation Research of the Tire Basic Relaxation Model in Conditions of the Wheel Cornering Angle Oscillations. *IOP Conf. Ser. Mater. Sci. Eng.* **2016**, *148*, 012015. [\[CrossRef\]](#)
40. Shaju, A.; Kumar Pandey, A. Modelling Transient Response Using PAC 2002-Based Tyre Model. *Veh. Syst. Dyn.* **2022**, *60*, 20–46. [\[CrossRef\]](#)
41. Alcázar Vargas, M.; Pérez Fernández, J.; Velasco García, J.M.; Cabrera Carrillo, J.A.; Castillo Aguilar, J.J. A Novel Method for Determining Angular Speed and Acceleration Using Sin-Cos Encoders. *Sensors* **2021**, *21*, 577. [\[CrossRef\]](#)
42. Ljung, L. *System Identification Toolbox User's Guide*; The Mathworks: Natick, MA, USA, 2022.
43. Cabrera, J.A.; Ortiz, A.; Simón, A.; García, F.; Pérez de la Blanca, A. A Versatile Flat Track Tire Testing Machine. *Veh. Syst. Dyn.* **2003**, *40*, 271–284. [\[CrossRef\]](#)

44. De Rosa, R.; di Stazio, F.; Giordano, D.; Russo, M.; Terzo, M. ThermoTyre: Tyre Temperature Distribution during Handling Manoeuvres. *Veh. Syst. Dyn.* **2008**, *46*, 831–844. [CrossRef]
45. D'Errico, J. Polyfitn. Available online: <https://es.mathworks.com/matlabcentral/fileexchange/34765-polyfitn> (accessed on 28 June 2022).